DEVELOPMENT OF A SEMI-AUTONOMOUS ROBOTIC PLATFORM FOR INTERCULTURAL OPERATIONS IN ROW CROPS

by

ATHIRA P.

(2018-18-011)

DEPARTMENT OF FARM MACHINERY AND POWER ENGINEERING

KELAPPAJI COLLEGE OF AGRICULTURAL ENGINEERING AND TECHNOLOGY, TAVANUR, MALAPPURAM– 679573

KERALA, INDIA.

2020

DEVELOPMENT OF A SEMI-AUTONOMOUS ROBOTIC PLATFORM FOR INTERCULTURAL OPERATIONS IN ROW CROPS

by

ATHIRA P.

(2018-18-011)

THESIS

Submitted in partial fulfilment of the
requirement for the degree of
MASTER OF TECHNOLOGY
IN
AGRICULTURAL ENGINEERING
(Farm Power and Machinery)

Faculty of Agricultural Engineering & Technology
Kerala Agricultural University

DEPARTMENT OF FARM MACHINERY AND POWER ENGINEERING
KELAPPAJI COLLEGE OF AGRICULTURAL ENGINEERING
AND TECHNOLOGY, TAVANUR, MALAPPURAM– 679573
KERALA, INDIA.

2020

DECLARATION

I, hereby declare that this thesis entitled "**DEVELOPMENT OF A SEMI-AUTONOMOUS ROBOTIC PLATFORM FOR INTERCULTURAL OPERATIONS IN ROW CROPS**" is a bonafide record of research work done by me during the course of academic programme in the Kerala Agricultural University and the thesis has not previously formed the basis for the award to me of any degree, diploma, associate-ship, fellowship or other similar title, of any other University or Society.

Place: Tavanur

Date: 04-01-2021

ATHIRA P.

(2018-18-011)

CERTIFICATE

Certified that this thesis entitled "**DEVELOPMENT OF A SEMI-AUTONOMOUS ROBOTIC PLATFORM FOR INTERCULTURAL OPERATIONS IN ROW CROPS**" is a bonafide record of research work done independently by Er. Athira P. (2018-18-011) under my guidance and supervision and that it has not previously formed the basis for the award of any degree, diploma, fellowship or associate-ship to her.

Place: Tavanur

Date: 04-01-2021

Dr. Shaji James P.
(Major Advisor)
Professor (FPME),
Agricultural Research Station,
Kerala Agricultural University,
Mannuthy, Thrissur.

CERTIFICATE

We, the undersigned members of the Advisory Committee of Er. ATHIRA P. (2018-18-011), a candidate for the degree of Master of Technology in Agricultural Engineering with major in Farm Power and Machinery, agree that the thesis entitled "**DEVELOPMENT OF A SEMI-AUTONOMOUS ROBOTIC PLATFORM FOR INTERCULTURAL OPERATIONS IN ROW CROPS**" may be submitted by Er. ATHIRA P., in partial fulfilment of the requirement for the degree.

Dr. Shaji James P.
(Major Advisor)
Professor (FPME)
Agricultural Research Station
Kerala Agricultural University
Mannuthy, Thrissur.

Dr. Jayan P. R.
(Member, Advisory Committee)
Professor and Head
Department of FMPE
KCAET, Tavanur.

Er. Shivaji K. P.
(Member, Advisory Committee)
Assistant Professor (FPME)
RARS, Ambalavayal
Kerala Agricultural University
Wayanad.

Dr. Sunil V. G.
(Member, Advisory Committee)
Assistant Professor (Agrl. Extn.)
Communication center
Mannuthy.

ACKNOWLEDGEMENT

I feel great pleasure in expressing my deep sense of gratitude towards all those who had made me possible to complete this research with success.

With due respect, I record my sincere gratitude and indebtedness to my major advisor, ***Dr. Shaji James P.****, Professor (Farm Power Machinery and Energy), Agricultural Research Station, Mannuthy, Thrissur, for his valuable advice, guidance, encouragement, deemed support and creative criticisms during the course of the research work and in the preparation of the thesis. I consider it as my greatest fortune to have him as the major advisor for my research work.*

*It is my privilege to acknowledge Prof. (****Dr.) Sathian K. K****., Dean (Agrl. Engg.) and Head, Dept. of SWCE, KCAET, Tavanur for the valuable help rendered to me.*

I am indebted to ***Dr. Jayan P. R.****, Professor and Head, Dept. of FMPE, KCAET, Tavanur and also my advisory committee member for the support and facilities offered while carrying out the research. It is my pleasure to express my sincere gratitude to the members of my advisory committee* ***Er. Shivaji K. P****., Assistant Professor (FPME), RARS Ambalavayal, Wayanad, and* ***Dr. Sunil V. G.****, Assistant Professor (Agri. Extn.), Communication center, Mannuthy. I gratefully acknowledge the valuable suggestions, helpful advice and encouragement extended by them during the course of research. I extend my sincere thanks to* ***Er. Sindhu Basker****, Assistant Professor, Dept. of FMPE, KCAET, Tavanur, for the facilities offered while carrying out the research.*

Words may become trivial while expressing gratitude towards ***Er. Joe Joe L. Bovas****, PhD Scholar, Gandhigram Rural Institute (Deemed to be University), Dindigul, Tamil Nadu, for his dynamic and valuable guidance, support and keen interest during this research work. I gratefully acknowledge* ***Mr. Rubesh*** *for his support and help during the research work.*

With a profound sense of gratefulness, I also acknowledge ***Dr. Dipak S. Khatawkar****, Senior Research Fellow, Dept. of FME, KCAET, Tavanur, for his critical and vital guidance, valuable critics and support throughout my research work.*

I extend my sincere thanks to ***all faculty members, technical, non-teaching and library staff of KCAET****, for their ever willing help and co-operation. Special thanks are also to* ***FMPE Workshop team in KCAET****. I also express my sincere gratitude to* ***Kerala Agricultural University*** *for the financial support to do this research work.*

I remain indebted to all ***my friends****,* ***classmates****,* ***juniors*** *and* ***seniors*** *for their unfailing help and support which enabled me to have everything on reach. It becomes difficult to pen down everybody's name. However, I am forever thankful to each and every one, for their help rendered.*

Above all, I bow my heads before ***The God Almighty*** *for the blessings bestowed upon me which made me to materialize this endeavour.*

At last but not the least, I am greatly indebted to my ***beloved parents and all family members*** *for their love, blessings, and support which gave strength to complete the study.*

Athira P.

TABLE OF CONTENTS

LIST OF TABLES

LIST OF FIGURES

LIST OF SYMBOLS AND ABBREVIATIONS

&	:	And
µm	:	Micrometer
2D	:	Two Dimensional
3D	:	Three Dimensional
AC	:	Alternating Current
Ah	:	Ampere hour
AR	:	Application Rate
AUCI	:	Arduino Uno Control Interface
CAN	:	Control Area Network
CCD	:	Charge Coupled Device
CCU	:	Central Control Unit
CFRP	:	Carbon Fibre Reinforced Polymer
CI	:	Cone Index
CPDGPS	:	Carrier Phase Differential Global Positioning System
DC	:	Direct Current
DoD	:	Drop on Demand
DoF	:	Degrees of Freedom
DPDT	:	Double Pole Double Throw
DTMF	:	Dual-Tone Multi Frequency
EEPROM	:	Electrically Erasable Programming Read Only Memory
EFC	:	Effective Field Capacity
ESOINN	:	Enhanced Self Organizing Incremental Neural Network
et. al.	:	and others
etc.	:	Etcetera

FAO	:	Food and Agriculture Organization
FESS	:	Finite Element Skid Steering
FoS	:	Factor of Safety
Fig.	:	Figure
GB	:	Giga Bytes
GDP	:	Gross Domestic Product
GHz	:	Giga Hertz
GND	:	Ground
GPS	:	Global Positioning System
GSM	:	Global System for Mobile communication
GUI	:	Graphical User Interface
HTTP	:	Hyper Text Transfer Protocol
I2C	:	Inter-Integrated Circuit
IEEE	:	Institute of Electrical and Electronics Engineers
IMU	:	Inertial Measurement Unit
IC	:	Integrated Circuit
ICSP	:	In-Circuit Serial Programming
IDE	:	Integrated Development Environment
I/O	:	Input/output
IP	:	Internet Protocol
IoT	:	Internet of Things
ISM	:	Industrial, Scientific and Medical
KAU	:	Kerala Agriculture University
kB	:	Kilo bytes
KCAET	:	Kelappaji College of Agricultural Engineering and Technology

kg_f	:	Kilogram-force
LED	:	Light Emitting Diode
LIDAR	:	Light Detection and Ranging
LiPo	:	Lithium Polymer
Min	:	Minute (s)
MOSFET	:	Metal Oxide Semiconductor Field Effect Transistor
PC	:	Personal Computer
PID	:	Proportional Integral Derivative
PWM	:	Pulse Width Modulation
RAM	:	Random Access Memory
RF	:	Radio Frequency
ROM	:	Read Only Memory
Rs.	:	Rupees
RPiI	:	Raspberry Pi Interface
RPM	:	Revolutions Per Minute
RR	:	Rolling Resistance
RTKGPS	:	Real Time Kinematic Global Positioning System
SD	:	Secure Digital
SIM	:	Subscriber Identity Module
SLAM	:	Simultaneous Localization and Mapping
SMC	:	Steering Motor Control
SMPS	:	Switched Mode Power Supply
SPDT	:	Single Pole Double Throw
TFC	:	Theoretical Field Capacity
UART	:	Universal Asynchronous Receiver Transmitter

UK-RAS	:	United Kingdom – Robotics and Autonomous Systems
USB	:	Universal Serial Bus
Wi-Fi	:	Wireless Fidelity
WLAN	:	Wireless Local Area Network

Introduction

CHAPTER I

INTRODUCTION

The population of the world is growing at an alarming rate, leading to resource management problems (Coccia, 2013). Food demand is one of the major challenges faced by the people, in fact, various studies have shown that 820 million people in the world are not fed properly (Tamburino *et al.*, 2020; O'Neill *et al.*, 2018). The world population is expected to be 9.7 billion by 2050, which is 26% higher than that of 2019 (World Population Prospects, 2019; Tedla *et al.*, 2019) while the agriculture productivity is estimated to increase by only 25% (Madhusudhan, 2015). It is estimated that the production should increase by 70% by 2050 to meet people's demand (FAO, 2009; Natu and Kulkarni, 2016; Tedla *et al.*, 2019; Vasconez *et al.*, 2019). Out of the 17 Sustainable Development Goals set by United Nations General Assembly, to be achieved by 2030, the top two goals are no poverty and end to hunger (Dhahri and Omri, 2020). Past experience show that precision agriculture can play a vital role to fight against poverty and hunger (Sud *et al.*, 2015).

Agriculture is the primary source of livelihood in many countries all over the world, including India (Kadiyala *et al.*, 2014). The Indian economy mainly depends on agricultural sector which accounts for 18% of India's Gross Domestic Product (GDP) and ensures employment for more than 50% of countries workforce (Madhusudhan, 2015). Globally, India is an important player in terms of consumption, production and trade of agricultural commodities (Mohanty and Mishra, 2019). India is world's largest producer of food grains, pulses, spices and spice products. The food grain production was 283.37 million tonnes during 2018-19 (Anon., 2019). Apart from this, India stands second in the production of fruits and vegetables. During 2018-19, the vegetable production was 187.36 million tonnes (Anon., 2019). The efficiency and productivity of agriculture has to be improved to meet people's requirement because lands for agriculture decrease due to the increase in population. Several countries around the world are facing a decline in crop production rates due to labour shortages (Jokisch, 2002; Cook & Frank, 2008). The movement of labour force from rural areas to cities in search of better job opportunities is

a cause of major concern (Vasconez *et al.*, 2019). The conventional methods of farming and labour shortages make agriculture uneconomical and inefficient (Grift, 2007; Yaghoubi *et al.*, 2013; Sreekantha, 2016). This has led to the increased use of agricultural machines, even though they are costly. To be precise, the costs of most agricultural machines have increased by fivefold, while its use has been increased eight-fold in the last forty years. This led to the increase in farm production, in spite of more households engaging in off-farm labour (Michler, 2020). The other means to tackle labour shortage is by technological process, through the application of automation and robotics in agriculture (Vasconez *et al.*, 2019).

Automation in agriculture has emerged as a promising technological option for increasing the crop productivity without sacrificing the product quality, by which saving of time and labour is achieved through specialised tools and technology (Bonadies and Gadsden, 2019). By reducing human interventions and related errors, the enhanced efficiency, reliability and precision will help to improve the productivity of agricultural machinery. Automation in farm vehicles has been studied for many years, even as early as 1920s. The concepts of autonomous agricultural machines were practically applied in the field during 1950s. One of the first developments was the modified driver less tractor prototype using leader cable guidance system by Morgan in 1958 which was seen cited by Hague *et al.* (2000).

Robotics in agriculture induces a revolutionary change through improved productivity with greater precision (Bawden *et al.*, 2014). Because of reduced soil compaction, less impact on environment, low cost, less input energy required, multi-purpose use and high precision, most of the researchers are interested in developing smaller autonomous farm vehicles instead of larger machines. By employing autonomous agricultural robots, the modern agriculture could reduce the labour dependency thus decreasing labour intensity (Bechar and Vigneault, 2017). However, successful implementation of completely autonomous robots in agriculture is still far away due to the complexity of agricultural processes and higher investment requirement (Sistler, 1987; Vasconez *et al.*, 2019).

In addition to labour dependency, robots increase the labour productivity on various agricultural operations. They have the ability to operate under difficult agricultural environments, imitate human skills, continuous precise operations, and provide higher possibility for increasing agricultural productivity and production (Auatcheein and Carelli, 2013; Bochtis *et al.*, 2014). This will result in sustainable economic growth and development (Eberhardt and Vollrath, 2018; Marinoudi *et al.*, 2019).

The trend of using and developing robots for various agricultural operations was accelerated due to the acute shortage in sufficient skilled manpower in many countries (Dattatraya *et al.*, 2014). Now a days, use of robots in agriculture are being investigated for repetitive jobs such as mapping (Cheein *et al.*, 2011), land preparation (Yaghoubi *et al.*, 2013), seeding (Shivaprasad *et al.*, 2014), harvesting (De-An *et al.*, 2011; Nuske *et al.*, 2011; Bac *et al.*, 2014), pruning (Akbar *et al.*, 2016), spraying and irrigation (Moreno *et al.*, 2013; Oberti *et al.*, 2013; Adamides *et al.*, 2017a,b), monitoring and inspection (Pace *et al.*, 2011; Lunadei *et al.*, 2012; Munera *et al.*, 2017) and weeding (Bak and Jakobsen, 2004; Sujaritha *et al.*, 2017; Utstumo *et al.*, 2018). According to the UK RAS network (2018), there will be a time when humans and robots work together for performing simple to complex works.

The farm power availability in India was 1.84 $kWha^{-1}$ during 2013-14 and it has to be increased to 4 $kWha^{-1}$ by 2022 (Anon., 2019) for improving agricultural productivity. Agricultural operations are usually carried out by means of human, animal and mechanical power sources and apart from improving power availability, efficient use of available power is also equally important. Now, researchers in India are also stepping forward to implement robotics in the agricultural field to reduce labour dependency and improve precision in agricultural operations. The concept of “Agribot” is an agricultural robot designed to execute basic farming functions like seeding, weeding, spraying and harvesting. In one such initiative a “robo kisan” to monitor powdery mildew of grapes was developed at Allahabad Agricultural Institute during 2008 (Srivastava, 2010).

Kerala people depend on the neighbouring states to a great extent to meet the food demand in spite of the quality concerns on the commercially produced food products brought to the state. Growth of agriculture sector in Kerala is facing various labour related challenges such as high cost of labour as well as its shortage and non-availability. The initiation of farm mechanisation could commensurate the decline in farm labours to an extent. But the fact that 98% total farm land in Kerala is occupied by small and marginal holders pose technological challenges to agricultural mechanisation. Considering all these facts, automated technologies need to be implemented for increasing the agriculture growth rates with precision farming. Taking into consideration the conditions prevailing in the agriculture dominated areas, the robot should be easy to operate and service and should work based on the command of a human operator (Bechar and Vigneault, 2017). The present advancements in programming and technology have made robotics easy and less complicated (Decker *et al.*, 2017). In addition to the technological easiness, the cost factor should also be considered such that it is compatible to the common farmer (Pedersen *et al.*, 2006; Bechar and Vigneault, 2016; Lampridi *et al.*, 2019; Marinoudi *et al.*, 2019).

Robots are successfully used in many agricultural tasks but still its cost is not affordable to majority of the farmers of India. Taking into consideration the present needs and the present technological availability, it is desirable to develop an economically feasible semi-automatic agricultural robot for the farmers. In Kerala, no notable research works are seen done in the field of agricultural robots and an attempt is hence made to develop a semi-autonomous robotic platform. This work is expected to aid the development of automated gadgets that can be a boon to the farmers in Kerala as well as for other areas of the developing world. The present study is envisaged with the following objectives:

1. To study the technical requirements for a semi-autonomous robotic platform for row crops.
2. To develop a prototype semi-autonomous robotic platform.
3. To test the prototype in laboratory and assess the feasibility in field condition.

Review of Literature

CHAPTER II

REVIEW OF LITERATURE

Autonomous agricultural robots can automate slow, repetitive and difficult tasks for farmers, allowing them to focus more on improving overall production so as to achieve potential yields. Hence, the development of an economically feasible agricultural robot for row crops based on the existing technologies will be boon to the farmers in India. These were developed for harvesting and picking, weed control, spraying, monitoring of crops, seeding, soil analysis etc. A review of various research works carried out in the design aspects and development of autonomous agricultural machines are presented in this chapter.

2.1 Automation in Agriculture

Agriculture plays an important role in Indian economic growth as agriculture is the livelihood for the people in India. The decreasing availability of labour in agricultural sector has threatened the efforts to meet the ever increasing food demand. Automation and IoT techniques were introduced in the field of agriculture to enhance its productivity by making it smart and efficient. The productivity and quality of crops could be increased by the application of various kinds of automated technologies in agriculture (Zhang, 2013). Automation in the field of agriculture led to the usage of agricultural robots and there is a possibility that fuel consumption and air pollution could be reduced by using robots or autonomous tractors for various agricultural tasks (Gonzalez-de-Soto *et al.*, 2015). Agricultural automation could result with increased productivity for supporting the sustainable economic growth and development (Eberhardt and Vollrath, 2018).

Human efforts can be minimized for a maximized productivity by using smart farming techniques (Kashyap *et al.*, 2019). In smart farming, data from various fields will be gathered by means of sensors and transferred to an on-board computer. The data received by the on-board computer will check the threshold values for taking necessary action. The development of various sensors, innovative control algorithms, artificial

intelligence, computer vision, and other technologies, along with the cost reduction achieved owing to their mass production, led to advancements in the field of robotics (Corollaro *et al.*, 2014; Donis-Gonzalez *et al.*, 2016; Diels *et al.*, 2016). As technology advanced in various fields like on-board computer speed, memory, sensors and internet, the robots became more intelligent and could serve the ever demanding applications in the fields of agriculture, industry, defence, surveillance, medical, and so on. Other than agriculture, many researchers were focused on automated video surveillance as their core area for research. The surveillance robots were developed with the ability to execute emergency monitoring, searching and rescue operations in places where humans were unable to go. Various industrial applications of the robots included material handling in hazardous places, pick and place, assembling of subsystems, painting etc. (Dixit and Dhayagonde, 2014).

2.1.1 Characteristics of agricultural robots

The agricultural robots are intended to operate in a complex real world environment characterised by complicated and dynamic field conditions in a rough terrain (Edan *et al.*, 2009). They could perform different tedious agricultural operations such as land preparation, seeding, weeding, spraying, irrigation, harvesting, monitoring and mapping which were based on an autonomous or semi-autonomous system depending on the human-robot interaction approaches (Vasconez *et al.*, 2019). In case of an 'AgriRobot', the user (farmer) could receive various data from the sensors installed in the robot and simultaneously control the motion and operation of the robot from a safe distance under comfortable conditions (Adamides *et al.*, 2017a). Robots were also employed in greenhouses to perform agricultural tasks (Slaughter *et al.*, 2008; Van Henten *et al.*, 2013; Hassan *et al.*, 2016; Gat *et al.*, 2016). Many workers expected that the introduction of feasible multipurpose robots would overcome the limitations in production inefficiency due to less potential resource utilization, and thus could be economically justified (Belforte *et al.*, 2006; Arguenon *et al.*, 2006).

2.1.2 Autonomous navigation of agricultural robots

Autonomous navigation was one of the basic components of automation in agriculture (Nof, 2009). Combination of various sensors and their control algorithms made the guidance system more precise (Morimoto *et al.*, 2005; Khot *et al.*, 2006). Machine vision was a guidance assistance system based on image processing technique (Bakker *et al.*, 2008; Dar *et al.*, 2011). Camera sensors with computer vision based navigation were used in the robots (Hiremath *et al.*, 2014). Global Positioning System (GPS) based autonomous guidance was recently used because of its increasing accuracy in mapping and precise operation (Nagasaka *et al.*, 2004; Bergtold *et al.*, 2009; Bakker *et al.*, 2011; Rovira-Mas *et al.*, 2015).

2.1.3 Autonomous agricultural tractors

Efforts to automate operation of agricultural tractors started as early as 2000 (Cordesses *et al.*, 2000). Bell (2000) developed automatic steering control in John Deere 7800 tractor using Carrier Phase Differential Global Positioning System (CPDGPS) and demonstrated automatic seeding. Subramanian *et al.* (2006) designed a guidance system in John Deere 6410 tractor based on machine vision and LIDAR to enable autonomous navigation in orchards or forests where GPS limits. Tamaki *et al.* (2013) developed an autonomous tractor, installed with RTK-GPS and Inertial Measurement Unit, for autonomous navigation in rice field. Tractors could be automated using viable, cost effective and highly accurate technologies to perform the agricultural tasks (Tarannum *et al.*, 2015).

2.2 Technical aspects of robotics

A robot is a machine to perform specified tasks by eliminating the human labour according to the predetermined program/algorithm. Autonomous robots are completely under computer program control while semi-autonomous robots depend on both computer program and human labour. In remote-controlled robots, joystick or other handheld devices are used by humans to control the robot. Application of robotics in agriculture

offers a precision and promising farming method for higher production efficiency and safer operations (Yaghoubi *et al.*, 2013).

Krinkin *et al.* (2016) created a small sized omni-directional robot for testing Simultaneous Localization and Mapping (SLAM) algorithm. Centro-symmetric design was selected with rubber roller omni-wheels in order to avoid wheel slip. All wheels were individually driven by electric motors. The system consisted of Arduino based controller, Raspberry Pi on-board computer, L293 motor drivers and Li-Po battery (7.4 V). The controller, motors and motor drivers were powered by battery and a 5V regulator was used as Raspberry Pi power unit. The controller and on-board computer were communicated by UART at 115200 broad rates. The experimental tests conducted indoors as well as in outdoor environment showed that the robot was capable to operate even in limited spaces without any damage to it at maximum speed and acceleration. The robot had provisions to mount additional sensors and electronic equipments.

The mechanical structure of an agricultural robot consists of the robot's body and driving wheel unit. Xue *et al.* (2018) tested two wheel drive agricultural robot with differential drive for verifying its performance. Basic Atom microcontroller was the slave controller of the robot and laptop was its host controller. Trajectory tracking was achieved by using RTK-GPS receivers mounted on the platform. MATLAB software verified the performance of the control algorithm. The field test results indicated a good tracking performance with a maximum error of 0.21 m. The effectiveness of sliding mode controller for trajectory tracking was also verified.

Oltean (2019) developed a robot platform based on four-wheel configuration driven independently by four DC motors powered by 7.4 V 4000 mAh capacity Lithium Polymer battery. All the four motors were driven in the same direction at the desired speed for getting a forward/reverse movement. For a turning or rotation, motors on different sides were driven in counter clockwise direction. The robot consisted of a Raspberry Pi camera, ultrasonic sensors and three infrared sensors. The robotic arm having one degree of freedom was installed in the robot along with a gripper for lifting

and transporting the obstacles present in its way. Two servo motors were used for actuating the arm and the gripper. The major components of the robot included a Raspberry Pi Interface (RPiI) and Arduino Uno Control Interface (AUCI) which were communicated via I2C (Inter-Integrated Circuit) protocol. ATMega328P was the microcontroller used and Raspberry Pi 3 Model B was the small single board computer used which serves as the brain of mobile robotic platform. Arduino Uno was programmed in Arduino Integrated Development Environment (IDE) using C/C++ language and Raspberry Pi worked under Raspbian operating system. RPiI had direct connection with Pi camera and robotic arm servomotors, thus ensuring 2D mapping, route planning, navigation, and catching and lifting of the obstacles. AUCI had direct access to Infrared sensors for line detection, Ultrasonic sensors for avoiding obstacle and controls the DC motors for the movement of the robot in desired direction.

2.2.1 On-board microcomputers for system control

Arduino Mega 2560 and Raspberry Pi are the most widely used open source on-board microcomputer boards. Reguera *et al.* (2015) proposed a low-cost solution-oriented scheme to control education where Raspberry Pi was used for remote communication and Arduino microcontroller with an adapter card helped to upgrade the system for enabling configurable practices with easy signal acquisition. Adapter card was used to adapt the voltage to 0-5V Arduino's I/O from +15V feedback system. It also suppressed the high frequency noises for Arduino's input and output since a stable supply was required to avoid improper running programs in Arduino. Thus the proposed system took the advantages of both raspberry Pi and Arduino microcontrollers.

A Raspberry Pi and Arduino Mega were interfaced in a wirelessly controlled mobile robot through internet using a webpage (Al-Sahib and Azeez, 2015). Because of high flexibility in dealing various operations, Raspberry Pi was used as the microcomputer with Raspbian operating system. WebIOPi web application was installed on the Pi board which allowed the user to control the board. Arduino Mega was the microcontroller used to control the servo motors for robotic arm movement and camera

position. Microcomputer was programmed in python language and microcontroller was programmed in C language. Wireless communication using webpage reduced the time delay and increased the communicating distances between the robot and the user depending upon the type and strength of the internet package.

2.2.1.1 Raspberry Pi micro-computer

Raspberry Pi was a low-cost open-source single board computer. Raspberry Pi model B+ had RAM memory of 512 Mb, HDMI, four USB ports, 3.5 mm audio jack and a MicroSD card slot for storing the software. Raspberry Pi projects usually ran on Raspbian operating system using python language. SciPy, Matplotlib and NumPy were the most important open source libraries used in python which had a wide application in signal processing and mathematical algorithm. The physical communication between the Pi board and the outside world was achieved through General Purpose Input/Output (GPIO) interface. Raspberry Pi was capable of allowing both wired and wireless communication to perform a network-based control or remote control. All the hardware and software tools could be used to propose a whole control education project (Hoyo *et al.*, 2015).

Vanitha *et al.* (2016) developed a mobile robot to detect fire accidents and to trace out the intruders. The robot was fully controlled by Raspberry Pi model B+ with programming language based on LINUX platform. The robotic vehicle was driven by DC motors with motor driver circuits (5V, 600 mA). The internet connection was established between the robot and the user for its communication. Webcam installed in the robot had captured the images and were stored in the memory card. The motion of the robot was controlled by a webpage through Raspberry Pi using the live images captured. A unique username and password of the webpage made a secured control of the robotic movement by the user from anywhere in the world.

2.2.1.2 Arduino microcontroller board

Various microcontrollers are available in the market for specific purposes which can be selected according to capability requirement. Yusoff *et al.* (2012) developed a wireless mobile robot with robotic arm based on Arduino Mega 2560 microcontroller. The microcontroller had a total of 54 digital input and output pins which included 15 Pulse Width Modulation (PWM) inputs, 16 analog inputs, a 16 MHz oscillator, 4 hardware serial ports, an ICSP header, a power jack and a reset button. Arduino was programmed in Arduino IDE environment using a wiring-based language similar to C/C++. PS2 wireless controller was used for wireless communication. The developed system could overcome the obstacles in an easy and fast way by picking the obstacles and placing it away from the way.

Budiharto (2014) proposed a low cost remote controlled AVR-based mobile robot to avoid obstacles. ATMega32 microcontroller was used because of its ability to store 32 kB program at EEPROM. In order to handle heavy load for carrying the task, the system was proposed with a DC motor driver and a geared DC motor having 56 RPM and 588 mN-m torque. Because of the use of geared DC motor and high quality frame for the robot, it was able to handle 10 kg load during testing.

Umarkar and Karwankar (2016) developed an automated seed sowing Agribot with Wi-Fi interface between the server and Android application using Arduino Nano. All sensors and hardware were connected to Arduino board to perform the desired work. Arduino Nano was a low-cost easily-available micro-controller, based on ATmega328 having 32 kB flash memory, 2 kB SRAM and 1 kB EEPROM. The software programming was run on Arduino Integrated Development Environment (IDE) which enabled easy writing and uploading of the code to the board. REST API and MQTT API were the two different libraries used in Arduino Nano to access Adafruit cloud server, which enabled the IoT communication. Data collected from the Agribot was sent on the Adafruit server and controlled using Android application.

A new approach for detecting and locating the target for controlling a distant mobile robot was proposed by Kebir *et al.* (2016). Image processing technique using webcam was employed for target detection and localization, and the results from these operations were used to generate control signals. The control signals were transferred to the robot via Wi-Fi communication based on Arduino microcontroller and Arduino-WiFi shield. Arduino Uno was the microcontroller used which had 6 analog inputs, 14 digital I/O pins, 16 MHz clock speed, a power jack, a USB connection and a reset button. Arduino board was connected to the internet having 802.11 wireless specifications by means of Wi-Fi shield. After locating the target by image processing technique, the direction of rotation and speed of two DC motors of the robot were controlled using Arduino microcontroller in order to ensure its desired movement.

2.2.1.3 Other on-board micro-computers

Ramya and Palaniappan (2012) proposed a robot for safety and security purposes driven by 12V DC geared motors and controlled the direction and movement of the robot according to the command. Wireless AV camera with 100 m transmission distance was installed in the robot for getting high quality picture and sound and these could be viewed on TV, monitor or LCD. The controller used was Atmel AT89C51, embedded with C program, having 4 kB flash memory and 12 bytes RAM. The robot was remotely controlled via Zigbee communication. This intelligent robot had application on security purposes and rescue operation like war fields, disaster situations and high density gas leakage regions where humans cannot go.

Gohiya *et al.* (2013) developed an agricultural mobile robot for monitoring the soil and atmospheric parameters wirelessly based on ARM-LINUX platform. The host controller (PC) was based on Linux platform using Ubuntu 10.04. The ARM9 Samsung S3c2440 microcontroller was used by the target devices to control the tasks. The host and the target devices were communicated wirelessly via Zigbee wireless protocol. The microcontroller had ARM920T processor-core integrated with S3c2440A having 400 MHz maximum frequency for accomplishing the on-board image processing task using

an open-cv library. All modules of the system were powered by 7 Ah lead acid battery. Driver module included three DC motors for driving the robot and three servo motors for performing its various tasks. The sensor module comprised of a camera, humidity sensor, temperature sensor, soil sensor and an Infra-red sensor. A real-time digital PID controller was adopted to control the speed of the DC motor by ARM based microcontroller using L293D interfacing circuit. Precision speed control and higher operation speed was accomplished by ARM board since it was a 32-bit microcontroller with additional facility for concurrent programming and real-time operation control.

A microcontroller PIC 16F877 was used to control a pesticide spraying robot especially for greenhouse (Sulakhe and Karanjkar, 2015). PIC 16F877A had 14 bit core, 40 pin count and flash memory for rewritable purpose. It was operated at frequencies up to 20 MHz and already had 368 bytes RAM inside it. The program code of only about 8000 words size could be stored inside PIC16F8777A ROM. Once a new program was loaded, it immediately erased the old program automatically. This low-cost microcontroller was very easy to assemble and program and had good stability and reliability.

2.2.2 Wireless communication and data acquisition

Various wireless standards are established as communication protocol such as Wireless Local Area Network (WLAN), Web-based communication (internet), Bluetooth technology, ZigBee technology, Wi-Fi communication, LoRa CSS, RF transmitter-receiver, I2C protocol, PS2 wireless controller, etc. Wireless communication reduced and simplified the wiring and harness. It also enhanced the reliability of signal transmission.

Wired local area network was extended and substituted by a flexible data communication protocol, namely WLAN based on IEEE 802.11. WLAN was operated at a frequency of 2.4 GHz and bandwidth 11 Mbits. Bluetooth (IEEE 802.15.1) was a short range wireless communication protocol operating at 2.4 GHz, 915 MHz and 868 MHz radio band frequencies to communicate at a bandwidth of 1 Mbit in between maximum of eight devices. Zigbee technology (IEEE 802.15.4) was considered as the most promising

wireless standard which addressed the network problems of wireless sensors because of its low power consumption and simple networking configuration. It was an ideal communication protocol for monitoring, sensing, automation, control, and tracking applications for the home, medical, agricultural and industrial environments (Wang *et al.*, 2006).

2.2.2.1 Wi-Fi Communication technology

As automation plays an important role in this developing world, the implementation of wireless sensing and control networks came into existence. Jadhav and Hambrade (2016) presented a fully automated drip irrigation system using Raspberry Pi via Wi-Fi communication. WiFi dongle had provided additional forms of wireless connectivity to devices with 2.4 GHz operating frequency band and high speed USB 2.0/1.1 host interface. The video stream captured by the webcam was saved, viewed and send to other networks through internet. Similarly, a remote controlled Agribot for performing agricultural operations like seeding, weeding, and fertilizing could be developed by using an internet protocol for transmitting and receiving the functional signals. There was no limitation on the range or distance between the robotic vehicle and the user while using internet. (Shivaprasad *et al.*, 2014; Amer *et al.*, 2015).

The control signals for target detection and localization of a distant robot could be generated through WiFi communication with the help of a microcontroller and WiFi Shield. Wifi Shield was an interface between the Arduino microcontroller board and the internet using 802.11 wireless specifications. WiFi technology was a WLAN in which an internet access could be obtained using a router connected to the internet service provider (Kebir *et al.*, 2016).

A WiFi module CC3000 was used in an automated seed sowing Agribot with Adafruit I/O server and Smatphone Android application. It was an IEEE 802.11 b/g protocol with softAP and WiFi Direct (P2P). This module simplified the internet connectivity because it was equipped with its own wireless processor (Umarkar and Karwankar, 2016).

2.2.2.2 Bluetooth technology

Bluetooth technology could be utilized for communicating between the user and robot within a limited range. Sulakhe and Karanjkar (2015) developed a prototype of pesticide spraying robot especially in greenhouse using Bluetooth technology for wireless communication. The robot had used PIC16F877A as the microcontroller. Bluetooth technology was interfaced between the controller and Android app in Smartphone. The controller was interfaced to the Bluetooth module through UART protocol. The robotic motion was controlled according to the commands received from the remote buttons in the Android app. HC-06 Bluetooth module contained Bluetooth serial interface module and a Bluetooth adapter. The normal serial port line had been converted to Bluetooth module using a Bluetooth serial module in which one is connected to Bluetooth master device and the other connected to the slave device. The Bluetooth module was paired with android Smartphone before starting the operation. The data collected by the sensors and camera were received by Bluetooth module from the Smartphone and was fed to the microcontroller. The controller processed the data and acted accordingly to control the robot and its operation.

An Arduino based surveillance robot developed by Azeta *et al.* (2019) had utilized WiFi network for live video transmission and Bluetooth technology for remote control of the robot based on the video stream. Bluetooth had a limited range of communication as compared to WiFi network. So, for controlling the robot, both the remote controller and the robot should be under its line of sight. The experimental results showed that it got a communication range of 50 m which was good enough for many surveillance applications.

2.2.2.3 Web-based communication

Ishibashi *et al.* (2013) described a Web-based remote monitoring system of the agricultural robot. Information regarding the condition of the robot, sensor data, speed of motor rotation, latitude and longitude of the field, etc. were gathered by PC installed on the robot. PC server used FreeBSD 7.3-STABLE operating system. The gathered data

was send as binary dataset to the Smartphone via Bluetooth. The datasets were checked by the Smartphone and transferred to database server via 3G mobile communication using Hypertext Transfer Protocol (HTTP). The database server had accumulated all the datasets accepted in series. Finally, user could browse the specified Webpage to get the data of this agricultural robot. SQLite 3.7.12.1 was the database server and HTTP Server 2.2.22 (The Apache Software Foundation) was the Web server. Firefox 17.0.1 (Mozilla Foundation) was used to check the operation of Web page. The system was developed to know the exact condition about robot combine and adequately manage the data for agricultural tasks.

2.2.2.4 ZigBee communication protocol

Gohiya *et al.* (2013) introduced a mobile robotic system based on ARM-LINUX platform for monitoring the plant and environmental parameters where XBee-Pro ZigBee module from Maxstream was used for the wireless communication between the host and target. This ZigBee wireless protocol had accomplished the acquisition of monitored data and the wireless control of the robot.

Ferdoush and Li (2014) developed a wireless communication between open source hardware platforms using Zigbee module, XBee Pro S2B from Digi11. This module was operated at 2.4 GHz ISM band and had 250 kbps data speed. The communication range of this module was 90 m and nearly 2 miles in indoor and outdoor environment respectively. The XBee module encapsulated the ZigBee protocol stacks and 802.15.4 radio transceivers, and could be integrated to the microcontroller or microprocessor through UART serial communication interface. This helped to reduce the complexity of developing a wireless sensor network system.

Wireless network communication for an autonomous mobile robot with GUI could be achieved through XBee modules. More than 64000 units of meshing network connection at 500 kbps data speed was created by these modules. The communication range of XBee module was about some hundred meters and had consumed very less energy of few milliWatts. The module could receive the data from sensors and then

transmitted to the microcontroller and PC control centre through meshing wireless network in order to enhance the computation ability of the robot (Tamre *et al.*, 2018).

2.2.2.5 DTMF technology

A robotic vehicle, with multi-tasking agricultural features, developed by Srivastava *et al.* (2014) uses a wireless communication system based on Dual Tone Multi-Frequency (DTMF) technology which allowed a greater range as this machine could be controlled from anywhere in the world.

Similarly, Rashid *et al.* (2016) developed a room cleaning robot using Arduino Uno platform which utilized DTMF technology for remote control operation from any distance using cell phones. The remote control was achieved through DTMF receiver MT8870 having the capacity for decoding 16 DTMF signals to its pairs for coding 4 bits. The frequencies of the signals were detected and verified by the decoder, corresponding to the standard DTMF frequencies, using digital counting techniques. DTMF module was interfaced to the microcontroller via 7404 NOT gate IC. Two cell phones were used for controlling the robot, one connected to DTMF module and other used as remote control. From the remote control phone, user made a call to the other phone connected to DTMF module which helped to send the proper symbol pulse according to the command key pressed on the remote control. Hence, the control signals for the robot was received by the cell phone via DTMF receiver and according to the commands from the remote cell phone, signal was transmitted to the Arduino Uno through DTMF transmitter for the movement and control of the robot.

2.2.2.6 Other wireless communication technologies

PS2 wireless controller was another communication system having vibration feed-back capability and operated at 2.4 GHz. Yousuff *et al.* (2012) developed a mobile robot with robotic arm controlled wirelessly. The movement of the robot as well as the robotic arm was controlled by the signal transmission between transmitter and receiver in PS2 controller. It consisted of a transmitter and a receiver for wireless communication and had

maximum wireless control up to 8 meters and 45 degree angle. The signal strength between transmitter and receiver got weak due to the reduction in its battery power.

Joe Joe *et al.* (2019) developed a low-cost automatic irrigation system based on Global System for Mobile Communication (GSM) for its wide adaptability. GSM mobile phones were the most convenient means of communication among farmers. In order to facilitate communication with the user via text messages, usually a Subscriber Identity Module (SIM module or GSM module) was used. A cheap and reliable communication was established with the farmers by inserting an activated SIM card into the module (SIM 900A GSM module). The data transmit pin of the GSM module was connected to the data receive terminal of the Arduino and vice versa. The experimental result showed that the system could manage its irrigation efficiently and continuously.

Oltean (2019) designed a mobile robot based on Raspberry Pi Interface (RPiI) and Arduino Uno Control Interface (AUCI) which communicated each other through an Inter-Integrated Circuit (I2C) synchronous communication protocol. AUCI received the data from various sensors and controlled the DC motor for driving the platform, while RPiI was used to process the data for performing the robotic task. According to I2C protocol, the address frame represented the address to which the message was sent and the data frame had one or more 8-bit fragments. The data frame consisted of two types of messages, command message and request message. The first byte of data frame was the identification code of the message. When a command message was received by AUCI through this protocol, it performed according to the command; whereas necessary information would be transferred to RPiI when AUIC received a request message.

2.2.3 Motion and direction control

Motion and direction control of a robot become an important sub-system as it directs the platform in desired orientation at desired speed for performing the specified tasks (Benson *et al.*, 2003; Bak and Jakobsen, 2004; Bergtold *et al.*, 2009; Grimstad *et al.*, 2015; Gat *et al.*, 2016). Usually the agricultural platforms had 4 wheels with 2 or 4 wheel drive and 2 or 4 wheel steering. Six wheel drive and tracked platforms were also in use.

Lin *et al.* (2015) developed a 4-wheel drive, 4-wheel steering platform suited to precision wheat seeding techniques. The platform could allow proper and desired orientation of the vehicle even during turning. Field test results showed that more than 93% seeding rate was achieved during different sowing speeds.

As agricultural robots were operated on off-roads, skid steering was most suitable for them because of its simplicity and robust performance. All wheels should be skid laterally to achieve a proper steering along the curved path. Juman *et al.* (2019) designed a four wheeled, differentially driven, skid steered mobile robot for navigating in an oil palm plantation. To change the direction of travel of the robot, the wheels should differentially drive the wheel pairs on each side (left/right). This skid steering could provide a high level of manoeuvring and rigid mechanical structure for the robot, because of its less moving parts. This configuration made the overall construction simple and minimized the maintenance work. The electric motors had driven the wheels and encoders gave feedback on the rotational speed of the wheels. These motors and encoders were connected to on-board microcontroller, Arduino Mega, which in turn was connected to a laptop computer for data collection and control processes. Microcontroller controlled the speed of the motor using Pulse Width Modulation (PWM) signals via motor driver. The control system was based on Enhanced Self Organizing Incremental Neural Network (ESOINN). The proposed system indicated higher accuracy in path planning and short processing time for learning during its field testing.

The major constraint for skid steering system was its higher power consumption than other conventional steering systems, which could be addressed by modelling the skid steering. Guo *et al.* (2019) introduced a universal skid steering model, Finite Element Skid Steering (FESS) model, which considered both the wheel and track conditions to make it suitable for both wheeled and tracked vehicles. A six-wheel drive track-wheel interchangeable mobile robot was used in the field test to validate the model and the results indicated high accuracy of FESS model.

Tu *et al.* (2019) implemented a Steering Motor Control (SMC) based navigational controller on a small 4WD/4WS autonomous agricultural robotic vehicle, 'AgRover'. To provide the location information, two RTK-GPS receivers were installed on the platform. During field test, the controller showed promising performance with an overall RMS error about 0.1 m.

2.4 Application of robots in various agricultural operations

There are reports that the use of conventional agricultural machinery resulted in soil compaction due to its heavy weight (Bechar and Vigneault, 2017). This could be overcome by the use of small agricultural robots which are suitable for precise agricultural operations. Jinlin and Limin (2010) proposed an agriculture robot for row guidance. The basic design comprised of a front cabin with a portable PC, motor controllers, power supply, electronic components, camera and other sensors. The storage boxes for materials like fertilizers, pesticides, water etc. were placed on the rear cabin. The robotic platform was driven by DC motors via wheels. The crops were detected for vision based row guidance using CCD camera with 8 mm focus lens. The crops and rows got differentiated based on their pixel sizes and thus the targeted area was extracted from the binary image for the row guidance. The preliminary test conducted on a vegetable field showed that the robot moved along the crop rows effectively and accurately.

'Bonirob' was a small autonomous agricultural robot used to detect and map individual plants. The crop rows or single plants were detected and mapped to achieve navigation and localization of the robot. The basic components in the navigation module consisted of GPS and 3D laser sensor. The precise operations performed by the robot led to the reduction of operation cost and a tremendous improvement in agricultural operation. The agricultural robots, 'Agrobots', could be classified into harvesting or picking, planting, weeding, spraying or maintenance robots with GPS or other sensors for its navigation. These new robots were becoming smaller and smarter using new advanced technologies in its hardware and software. Some of the examples included an 'Ag Ant' robot for detecting the weeds, insects or diseases and applying pesticides, herbicides or

soil nutrients, a ‘Slugbot’ for catching the slugs and a mushroom picking robot (Yaghoubi *et al.*, 2013).

Grimstad and Johan (2017) designed a modular reconfigurable mobile robot, ‘Thorvald II’, to enable a low cost, light weight and high quality robot for agricultural domain. The system used a reconfigurable aluminium frame and different modules to make it a multipurpose and multi-sized robot. It could carry 200 kg payload and had four-wheel drive and four-wheel steering configuration using 48V lithium battery. All components of the robot like on-board computer, motor drivers, and battery were connected each other by CAN open network. The robot performed well during the field test at different environments.

2.4.1 Weeding

The potential yield of the crop would be affected by several biotic and abiotic stresses. Weeds and insects could decrease about 40% of World’s food production (Oerke and Dehne, 2004). In agricultural robotics, several weed control systems had been developed over last few decades in order to overcome the production loss (Perez *et al.*, 2000; Choi *et al.*, 2015; Obert *et al.*, 2016).

Bak and Jakobsen (2004) developed a robotic platform for mapping the weed population. The system comprised of a station, robotic platform and an implement for carrying out the agronomic operation. Communication between the station and robotic platform was achieved by means of wireless network. Transmission Control Protocol/Internet Protocol (TCP/IP) was the standard communication protocol used. The robotic platform was especially designed for row crops with 25 cm and 50 cm row spacing. It had a water tight compartment for mounting all electronic components. PC/104 system was used as the platform computer and the motion of the platform was controlled by the computer software based on LiNUX operating system. It ensured the real-time execution of the task. All the electronics components and the embedded controller controlled the robotic platform. Four wheel steering was introduced to provide a highly flexible robotic platform. Since all the four wheels were steered, wheel slip got

reduced and allowed a parallel displacement of the vehicle while turning. The experiment showed that the platform followed the predetermined path and maintained fixed orientation relative to the path.

Patnaik and Narayanamoorthi (2014) proposed a weeding robot using image processing technique. This four wheel drive robot was driven by four high torque DC servo motors having 100 RPM and employed with skid steering mechanism in order to make it robust for semi-cultivated field. It was controlled by Arduino Mega microcontroller which was interfaced with the motor via L293D motor driver circuits and XBee modules were used for wireless communication. A rechargeable battery (12 V, 3 Ah) was used to power the robot. Weeding was achieved through 2 blades fixed on the gripper mechanisms at the front of chassis which was driven by a DC motor. For weed detection, a static camera was used for capturing the images and thus employed with an image processing technique using NI VISION in LAB VIEW software with which the characteristics of weeds were defined for further detection. Hence, the location and coordinates of the weeds were identified and sent to the microcontroller for activating the navigation and weeding via XBee modules. This robot could help in reducing the farming cost, saving a lot of time and also increasing crop production.

Sujaritha *et al.* (2017) designed and developed a weed detecting robotic prototype using Raspberry Pi microcontroller. The other components for weed detection included cameras, light sources and motors with power system. Weed detecting mechanism was carried out using Raspbian operating system and python programming language. An image classification system has been developed for extracting the leaf texture and fuzzy real-time classification techniques were employed for achieving the weed detection. Inter-row images were captured and processed by using an intex IT-105 web cam (3264 x 2448 resolution) and crop-row images were acquired by using Raspberry Pi camera (2592 x 1944 px). This Pi camera supports 1080p, 720p and 480p videos with 30-60 frames per second. After weed detection process, the weed removal was carried out by the prototype using a total of seven DC motors. A set of two motors were used to drive the rotavator, one for spinning the rotavator and other for raising and lowering the rotavator. Another

two motors were used for driving the robot which was controlled by PIC 16F877A microcontroller with embedded C program. The other three motors were used for the movement of robotic arm controlled by another PIC 16F877A microcontroller with embedded C program. The output from the texture algorithm may be either crop or weed. When the output was crop, navigation continued and the robotic arm stopped working. If the output was weed navigation stopped and the robotic arm started working. In the colour based algorithm, if the output was green then the rotavator got lowered for weed removal. If the output was yellow the robot will take 90° right turn and if output was blue then robot turns 90° left. The prototype was tested in sugarcane field and gave 92.9 % overall accuracy and 0.02 s processing time.

2.4.1.1 In-row weeding by robots

The weed removal in between the crop rows was achieved by flaming, spraying, row-harrowing or by using manual or powered weeders. But in-row weeding was a great challenge among the farmers. In transplanted crops, in-row weed removal could be achieved by vision-controlled in-row harrowing using Robovator, Steketee IC weeder or Garford Robocrop In-row weeder or by selective spraying of herbicides/weedicides using robots under Ecorobotix or Blue River Technology Company. The Drop on Demand (DoD) spraying system was employed in which the weeds were detected within the crop row and selectively sprayed the herbicides (Slaughter *et al.,* 2008; Fennimore *et al.*, 2016).

Utstumo *et al.* (2018) designed the 'Asterix' robot with a highly specialized tool for in-row weed control based on DoD system. They focused on a light weight robotic platform having a gross weight under 300 kg, in order to reduce the soil compaction and human-robot interaction risk. An operating speed of 0.8 m/s was selected for the robot which provides uniform area coverage and proper timing requirements for DoD system. GPS modules and Omnivision 46824MP sensor (camera) was used for row detection and CAN bus modules had been connected to the computer for providing necessary operational commands to control the robot. Each weed was detected separately using

machine vision system and treated separately without affecting the crop using DoD system. This system resulted in the reduction of herbicide use and its exposure to the operator.

2.4.2 Spraying robots

Robotic spraying is a precise operation in which the spraying liquid is saved with simultaneous prevention of health hazard due to direct exposure of the operator to the chemical. Sammons *et al.* (2005) constructed an autonomous mobile robot for pest and disease control in greenhouses. Its modular design enabled to perform various agricultural tasks. The drive system comprised of a worm gear motor driven by high power PWM controller board, which took all input and output signals from on-board microprocessor. The mobility of the platform was controlled by using Platform Control Program which had monitored the robot speed and sensor inputs. On-board microprocessors would electronically control the spray system by receiving the input signals from Infra-Red sensors placed at downside of the robot. The pump got turned ON/OFF when the robot passes over the reflective lines on the field in order to enable selective spraying. Web hosting ability of microprocessor allowed monitoring and controlling of the robot from any remote location. The platform could navigate through the field and spraying system could evenly cover the plants efficiently.

Similarly, Ogawa *et al.* (2006) developed a robot for spraying chemicals in vineyard. The robot was employed with crawlers for its movement since the field was not tilled. A manipulator having five DoF was applied in the system with spraying end-effect or at its end. Manipulator consisted of prismatic joint mechanism in order to work at high speed using a simple control method. The plants would be sprayed uniformly with certain quantity of chemicals per unit area. A constant distance was maintained between the spray nozzle and the target by controlling the manipulator, based on the distance information from the ultrasonic sensor, in order to spray the target uniformly. The experimental results revealed that a precise spraying operation could be achieved and

recorded by this robot system so that an optimum management of chemicals would be achieved.

Aishwarya *et al.* (2015) developed a robotic vehicle for spraying pesticides on crops. It consisted of a micro-controller board, programmed using embedded C software to control the movement of the robot with the help of a transmitter (joystick) and a receiver. A wireless camera mounted on the top of the vehicle helped in its guidance. Sprinkler motor with PID controller was used for spraying. This cost effective robotic vehicle could aid in improving productivity, safety in agricultural operations and also met the labour demand.

Oberti *et al.* (2016) performed selective spraying in grapevines for disease control using a modular agricultural robot. The system comprised of a modular CROPS manipulator (arm) with 6 DoF, disease sensing unit and precise spraying unit with end-effector. Multispectral images of the canopy were acquired using 3-CCD, R-G-NIR camera (1912-1076 pixel and 8 bit) for sensing the diseases. The system consisted of PC for data acquisition from camera, unit for real-time image processing of multispectral images, target position computation, manipulator control computer and spraying control unit. The real-time control unit was hosted on Central Control Unit (CCU) which was a standard PC with CAN interface board. The robot was installed on a wheeled platform on which an absolute encoder was mounted for high resolution positioning. The experiments conducted on different vineyards showed that the robot was able to treat 85-100% of disease affected area with 65-85% pesticide reduction.

Adamides *et al.* (2017a) presented the design aspects of a semi-autonomous tele-operated agricultural robotic sprayer developed from a general purpose mobile robotic platform. For this purpose several modules like mobile robot platform, electric sprayer, robotic arm, various robotic actuators and sensors were adapted and integrated. The user interface consisted of different components viz main frame for camera representation, sonar sensor indicators, battery sensor indicators, operation mode control buttons and camera control buttons. Different modes of operation were achieved with operation mode

control buttons. In the electric sprayer, a stable nozzle was provided for mass spraying. So the end effector (nozzle) was attached on a low cost, light weight robotic arm for getting targeted spraying. Modbus IO was an Ethernet communication system connected directly to the robot's battery. PC keyboard and PS3 gamepad controller were the input devices for remote operation of the robot, which was programmed to send ON/OFF command to the sprayer through Modbus IO. The controller was connected through Wi-Fi and a PC Keyboard was added as an alternative for input devices in order to solve the limited distance communication of PS3 gamepad controller. Small size of the robot and the sprayer tank were the limitations of this system for large vineyards.

2.4.3 Harvesting

Harvesting is one of the most demanding and challenging tasks for agricultural robots. The research activities on harvesting orchard and open field crops such as apple, cucumber, citrus, tomato, watermelon, cotton etc. were started over last three decades (Ceres *et al.*, 1998; Ceccarelli *et al.*, 2000; Bulanon *et al.*, 2009; Cui *et al.*, 2013). Several robots were designed for selective robotic harvesting in fruits and vegetables. Cho *et al.* (2002) developed a lettuce harvesting device consisting of machine vision system, fuzzy logic controller, photoelectric sensors, air blower, feeding conveyor, 3-DoF manipulator and an end effector. The field test showed 94% harvesting efficiency with a cycle time of 5s per plant.

Advancement and integration in sensory systems and related algorithms had modified the robotic technology for harvesting (Yuan *et al.*, 2009; Irie *et al.*, 2009; Arefi *et al.*, 2010; Mehta and Burks, 2014; Luo *et al.*, 2016). Hayashi *et al.* (2010) developed a strawberry harvesting robot with an objective to overcome the problems in robotic harvesting like low success rate, difficulty in fruit detection, fruit damage, less work efficiency and higher cost. The system composed of a machine vision unit, cylindrical manipulator, end-effector, storage unit and a travelling unit. Machine vision system consisted of three aligned CCD cameras and five light sources with 120 LED's each. The central camera would calculate the inclination of the peduncle while 3D position of the

fruit was determined by other two cameras. After positioning the target fruit, it got grasped by the end-effector and cut the peduncle to avoid fruit damage. Field test resulted that machine vision unit could detect 60% of the target fruits for harvesting. The successful harvesting time (from detection to cutting) of a single fruit was found to be 11.5 s.

A robotic device with image-based vision servo control system was developed for apple harvesting by Zhao *et al.* (2011). It consisted of a manipulator with 5 DoF and for simplifying the control strategy it was optimized geometrically to enable quasi-linear behaviour. The spoon shaped end effector with pneumatic gripper could harvest 77% of apples at a harvesting time of 15s per fruit.

Davidson *et al.* (2016) presented a robotic system for apple harvesting in which harvesting was achieved by means of a robotic arm. The movement of the arm was actuated by NEMA 23 bipolar stepper motors and digital output board with Windows C++ API was used to control the motor. The arm had an “elbow-up” configuration for getting the catching position. Robotic arm was assisted with machine vision system to detect and locate the individual fruit and picked up the fruit based on some harvesting criteria like maturity, size, colour etc. The robotic system was equipped with grasping end effector in order to minimize the fruit damage.

2.4.4 Multipurpose robots

Noguchi and Barawid Jr. (2011) introduced the application of robot farming system in Japan agriculture using multiple robots like rice transplanting robot, seeding robot, combine robot harvester, robot tractor etc. They developed one electronic robot vehicle and two robot tractors. Autonomous data acquisition and monitoring of crop was obtained through the robot vehicle. The robot tractor could perform various operations by attaching suitable implements to it. GPS and IMU sensors were the navigation sensors used for autonomous navigation which could be replaced with low-cost AGI-3 sensors also. In robot farming, the commands from the control centre were received by the robots and information was send via wireless LAN and packet communication. Thus the robots

had performed their desired operations accordingly. The real-time monitoring of the robot enabled to understand its current location and status. Details about the working robot would be obtained by clicking its own Robot ID to the computer. This robot farming system had contributed a lot to increase the crop productivity in Japan with minimum cost and labour.

Shivaprasad *et al.* (2014) designed a remote operated agricultural robot for seeding and fertilizing, controlled via internet. The robot could navigate to the destination, perform the agricultural task (seeding/fertilizing) and check the soil parameters like pH, temperature, humidity and moisture content using various sensors. Six DC motors were used for navigating the robot such that three would be activated at a time. Arduino ATMega 323 microcontroller controlled the system and acted as the brain of the project. Microcontroller was interfaced with DC motor with L293D motor driver circuit. The input data sensed by the sensors was processed by the controller and triggered the particular actuator to perform that particular task. Raspberry Pi on-board computer was used in remote control of the robot on the basis of live video captured by the camera. The LED got lighted when the seed/fertilizer tank became empty. The robot moved in proper direction and placed the seed/fertilizer at specified distance in the field according to the signal received from the microcontroller.

Xue *et al.* (2017) developed a multipurpose robotic platform with modular attachments for interchangeable modules to achieve spraying and weeding. A sensing unit, control unit, actuating unit and mobile platform were the major parts of this robot. The sensing unit acquired necessary information for navigation and operation through sensors such as vision, encoders, gyro, laser radar etc. The sensed information was processed by Basic ATOM Pro 40m microcontroller for producing the output command to the robot for its motion and field operation. Field operations were carried out by the actuating unit consisting of elevating-translating mechanism and an actuating tool for each operation. This actuating unit was installed at the middle of the robot frame. The four identical wheel modules of the robot was composed of wheels along with the frame and it was differentially steered by four geared DC motors in such a way that two motors

on same side shares one motor driver. The overall dimension was 1200 mm x 780 mm x 970 mm with a wheel base of 740 mm. The robot was electrically powered by 24 V battery. Machine vision sensors were used for row guidance and also for detecting the operation tools along with the combination of other sensors. The preliminary test showed that the robot travelled well in the field with a lateral error of 47mm. The spray capacity was found to be 16-20 plants/min and weeding was achieved in time. Since different operations could be achieved on the same platform, the robot was found to have high adaptability and versatility.

Similarly, a multipurpose autonomous agricultural robotic vehicle for ploughing, seeding, levelling and irrigation system was developed by Sowjanya *et al.* (2017). The system was wirelessly controlled by Bluetooth technology operated through Bluetooth app from an Android smart phone. The robot had four wheel chassis where only the rear wheels got powered using DC motors. DC motors, Bluetooth module, ploughing unit, seeding unit, levelling unit and water spraying unit were interfaced to the AT89S52 microcontroller through L293D motor drivers. The software was embedded with C programming. Once the Bluetooth was paired, the robot would move and perform various operations according to the applied command and program loaded to the microcontroller. This multipurpose robotic vehicle could ensure proper irrigation and efficient resource utilization without human intervention.

2.4.5 Monitoring and Surveillance

Kulkarni *et al.* (2014) proposed a remotely controlled surveillance robot via internet. The robot consists of an Android Smartphone, Arduino microcontroller, remote controller and necessary hardware like chassis, DC motors, motor drivers, power supply unit etc. Android phone acts as a communication link between the remote controller and the Arduino microcontroller which was accomplished by running two separate apps simultaneously on the phone. First app was a freely available android app called ‘IP Camera’ for live video transmitting feedback to the remote controller and the second app for receiving the control signal from the remote user and sending it to Arduino

microcontroller. The control of direction of travel of the robot based on visual feedback from the Smartphone was achieved during testing. Similarly, Dixit and Dhayagonde (2014) proposed a wireless control of e-surveillance robot through internet for video monitoring and living body detection using camera and Pyroelectric Passive Infrared (PIR) sensor.

Bokade and Ratnaparkhe (2016) described the method for controlling a wireless surveillance robot using a Smartphone. Two DC motors were used for the movement of the robot which was connected to the Raspberry Pi board control unit via L293D motor drivers. The camera installed on the robot would capture live video and servomotors were used for the tilt motion of camera to get a wide capturing area. 12 V battery was used to power the components of the robot. Smartphone and robot control unit was connected to Wi-Fi. The video streaming was done using MJPG streamer program. The IP address allocated to the web server was initialized by the control unit and established a connection with LAN. As it was connected, the robot started video capturing and thus moved according to the wireless command received by the Pi board from the android smart phone. A quick and good quality video was obtained during field experiments. The result indicated that the use of smart phone rather than computer or laptop made the system reliable and easy to use.

Azeta *et al.* (2019) developed a cost effective android based mobile robot for surveillance applications. The mobile robots were navigated through the field for monitoring and other surveillance purposes where humans could not reach. The experimental results showed the varied flexibility of the mobile robot to avoid obstacles and got a communication range of 50 m which was good enough for many surveillance applications.

2.4.5.1 Monitoring robots

Monitoring of crop as well as environment would help to collect information for decision making about plant production actions like weed control, insect control, fertigation, irrigation etc. (Ortiz and Olivares, 2006). Kim *et al.* (2014) proposed a new

wireless sensor network with autonomous robot platform for real-time monitoring of agriculture. The atmospheric parameters like temperature, humidity, gas, and illumination got monitored by the robot. The robotic platform consisted of two wheels for its motion and could move at maximum speed of 30 cm/s. The system was controlled by using ATmega128L processor where the sensor modules were connected and ran on TinyOS software. The sensor modules in the system had gathered the information from the field. This study could demonstrate the wide application of Wireless Sensing Network (WSN) technology with mobile robot system for agricultural monitoring.

Kajol *et al.* (2018) proposed a model called Automated Agricultural Field Analysis and Monitoring System (AAFAMS) using IoT. AAFAMS was a line follower robot, based on Raspberry Pi, in which arrays of IR sensors would detect the black line and move along that line. Soil moisture sensors in the system could monitor the soil moisture at every 100 m distance and this information was stored at SQLite database in the cloud. The presence of pests was analysed through image processing technique using a camera and was send to the drop-box in the cloud. The analogue input from the sensor was taken by IC PCF8591P and the output in digital signal form was given to Raspberry Pi. For motor driving, two L293D IC's were used. All the stored data from the cloud was retrieved by the system for processing the moisture content and pest information in order to give required advisory to farmers through an Android application. The system was powered by either battery or a solar panel and could become an efficient and smarter way of monitoring the field.

Ramesh and Pasupathy (2019) designed an agricultural robotic platform for environmental monitoring using remote sensing techniques for precision agricultural application. The field data collected by the robot using sensing unit was sent to the central server which got further forwarded to a multifunction farmland mobile app for real-time farmland monitoring. Arduino mega based on ATMega 2560 microcontroller was the central control unit used. Environmental parameters were obtained via sensors like soil moisture sensor, digital humidity and temperature sensor, MQ 137 sensor and light intensity sensor. In this remote data collection system, Apache and MySQL databases

were used, which ran on ‘Virtual Machine’ using ‘Ubuntu 14.40’. The experiment was conducted with the robot in real world environment and results showed that the system was more suitable for real-time precision agricultural applications.

Materials and Methods

CHAPTER III

MATERIALS AND METHODS

In most of the developing countries, intercultural operations are carried out by human labourers and it is a tedious process. The availability of human labour is also declining tremendously. The scarcity of farm labour could be rectified by the establishment of mechanization and automation. Now, modern agriculture is focused on the development and utilization of autonomous technologies as it can address the problems like labour shortages, higher labour costs, lower crop productivity, higher investment, and operational costs. The agricultural farm vehicles are getting automated for the past few years and several agricultural robots (agrobots) were also developed to perform various agricultural operations. The concept of agrobots is becoming popular because of their wide range of applications. But still, the higher initial investment has always been a limiting factor in their usage among the small and medium farmers, especially in India. Hence a robotic platform, capable of providing all the advantages of agrobots at reduced cost could boost the pace of advancement of Indian agriculture. Therefore, this investigation was undertaken aiming at the development of a semi-autonomous robot capable of performing intercultural operations in row crops. The methodologies adopted for the design and development of this prototype are detailed in this chapter.

3.1 Agronomic characteristics of the vegetable crop cultivated in rows

A self-propelled robotic platform was conceptualized as a basic rover capable of performing intercultural operations on vegetable crops cultivated in rows. Chilli (*Capsicum annuum*) was the representative vegetable crop considered for the prototype development. Some of the chilli varieties developed by Kerala Agriculture University included *Anugraha, Jwala, Jwalasakshi, Jwalamughi, Manjari, Ujwala, White kanthari* etc. *Serra* is one of the hybrid variety normally cultivated in Kerala. The agronomic characteristics of chilli commonly cultivated in Kerala, relevant to the requirements of intercultural operations are given in Table 3.1 (KAU, 2011).

Table 3.1 Agronomic characteristics of chilli

Variety	Row-to-row spacing (cm)	Plant-to-plant spacing (cm)
Less spreading varieties	45	45
Spreading varieties	75	45-60

Usually, the seedlings are raised in the nursery and 4-5 weeks matured seedlings are transplanted to the main field. They are being planted on ridges/level lands during rainy season or in shallow trenches during summer. Intercultural operations are carried out at different growth stages of the crop. The plant protection chemicals are applied to the crop at its various growth periods according to the requirement i.e., after 10-15 days of transplanting, at the time of flower initiation, 10-15 days after flowering and at full growth period. The plant height will be changing throughout its growth period and the maximum plant height may vary according to the crop variety cultivated. Five plants from each crop varieties *Anugraha, Ujwala and White kanthari* were selected randomly and the plant height at its various growth stages was recorded for determining the maximum height. These agronomic parameters could define the dimensions of the robotic platform.

3.2 Design considerations for the development of semi-autonomous robotic platform

A semi-autonomous robotic platform was conceptualized for performing the intercultural operations on crops cultivated in rows. The platform would be required to move through the space between the rows and perform the intended operations like spraying. It should be capable of navigating within the field and performing the intended operation according to the user command. A wireless remote controller could be used to transmit the control signals from the operator and the signals received by the robot would be processed, via a microcontroller unit, for achieving the output functions. The dimension of the platform was decided in consideration with the agronomic characteristics of the crop. The number of crop rows to be covered and the row spacing

would determine the track width and the plant height would indicate the ground clearance to be provided for the chassis. The framework should also have a provision to adjust the wheel track to operate within different crop varieties with different row-to-row spacing. As it was expected to move through the inter row spacing, the wheel width should be less than the row spacing.

The functional unit composed of the user interface, signal processing unit (microcontroller) and end effectors. The input from the user would be transmitted to the robotic system via a remote controller. Two types of input signals was expected to be used, one for motion control and the other for controlling the operation unit. The signals received were required to be processed by a microcontroller unit for accomplishing the output functions. The robot could execute the motion control in forward, reverse, and turn on both left and right side directions using drive motors and the end effector. Similarly, in the operation unit, a provision for adjusting the position of functional components (such as boom in the case of a sprayer) should be provided along with the control of the operation unit (spray pump).

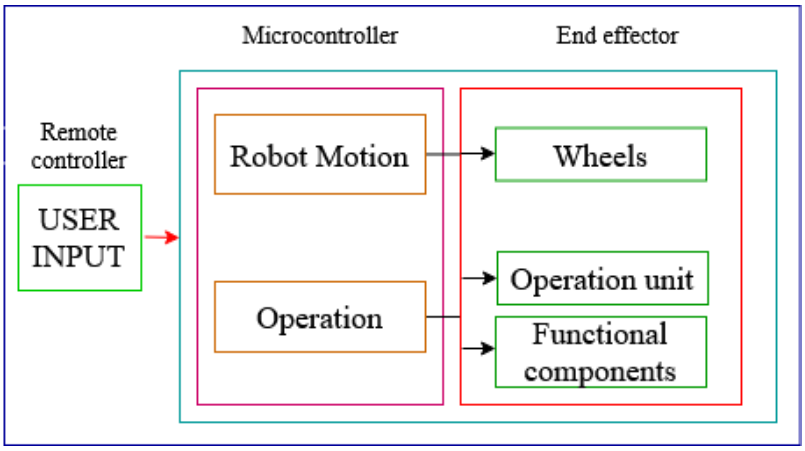

Fig. 3.1 Flow chart of functional unit of the system

3.3 Design of semi-autonomous robotic platform

The design of semi-autonomous robotic platform included the design of the chassis, selection of drive wheels, sizing of drive motors, and design aspects for the selection of functional components. The sequential design of the unit is detailed in the following sections.

3.3.1 Design of structural frame of the chassis

The structural frame of the chassis was envisaged to be capable of accommodating all the functions and handling all the resultant forces during field operations. In order to meet these requirements, the frame should be strong enough with minimal weight. The dimensions of the chassis would be decided relative to the agronomic characteristics of the selected crop. The platform was designed to operate over three crop rows, with 45 cm row-to-row spacing, in its single pass. Hence the maximum working width of about 135 cm should be provided to the chassis. As the robot was designed to operate over the crop, a minimum ground clearance of 100 cm should be provided to the chassis; because the maximum plant height was approximated to an average of 100 cm. For better stability and mobility of the platform, it was conceptualized as a rectangular carriage supported by six legs, three on each side. It was planned to provide a wheel-mounted geared motor on each leg for the self-propulsion of the platform. The movement of this six-wheel-drive robot in the field would be achieved in the space between crop rows. Six-wheel independent drive mechanism was considered to have better stability and performance for off-road manoeuvring and obstacles overcoming than four-wheeled configuration (Prasad and Ma, 2019).

The framework of the chassis should have a provision to adjust the wheel track to operate within different crop varieties with different row-to-row spacing. To adjust this track width each leg of the chassis should be attached to the frame via threaded rods, instead of a direct welded connection. Hence the adjustment of the leg would be possible within the lead screw length provided. It was designed to provide a 30 cm extendable length adjustment for each leg. Therefore, the wheel track of the chassis would vary from a minimum of 75 cm to a maximum of 135 cm. For ensuring better stability, the working width should be higher than the length of the chassis. Hence, a rectangular carriage having a length of 135 cm and breadth of 80 cm was suggested for the chassis. Thus the basic dimension of the chassis was selected as 135 cm × 80 cm × 100 cm. Structural stability could be improved by providing supporting members over the top of the carriage. It was also expected to help in the arrangement of all functional components

over the chassis. Galvanized iron tubes were selected for fabricating the chassis as this material was low cost and met the strength requirements.

3.3.2 Selection of drive wheels

As the wheel moves on soil it will result in wheel sinkage as well as deformation of the soil due to the Rolling Resistance (RR) acting horizontally. The soil strength is the maximum amount of force the soil can withstand without failure. It may vary depending upon the soil conditions including the type of soil, pore-volume, pore size distribution, moisture content, etc. Cone penetrometer is the device used to estimate RR. Cone index ($kgcm^{-2}$ or kPa), an index of soil strength, obtained from the device has great influence on RR (Wismer and Luth, 1974). From equation 3.1 and 3.2, it was understood that RR was dependent on soil strength, wheel characteristics and load acting on the wheel (Maria and Ishii, 2019).

$$C_n = \frac{CI * b * d}{W} \quad \text{....Eq. 3.1}$$

$$RR = W(\frac{1.2}{C_n} + 0.04) \quad \text{…. Eq. 3.2}$$

Where,

C_n = Wheel numeric

CI = Cone Index

b = wheel width, mm

d = wheel diameter, mm

W = Load acting on the wheel, kg

Soil-wheel interaction depicts the relationship between the soil conditions, the performance of the wheel, and its design parameters. The better characterization of soil-wheel interactions for the terrestrial vehicles was achieved from the terra-mechanics relations (Bekker, 1956). The pressure-sinkage characteristics and shear displacement characteristics describe the vertical and horizontal soil deformations, respectively.

According to Bekker's formula, the pressure-sinkage relationship (Chen *et al.*, 2018) is given as,

$$p = (\frac{k_c}{b} + k_\emptyset)z^n \quad \text{…. Eq. 3.3}$$

Where,

p = pressure generated at the contact point (compressive force), Pa

k_c and $k_\emptyset$ = cohesion and friction modulus of soil deformation

z = wheel sinkage, mm

b = width of wheel, mm

n = sinkage exponent

The Janosi's formula satisfying the relationship between shear stress and soil deformation, as proposed by Zhu *et al.* (2012) is given below:

$$\tau = (c + ptan\emptyset)[1 - e^{-(\frac{j}{k})}] \quad \text{…. Eq. 3.4}$$

Where,

τ = shear stress, Pa

j = soil shear displacement, mm

k = horizontal shear modulus of soil

c = soil cohesion

$\emptyset$ = angle of internal friction of soil

Table 3.2 Approximated values of geophysical properties of soil (Wong, 1993)

Soil type	**Moisture content (%)**	***N***	k_c	$k_\emptyset$	***C***	***Ø***
Dry sand	0	1.10	0.1	3.9	0.15	28°
Sandy loam	22	0.20	7	3	0.2	38°
Clay	38	0.50	12	16	0.6	13°
Heavy clay	40	0.11	7	10	3	6°
Lean clay	22	0.20	45	120	10	20°

When the compressive force acting on the wheel contact point exceeded the soil strength, the soil got failed and resulted in soil deformation and wheel sinkage. The amount of wheel sinkage depends upon soil properties, the load acting on the wheel, and the dimensions of the wheel. The required torque and wheel variables of a mobile robot have to be very specific. The dimensions of the wheel were assumed in consideration with these fundamental equations of terramechanics.

3.3.3 Technical requirements of the robotic platform

While designing a rover, there exists a trade-off between the gross weight of the rover (kg), drive motor torque (N-m), and battery capacity (Ah). The gross weight has a considerable influence on the selection of drive motors. With an increase in gross weight, the net torque required for driving the robot has to be increased. These will result in higher power consumption, and thus the battery capacity has to be improved.

3.3.3.1 Estimation of gross weight of the robot

The gross weight of the robot was composed of the dead load and the payload acting on it. The dead load included the weight of the structural framework, weight of drive motors, battery, electronic components and other supporting accessories while the payload included the weight of spray liquid and the sprayer unit. The estimated gross weight of the robot was given in Table 3.3.

***Dead load estimation*:** The weight of chassis, drive motors, battery, control unit, and all other functional components were contributing to the dead load. The dead load due to the chassis has been estimated after determining its dimensions and the weight of the material used. Galvanized iron tubes used for the construction of the chassis had variable weight depending upon the material cross-section and thickness. However, an optimum strength to weight ratio would be maintained always. Based on the conceptual design of the chassis, the chassis weight was approximated to a maximum of 20 kg. Weight of components were also approximated at its maximum and given in Table 3.3.

***Payload estimation*:** The payload due to the spray solution depends upon the tank capacity, which would be determined from the amount of spray discharged over the time

period. If AR is the application rate of the spray liquid in Lha^{-1}, v is the velocity of travel in ms^{-1} and w is the width of operation in meters, then discharge per unit time (Q) will be, (Kepner *et al.*, 1982),

$$Q = w * v * AR$$

…. Eq. 3.5

The normal application rate of any spray liquids (plant protection chemicals like pesticides, fungicides, insecticides, etc) for chilli is 500 Lha^{-1} (KAU, 2011) with conventional manually operated sprayers. The design considerations assumed for the calculation of spray volume includes:

- The velocity of travel for the robotic platform - 0.2 ms^{-1}
- The width of the spray boom - 3.35 m
- Number of nozzles - 5
- Nozzle discharge rate - 0.25 L per minute

Thus the total discharge of spray liquids per unit time would be $5 * 0.25 = 1.25\ L\ min^{-1}$. Area covered per unit time was calculated as 0.24 hah^{-1}. Therefore the spray volume, required to achieve a total discharge of 1.25 $Lmin^{-1}$ over unit area, was calculated to be 312.5 Lha^{-1}.

If we need to carry spray liquid for 0.2 ha, we need approximately 63 L as tank capacity. An increase in the payload necessitates a much heavier chassis, which will result in higher torque requirement as well as higher power consumption for the platform mobility. It will impart complications for a battery-operated robot. Therefore, the tank capacity was restricted under a safe limited value. In order to meet the spray demand over an area, with this limited tank capacity, either the number of fillings can be increased or more precise application of spray can be employed. Hence, a maximum design volume of 10 L was assumed to provide for the spray tank. It could reduce the payload exerted on the platform and can improve portability. Therefore, the maximum payload due to the weight of the spray solution was taken to be 10 kg. All other payloads were approximated at its maximum value for a safest design.

Table 3.3 Estimated gross weight of the robot

Components	Weight (kg)
Structural frame	20
Drive motors and wheels	6
Battery	10
Electronic components	3
Spray liquid	10
Sprayer unit accessories	6
Total	**55**

3.3.3.2 Criteria for selecting drive motors

One of the important aspects in consideration for the development of a mobile robot was the selection of drive motors. The parameters to be considered for sizing the motor included:

1. Gross weight of the robot (m)
2. Velocity of the robot (V)
3. Wheel diameter (d)
4. Traction characteristics

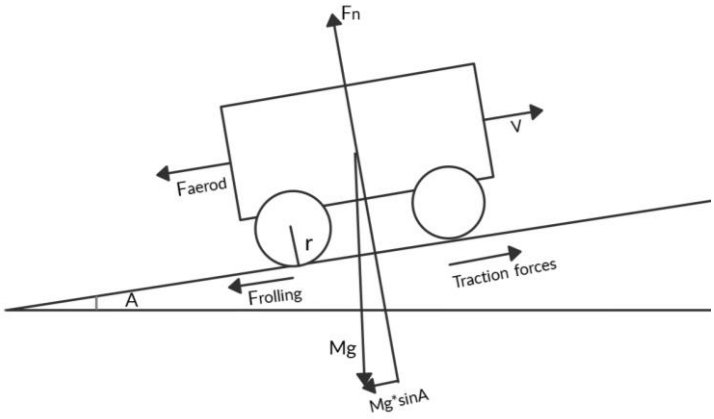

Fig. 3.2 Forces acting upon robotic platform moving on a terrain

The forces acting upon the robotic platform moving on a terrain was represented in the Fig. 3.2. According to the force balance equation, the net force acting on a moving vehicle is the sum of forces due to rolling resistance, gradient, acceleration and aerodynamic drag.

$$F_t = F_r + F_a + F_g + F_d$$

…. Eq. 3.6

Where,

F_t = Total force, N

F_r = Force due to rolling resistance, N

F_a = Acceleration force, N

F_g= Force due to gradient, N

F_d= Force due to aerodynamic drag, N

The rolling resistance is the resistance offered to the wheel when it comes to contact with the medium (soil). The force due to rolling resistance,

$$F_r = \mu * m * g * cosA$$

…. Eq. 3.7

Where,

μ = coefficient of rolling resistance

A = angle between the ground and the slope (usually taken as 10°)

Table 3.4 Coefficient of rolling resistance on various surfaces (McKibben and Davidson, 1940)

Surface	Coefficient of rolling resistance
Tilled soil/ Loose sand	0.2 – 0.4
Hard soil medium	0.04 – 0.08
Tar roads	0.02 – 0.03
Concrete	0.01 – 0.015

Acceleration force is the force required to accelerate the robot from its initial velocity.

$$F_a = m * a$$

…. Eq. 3.8

Where, a = acceleration of the robot, ms^{-2}

Gradient force is the force required to drive the robot up on a slope. It pulls down the robot on the slope due to gravity.

$$F_g = m * g * sinA$$

…. Eq. 3.9

The aerodynamic force is the force acted on the robot by the air due to the relative motion between the robot and air. Shape and area of the robot are the depending factors of aerodynamic force.

$$F_d = \frac{1}{2} * \rho * A_f * C_d * V^2$$

…. Eq. 3.10

Where,

ρ = density of air, kgm^{-3}

A_f = frontal area of robot, m^2

C_d = Coefficient of drag

V = Velocity of the robot relative to air, ms^{-1}

Hence the net tractive force,

$$F_t = (\mu * m * g * cosA) + (m * a) + (m * g * sinA) + (\frac{1}{2} * \rho * A_f * Cd * V^2)$$

…. Eq. 3.11

We know, Torque = Force * Perpendicular distance

$$\therefore \tau_{total} = [(\mu * m * g * cosA) + (m * a) + (m * g * sinA) + (\frac{1}{2} * \rho * A_f * Cd * V^2)] * \frac{d}{2}$$

…. Eq. 3.12

Torque on each motor, $\tau = \frac{\tau_{total}}{total\ no.\ of\ motors}$

The torque acting on each motor was calculated based on the above mentioned procedure. The suitable drive motors were selected on the basis of the torque-speed characteristics.

3.3.4 Design aspects of functional units of the semi-autonomous robotic platform

The functional units of the robotic platform were comprised of a drive mechanism, a real-time video transmission unit, a wireless control unit, a power supply unit, and a spraying unit. The selection of functional components is a decisive task because only the appropriate entity can regulate the intended operations of the robot. Suitable components for the functional units were selected according to the requirement as detailed in the following sub sections.

3.3.4.1 Drive mechanism

The chassis of the prototype would be adaptable for operating on various fields based on the different agronomic considerations. It should be strong enough to accommodate all of its functional units. The design dimensions of the platform were 135 cm × 80 cm × 100 cm. Since it has to operate over undulated terrain, a six-wheel drive mechanism with high torque geared motors was selected for ensuring better stability and steady movement. The selected drive mechanism consisted of drive motors with wheels, a microcontroller unit, and motor shields. The drive motor was selected based on the required torque-speed characteristics. The torque exerted by the motor should be higher than required torque. The movement of the robotic platform could be controlled by directing the rotation of drive motors using a pre-programmed microcontroller. An open source on-board computer, like Arduino or Raspberry Pi, could be selected for this project as they are small in size, programmable, good performer, support different programming languages, reliable, affordable and energy-efficient. The microcontroller and drive motors had to be interfaced with motor shields. The change in the direction of rotation of the motor could be accomplished by changing the direction of current through it with the help of these drivers. Usually motor drivers were enabled with both speed and direction control.

The skid steering mechanism was selected for the robotic platform because of its high manoeuvrability and robustness in motion. In skid steering, the wheels on each side of the robot should drive differentially for accomplishing a curved path or turn. If all the wheels on the left side were driven in the forward direction and the wheels on the right

side in the reverse direction, the robotic platform turn right about its centre with zero turning radius, and vice versa (Fig. 3.3). The advantages of skid-steering were simplicity in the driving system and increased traction due to multiple drive wheels on each side. The drawback of skid steering was the requirement of higher power and torque over other steering mechanisms due to kinematic constraints and complex wheel-soil interactions.

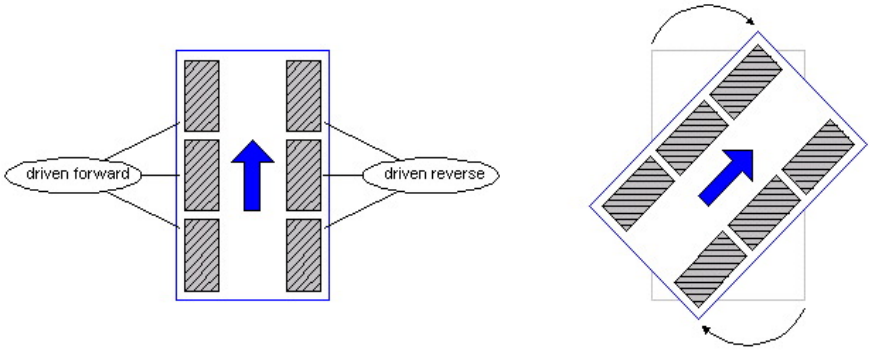

Fig. 3.3 Schematic representation of skid-steering mechanism

3.3.4.2 Wireless Control system

The autonomous or semi-autonomous robots are monitored, supervised, or controlled by the user/operator via wireless communication techniques. The wired connections make the control of a robotic system much complicated and thus limit its extensive application. Therefore, wireless communication systems are preferred over wired connections.

A wireless control system based on Radio Frequency (RF) protocol could be used in this project. A 2.4 GHz transmitter and receiver system would serve as the wireless communication system of the robotic platform. 2.4 GHz operating frequency band is a robust and most popular wireless communication network because of its advantages like lower interference, higher performance, safety, smooth data transmission and less power consumption over other frequency ranges. The transmitter-receiver would be connected each other via a unique ID for avoiding interference from noise signals. The user could transmit signals through a remote controlled transmitter. A receiver unit would receive the transmitted signals. In order to process these signals the receiver had to be connected to a microcontroller unit.

This wireless control system was expected to govern the robot's operations, viz, the forward movement, reverse movement, left-side turn or right-side turn of the robotic platform, switching ON/OFF the spray pump, lowering or raising of the sprayer boom unit, and bending or straightening of the sprayer boom.

3.3.4.3 Real-time video transmission system

The monitoring and the direction control of the robot could be accomplished with the help of a real-time video transmission system. Usually, the autonomous robots were equipped with navigational sensors like GPS, Laser Radar, LIDAR, Machine vision system, ultrasonic sensors, gyroscopes or combination of these sensors for achieving vehicle heading/navigation. For a semi-autonomous robot, the motion and direction control was carried out by human interactions, i.e., the user has to monitor the field conditions and control the robot accordingly. A Wi-Fi enabled camera could capture the video and enable the real-time transmission with its paired Android device. A two-way communication would be possible with this system. This could be used as a separate unit from the wireless remote controller.

3.3.4.4 Operational unit

The width of operation was one of the design considerations adopted during the development of the sprayer unit. The length of the spray boom would define the width of operation. A 3.35 m spray boom was considered for this design; which was also expected to improve the field coverage with minimum mobility of the platform. The sprayer unit was designed to be operated for spraying the liquid formulations over the crop. As the crop height may vary in its different growth stages, the height of spray had to be varied accordingly to the plant height. Therefore a provision for adjusting the boom position, as per the crop requirement, should be provided. Since the boom length was higher than the track width of the platform, there would be difficulty in turning or transporting the platform from one place to another. The boom had to be in its full span only during the operating condition. Therefore, a mechanism was required to be employed for the opening and closing of the spray boom. The position of the boom should be controlled as per the user commands. Therefore, this unit had to be integrated with the microcontroller

for processing the received signals from the remote controller. A simple and robust method for sprayer control was by means of relays with relay driver interfacing circuits.

The spray solution would be stored in two tanks having equal capacity. A sprayer pump had to be used for pumping the solutions from the tank. Necessary fittings should also be provided.

3.3.4.5 Power supply unit

All the functional components of the robotic platform could be powered by means of a battery. Suitable voltage regulators should be used for stepping down the input voltage, wherever necessary. The battery capacity was decided based on the total power requirement by the prototype. It was conceptualized for operating the platform for minimum of one hour. A provision for charging the battery could be provided when it got drained out.

3.4 Fabrication of the chassis

Fabrication of the chassis was accomplished as per the design dimensions. The selection of material for fabricating the framework was based on the consideration that the material should have the ability to carry a heavy load with minimum material weight. The material chosen for the structural frame was galvanized iron because it was having an optimum strength to weight ratio. Some of its features include higher reliability, durability, corrosion-resistance, easy to cut and weld, and anti-rusting property. Galvanized iron tubes with different cross-sections could be used for fabricating distinct members of the chassis. The mechanical properties of the material vary depending upon its cross-sectional areas. Rectangular tubes (16 gauge) of size 38 mm × 10 mm and square tubes (18 gauge) of size 25 mm × 25 mm were selected for fabricating the rectangular carriage and the legs of the chassis, respectively. Square tubes (16 gauge) of 12.5 mm × 12.5 mm was adopted for making the supporting members at the top of the carriage. The Fig. 3.4 depicts the conceptual design of the chassis.

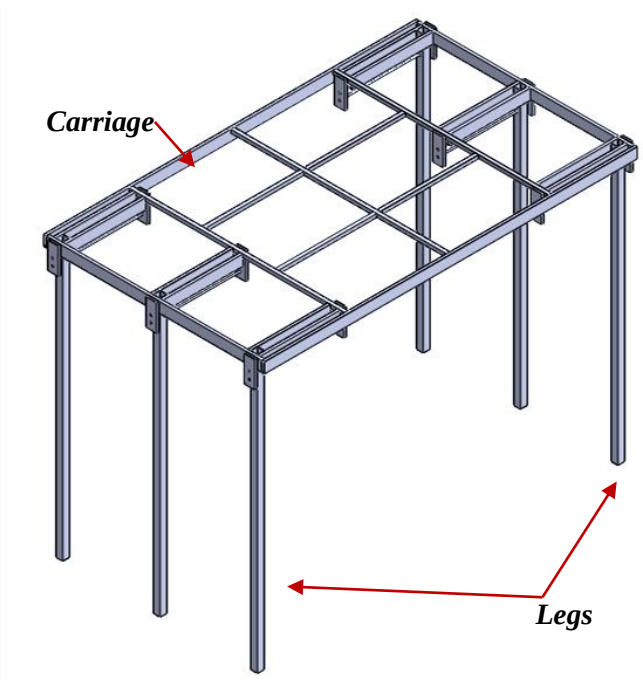

Fig. 3.4 Conceptual design of the chassis

3.5 Development of the prototype of semi-autonomous robotic platform

A conceptual design of a semiautonomous robotic platform was developed for the intercultural operations in row crops (Fig. 3.5). The basic robotic platform was intended to serve as a multipurpose platform by the attachment/detachment of suitable gadgets. Here, a spraying unit would be mounted on to the platform for the application of liquid plant protection agents. As the user could operate the robot from a safer distance, health hazards caused due to the direct exposure of spraying liquids could be avoided. The prototype was designed to operate in such a way that it could move through the crop rows and perform the spraying operation, according to the command from the operator. The operator could guide the robot as per the real-time-video streaming transmitted from the robot. All the operations of the robot could be controlled by the user via a remote control unit. The variable chassis of the rover platform could ensure various track width and allows the user to operate the platform accordingly with the agronomic characteristics of crops. Most of the agrobots are usually four-wheeled robots. A six-wheel-drive robot, equipped with high torque geared DC motors, was designed for carrying the loads and

providing better stability. All the functional units of the robot were properly assembled over the chassis for equal load distribution and sensible utilization of the space.

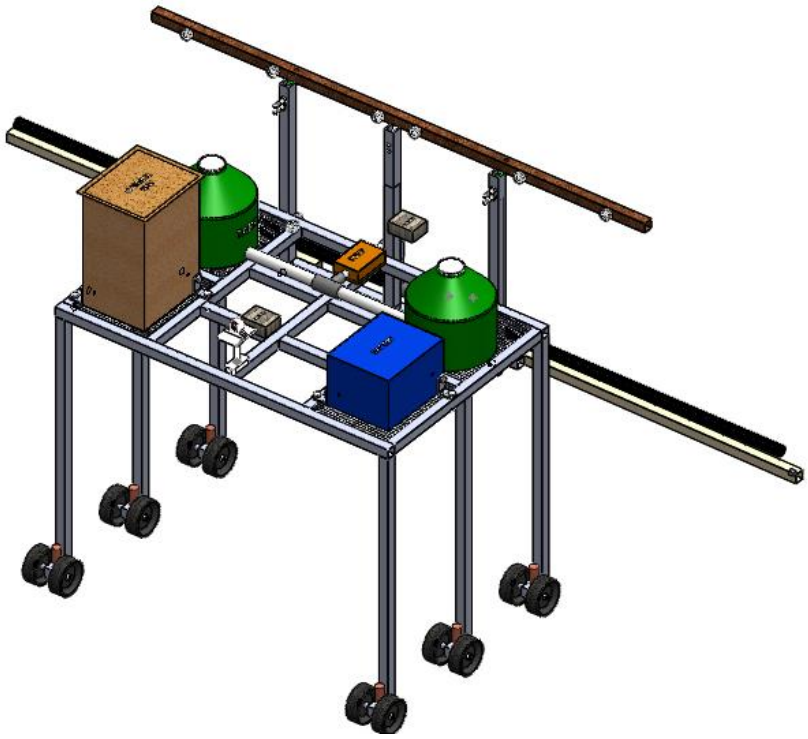

Fig. 3.5 Conceptual design of the prototype

3.5.1 Control unit of the robot

The principal control unit was the brain of the robot, consisting of a microcontroller or microprocessor board. It would be the principal functional unit of the robot where all the functions of the robot were controlled. The major functions of the control unit included motion control of the robot and spraying unit operation. The controller should be programmed using suitable software to process the commands from the user. The study on various microcontroller units helped for the proper selection of controller best suited to this project. All the supporting electronic units were selected accordingly to develop the control unit. Here the robot would be working wirelessly via a remote controller. The components of the control unit consisted of a wireless receiver unit, microcontroller board, voltage regulator, motor shields, relays and other minor electronic components. These should be properly connected to accomplish the indented operations. The Fig. 3.6 shows the block diagram of the control unit.

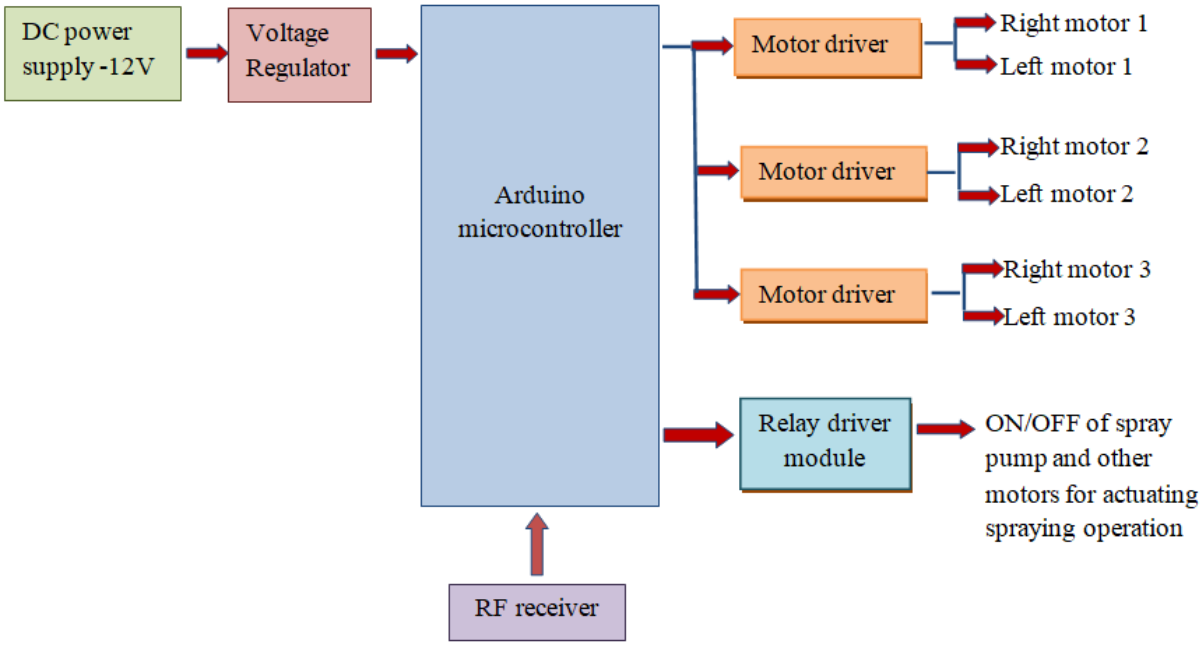

Fig 3.6 Block diagram of the control unit

3.5.2 Programming the microcontroller

After proper circuit connection of all hardware components, the microcontroller board had to be programmed. The major steps followed while programming the microcontroller were:

- Installation of the suitable software to interface with the hardware
- Development of the appropriate algorithm for the system
- Writing the computer code on the software using proper language
- Compilation of the program to remove errors
- Uploading the final program to the microcontroller via USB cable.

The algorithm defined the instruction for the processes and the order of their execution to solve a problem or computation. It helps to get an idea on how to write the computer program code directly on the Arduino environment and made it easily understandable. The Arduino microcontroller unit was programmed in the Arduino software (IDE) using C/C++ programming language. The Arduino working environment is shown in Fig. 3.7. The Arduino program should contain two main parts:

- **void setup ()**: At the start of every program, general instructions or the initialization of the program were provided under this function. This function was defined before the execution of the loop function.
- **void loop ():** Every statement under this function will be continuously executed when the microcontroller is turned on.

Arduino microcontroller should be programmed in such a manner that it could control the motion of the robot, switch on and switch off the spray pump, and move the sprayer unit according to the command given by the user through the remote controller. The system variables and its pin modes should be initialized first after starting the program. After setting up, the functions to be executed by the microcontroller would be defined. Control signals from the transmitter unit were received by the receiver unit, in connection with the microcontroller. Each channel of the transmitter was assigned for performing specified operations, as given below:

1. Left joystick up : Move forward
2. Left joystick down : Move backward
3. Left joystick right : Right turn
4. Left joystick left : Left turn
5. Left joystick at mean position : Stop robot
6. Switch on A (swA) : Spray pump ON
7. Right joystick down : Sprayer unit up
8. Right joystick up : Sprayer unit down
9. Right joystick right : Open spray boom
10. Right joystick left : Close spray boom

The received signals were read and analysed by the microcontroller and the function statement provided was executed. The motion control was accomplished with the motor drivers and sprayer control with relay circuits. Fig. 3.8 represents the flow chart of the prototype program.

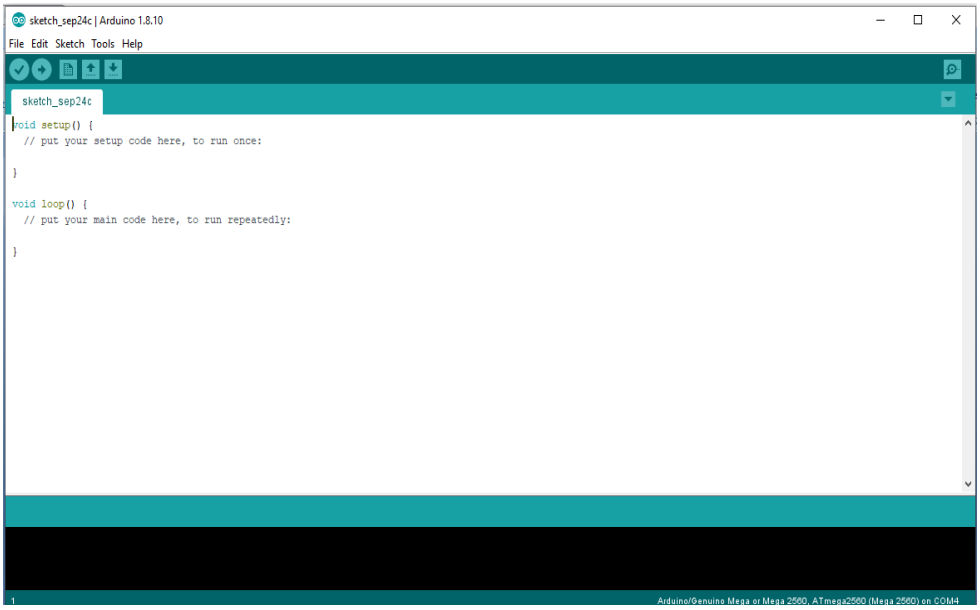

Fig. 3.7 Screenshot of Arduino working environment

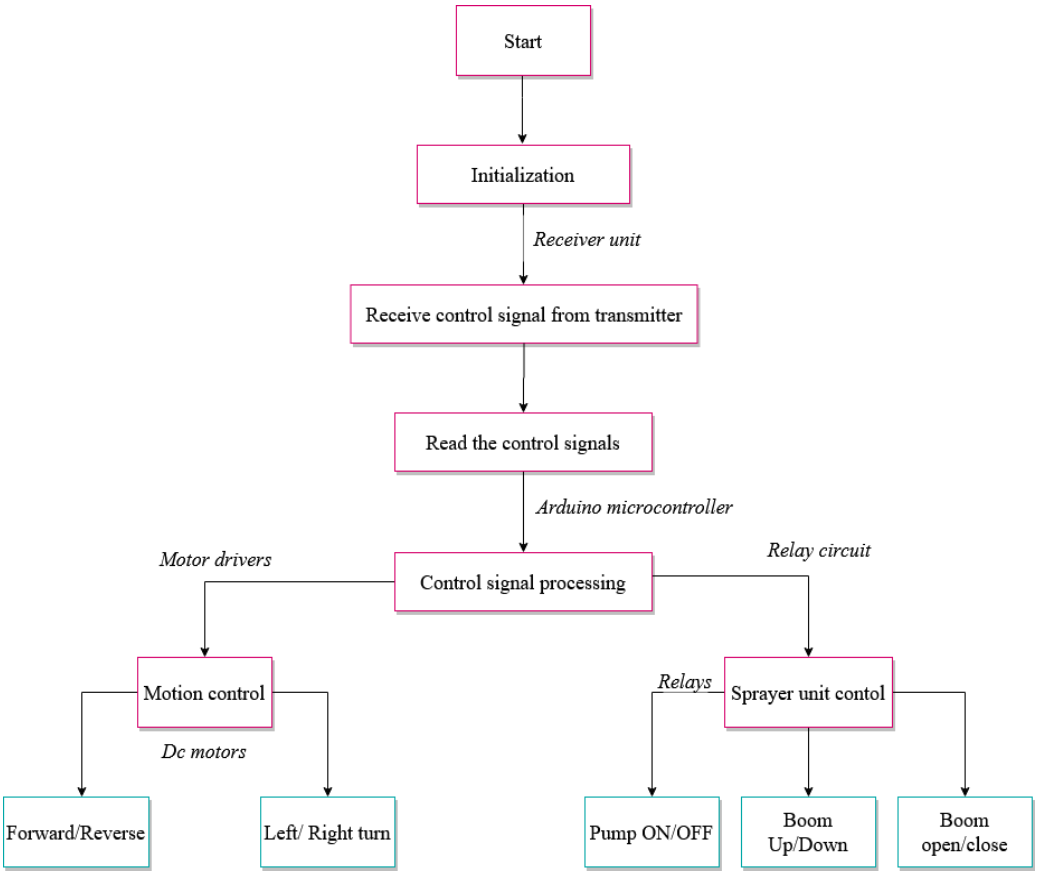

Fig. 3.8 Flow chart representing flow control of the prototype program

3.6 Operating procedure

The working of the robotic platform included the movement of the rover, real-time video streaming and the spraying operation. The operating procedures involved in the operation of the platform are given below:

- Uploading the programmed code to the Arduino microcontroller board after properly connecting all the circuits, for operating the prototype as per the commands.
- Connecting the entire system to the power supply unit (battery) indicated by the blinking of the LEDs in the circuit.
- Powering the six-channel transmitter (remote controller) using four 1.5V alkaline batteries. Before turning ON the transmitter, all switches on it was kept in OFF position.
- The transmitter wouldn't be armed at the initial state. Therefore, the right joystick has to trim (move) in upward direction for achieving the armed condition.
- Establishing the wireless connection.

After establishing the wireless communication, the user could command the robotic platform to perform the specified operations.

3.6.1 Real-time Video Streaming

A wireless IP camera was used for acquiring real-time video streaming from the robot through a mobile application, V380. The camera needs to be mounted at the front of the platform, for ensuring a maximum wide-angle view, using suitable fittings. It should be connected to the power source. The reset button should be pressed to reset the default settings. The camera had to be configured with the mobile application. The steps to be followed were:

- Turning on Wi-Fi option in the mobile
- Downloading V380 App from the Google play store
- Click on the “Local Login”
- The procedure for configuring the camera:

Click on Wi-Fi Smart link → Entering user name on the camera or scanning QR code → Set a password for Wi-Fi camera for security

- Entering the email address for further verification of the app if required

After configuring the device to the mobile phone, the real-time video can be obtained on the mobile phone display. The pan and tilt motion of the camera can be controlled by touching on the left/right and up/down arrows on the app screen respectively. The video can be recorded directly within the mobile or by inserting an SD card in the camera.

3.7 Evaluation of the developed prototype of semi-autonomous robotic platform

3.7.1 Laboratory tests

The developed prototype was evaluated in the laboratory. All the functional components of the robotic platform was analysed to identify its effectiveness of working.

3.7.1.1 Machine dimensions and weight

The Overall dimensions of the prototype were measured using a measuring tape. The gross weight of the platform was also determined, with all its functional components and tank at full capacity.

3.7.1.2 Speed of operation

The prototype was run over a fixed distance and time taken to cover that distance was noted. Then, $speed\left(\frac{m}{s}\right) = \frac{distance(m)}{time(s)}$

The number of revolutions of the wheel per unit time was measured to find the RPM.

3.7.1.3 Power requirement

The power consumption by the prototype was influenced by its gross weight and velocity of travel because it is a function of available torque and speed as shown in the equation 3.13.

$$Power\ (w) = \frac{2\pi * N * T}{60}$$

…. Eq. 3.13

Where,

N = Speed expressed in RPM

T = Applied torque, Nm = Force applied × perpendicular distance from axis of rotation

Power is the rate of energy transferred per unit time ($\frac{dU}{dt}$). In an electric circuit, current is the rate of flow of charge, and the energy transferred per unit of charge can be measured by voltage. Therefore, the power can be expressed as the product of voltage and current. The total power requirement of the prototype could be formulated by measuring the voltage and flowing current of the battery at working condition, using the equation 3.14.

$$Power = \frac{dU}{dt} = \frac{dU}{dq} * \frac{dq}{dt} = v * i$$

…. Eq. 3.14

A digital multimeter was used for measuring the voltage and current generated by the battery (Fig. 3.9). The specifications of the multimeter were;

Model : DT830D digital multimeter

Maximum capacity (DC) : 1000V, 10 A

Sensitivity : 0.1 µA, 10 µV

Accuracy : ± 0.5%

Fig. 3.9 Digital Multimeter

3.7.1.4 Operational or locomotion features

a. Straightness in motion

The prototype was allowed to had a straight forward motion for a fixed distance of 20 m. Straight-line tracks were marked on the ground. The prototype was run through the track and the deviations were recorded to determine the straightness in motion. The experiment was carried out under both with and without steering assistance.

b. Range of communication

The maximum communication range achieved with the available wireless communication system without any hindrance was verified. The range of real-time video streaming using the Wi-Fi IP camera was also checked.

c. Functioning of control unit

The effective functioning of the control unit has to be determined. The functioning of the drive mechanism and sprayer unit, in compliance with wireless communication, need to be assessed. The direction of drive motor rotation for accomplishing the skid steering mechanism was analyzed. The prototype was raised for achieving a free rotation of the driving wheels (no-load condition). The command for forward, reverse, left turn, and right turn motion of the prototype was provided and the rotation of the drive motors was observed. Similarly, the operation of the sprayer unit was also observed to assess the proper functioning of the control unit.

3.7.2 Field evaluation

The developed prototype was subjected to a basic field test for its performance evaluation. The prototype was operated on a prepared plot of 0.01 ha (20m x 5m) at KCAET, Tavanur, Malappuram District, Kerala. It was made to run between the chilli crop cultivated in rows having a row spacing of 45 cm and plant spacing of 45 cm. The plant was at the stage of 15 days after transplanting with 12 cm average plant height. Performance indices recorded during the field operation were:

3.7.2.1 Time of operation

The time required for operating the prototype on the field was noted.

3.7.2.2 Field capacity

The effective field capacity was the actual average rate of coverage by the robot based upon the total field time. The total field time consisted of the effective time of operation and time lost due to turning or other interruptions (Kepner, 1982).

$$EFC = \frac{A}{T_t}$$

…. Eq. 3.15

Where,

EFC = Effective field capacity, hah^{-1}

A = Actual area covered, ha

T_t = Total field time (effective operation time + lost time), h

3.7.2.3 Field Efficiency

Field efficiency is the ratio of effective/actual field capacity to the theoretical field capacity, expressed in percentage. Theoretical field capacity is the rate of area coverage by the robot when it is operating over 100% of time at rated speed and utilizes 100 % of rated width.

$$TFC = \frac{W * S}{10}$$

…. Eq. 3.16

$$E_f = \frac{EFC}{TFC} * 100$$

…. Eq. 3.17

Where,

TFC = Theoretical field capacity, hah^{-1}

W = Rated width, m

S = Travel speed, kmph

E_f = Field efficiency, %

3.7.2.4 Plant damage

The operation of the robotic platform may cause damage to the plant as it was run between the crops. Plant damage was the per cent of plants damaged due to the machine interaction to the total number of plants, present in a unit area.

$$Plant\ Damage, \% = \frac{q}{p} * 100$$

…. Eq. 3.18

Where,

p = Total number of plants in unit area before operation

q = Total number of damaged plants in the same unit area after operation

3.7.3 Cost estimation

The overall cost for the development of the prototype was estimated. It included the material cost of individual components, cost of fabrication and labour charges.

Results and Discussion

CHAPTER IV
RESULTS AND DISCUSSION

The salient results obtained during the development and testing of the semi-autonomous robotic platform is elucidated and interpreted in this chapter.

4.1 Agronomic requirements of the developed robotic platform

The agronomic characteristics of the crop were assessed for determining the wheel track and height of the robotic chassis. The track width of the chassis depended upon the row spacing and the number of crop rows to be covered in a single span. A wheel track of 135 cm was provided to the chassis, for a maximum coverage of three crop rows with 45 cm row spacing. However, as the representative crop (chilli) was having a row spacing of 45 cm for less spreading varieties and 75 cm for high spreading varieties, the number of crop rows covered would differ accordingly. Therefore, a variable chassis had to be provided for changing its track width from a minimum of 75 cm to a maximum of 135 cm in accordance with the varied requirements demanded by the crop characteristics. As the robot was intended to move between the crop rows, the width of the drive wheels should be less than the row spacing.

The plant height was an important parameter considered, because the robotic platform was designed to operate over the crop. The intercultural operations were practiced at different growth periods of the crop and hence the plant height of selected varieties at various growth stages were recorded (Appendix I). The average plant height and standard deviation of randomly selected five plants of each varieties of chilly is given in Table 4.1. The mean plant heights are shown in Fig. 4.1. The plant height was different for different varieties of chilli. It ranged from 0.5 to 1 m depending upon the growth stages. Thus, the maximum plant height was taken as 100 cm. As the prototype would be operating over the crop, a maximum ground clearance of 100 cm was allocated to the chassis in order to avoid the plant damage.

Table 4.1 Average plant height and standard deviation at various growth stages

Growth stages	Anugraha		Ujwala		White kanthari	
	Average, cm	Standard deviation, cm	Average, cm	Standard deviation, cm	Average, cm	Standard deviation, cm
15 days after transplanting (I)	12.4	3.04	12.8	3.01	15.2	1.82
Flowering stage (II)	43.5	4.60	48	5.33	60.6	3.57
15 days after flowering (III)	53.7	3.38	60.4	4.29	76.3	4.08
Full growth period (IV)	65.8	4.10	72.4	3.45	104.5	5.22

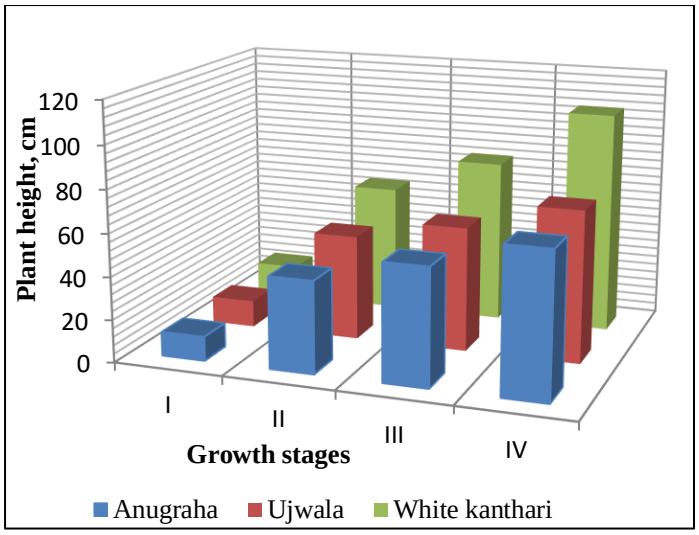

Fig. 4.1 Plant height of three chilli varieties at its various growth stages

4.2 Development of structural frame of the chassis

The design dimensions of the chassis were 135 cm × 80 cm with a ground clearance of 100 cm, considering the agronomic requirements. A rectangular configuration was provided to the frame for ensuring better stability. The constructional details of the chassis are shown in Fig. 4.2. The chassis was fabricated using galvanized

iron tubes having different cross-sectional areas, for various members of the frame in order to reduce the weight. A rectangular tube of 38 mm × 10 mm × 1.5 mm was used for the fabrication of rectangular frame (135 cm × 80 cm) of the chassis carriage. For improving the structural stability, three supporting members were provided along the width of the frame, one at the centre and the other two at 30 cm from each side. These members were fabricated using square tubes with 12.5 mm × 12.5 mm × 1.5 mm cross-section to reduce the dead weight. The carriage was supported by six legs, three on each side with 100 cm height for obtaining the required ground clearance. Square tubes of 100 cm length with 25 mm × 25 mm × 1.2 mm cross-section were used for fabricating the legs. Instead of directly welding the legs on the frame, lead screws were employed, through which the legs could be inserted for enabling the track width adjustment. Two rectangular tubes of 30 cm length were welded in the space between one side of the frame and the nearby supporting member, at 25 mm spacing. It would form a moving channel for the leg (25 mm × 25 mm cross-section) to adjust the track width. These were provided at the places where the legs have to be connected. Holes were drilled on the leg for inserting the 8 mm lead screws. Small pieces of the rectangular tubes were cut and welded at both ends of the moving channel and holes were drilled on it for inserting these threaded screws. The legs were fastened on the lead screws using suitable nuts (M8). Thus, the legs were connected to the body frame of the chassis which enabled a variable track width of 75 – 135 cm. The wheel mounted geared motors could be connected at the bottom of each leg. Fig 4.2 depicts the Front view (a), Side view (b), and Top view (c) of the frame assembly. Fig. 4.3 and 4.4 illustrate the carriage of the chassis and the leg assembly, respectively. Total weight of the chassis was tabulated and given in Table 4.2.

Grimstad *et al.,* (2015) developed an agricultural robotic platform “Thorvald” using slightly flexible materials, instead of completely rigid frame, which enable all wheels to be always in contact with the ground to ensure better traction capabilities in uneven terrains. However, some amount of uncertainty was still faced with this flexible design to properly position the tool mounted on it.

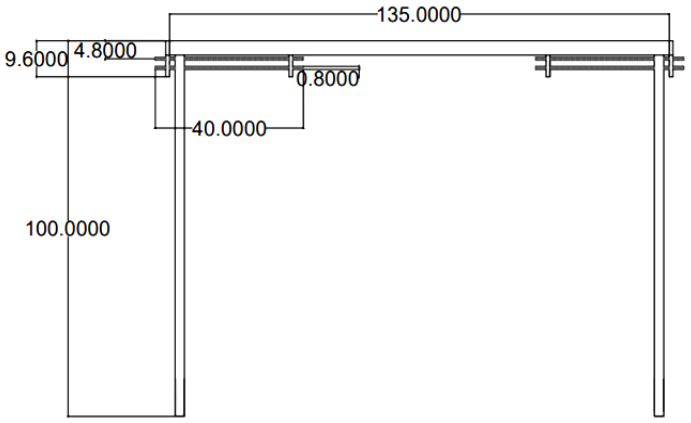

(a)

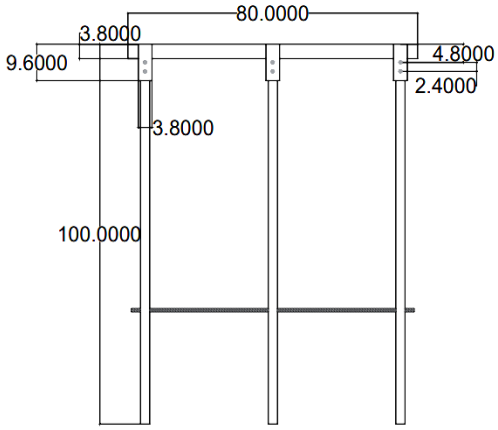

(b)

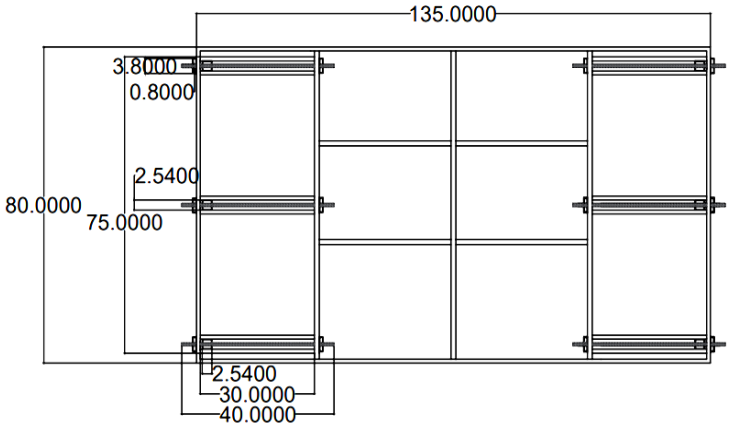

(c)

All dimensions are in cm

Fig. 4.2 Constructional details of the chassis

Fig. 4.3 Carriage of the chassis

Fig. 4.4 Leg assembly of the chassis

Table 4.2 Weight of the chassis

Material used	Length used	Weight (kg)
Rectangular tube – 38 mm x 10 mm x 1.5 mm (0.8 kg/m)	135 cm x 2 = 270 cm 80 cm x 2 = 160 cm 40 cm x 2 x 6 = 480 cm Total = 910 cm = 9.1 m	7.28
Square tube – 25 mm x 25 mm x 1.2 mm (0.9 kg/m)	100 cm x 6 = 600 cm = 6 m	5.40
Square tube – 12.5 mm x 12.5 mm x 1.2 mm (0.5 kg/m)	80 cm x 5 = 400 cm 55 cm x 2 = 110 cm Total = 510 cm = 5.1 m	2.55
Lead screws – 8 mm diameter (0.2 kg/m)	7.5 m	1.50
Miscellaneous accessories	-	1.72
Total		**18.45**

4.2.1 Determination of wheel variables

The dimensions of the wheel were determined based on the fundamental equations of soil-wheel interactions. Rolling resistance was highly dependent on the type of soil, ground contact devices and load acting. It varies with various terrain conditions. Sand surface has higher coefficient of rolling resistance than gravel, grass or bituminous surfaces (Steyn and Warnich, 2015). Pexa *et al.* (2020) had analysed effect of tire rolling resistance under different wheel diameter, inflation pressure, vertical load, and speed. The wheel diameter had a significant influence on the rolling resistance. It showed that the RR decreased with increase in diameter (Fig. 4.5). Similarly, the RR increases with increase in the load.

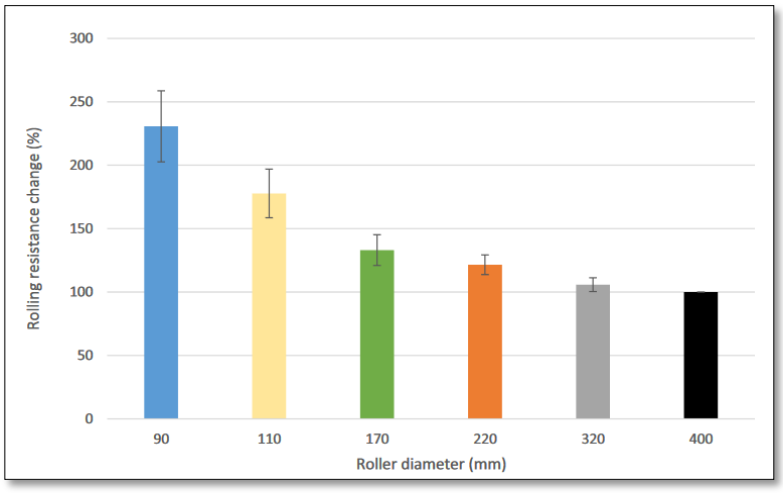

Fig. 4.5 Percentage comparison of rolling resistance with respect to the diameter (Pexa *et al.*, 2020)

From the pressure-sinkage relationship (Eq. 3.3) it was evident that wheel sinkage is a function of width of loading area (width of wheel) for any locomotive configuration. Smaller diameter wheels would not be recommended for off-road mobility because of its higher sinkage effect than bigger diameter wheels for the same load condition. The wheels with larger diameter and width cause a lesser sinkage effect (Wallace and Rao, 1993). From these studies it was clear that smaller diameter wheels had higher rolling resistance and sinkage effect while larger diameter had lesser effect on the rolling resistance and sinkage. But increase in wheel diameter could increase the net torque

required on the wheel which in turn increase the total power requirement of the robot. Therefore, it was decided to select medium-sized pneumatic wheels for the platform. But due to constraints in the market during the lockdown period, rubber wheels having 12.7 cm (5 inch) diameter and 2.54 cm (1 inch) width were procured.

4.3 Sizing of drive motors for the robotic platform

The important aspect in the development of a mobile robot was sizing of its drive motors. The capacity of the motor to drive the robot would be indicated with reference to motor torque. Gross weight of the robot, wheel diameter and velocity of travel are the dependant parameters of traction characteristics and they are directly proportional to the torque required by the robot. High torque - low speed was the ideal characteristics of a drive motor for traction applications in agriculture mobile robots. For a motor with given power rating, the torque drops hyperbolically with increase in the speed (Fig. 4.6). It would have a constant torque region below the base speed.

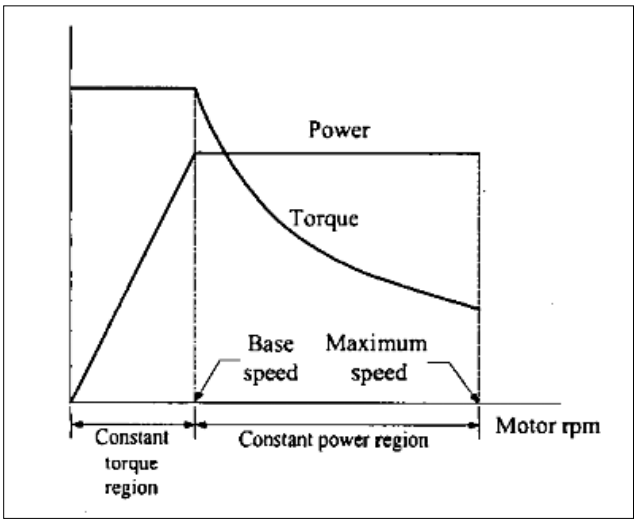

Fig. 4.6 Characteristics of drive motor

The torque acting on each motor of the prototype was calculated as per the procedure mentioned in Section 3.3.3.2. The gross weight of the robot and wheel diameter, 55 kg and 12.7 cm respectively, were taken into account for determining the total torque. The force due to rolling resistance and gradient force would be contributing to the net tractive force while force due to acceleration and aerodynamic drag were

considered as negligible. The net tractive force acting on the moving robot was calculated to be 199.75 N (20.38 kg_f). Therefore the total torque acting on the robot was 129.43 kg_f-cm and the torque on each motor was 21.57 kg_f–cm (Appendix II). The forward speed of the robot was assumed as 0.2 ms^{-1}. Therefore, the rotational speed for the motor was obtained as 30 RPM.

$$N = \frac{60 * V}{2\pi * r} = \frac{60 * 0.2}{2\pi * 0.0635} \approx 30\ RPM$$

4.4 Design characteristics of robotic platform

The design of each functional component of the robotic platform is detailed in this section. This includes selection and design of drive mechanism, wireless communication system, real-time video transmission system, operational unit and power supply unit. The specifications of the components are given in Appendix III.

4.4.1 Drive mechanism

The developed chassis of the prototype would be adaptable for operating on various fields based on the different agronomic considerations. It should be strong enough to accommodate all of its functional units. The design dimensions of the platform were 135 cm × 80 cm × 100 cm, with provision for varying the track width from 75 to 135 cm using lead screws. Since the robot was expected to be operated in the undulated agricultural fields, a six-wheel-drive mechanism with high torque DC motors was employed for ensuring better stability and sufficient power for movement. The drive mechanism consisted of DC motors, a microcontroller unit, and motor shields. Six high torque 12V DC geared motors (Model: DC worm gear motor GW5840-31ZY) were selected as the drive motors (Fig. 3.7). This worm gear motor was a dual-shaft motor with self-locking capability. The motor could withstand stall torque of 140 kg_f-cm and a no-load speed of 27 rpm. It had an output power of 10 - 20 W and a continuous current of 3A. The diameter of the motor's output shaft was 8 mm. As the output shaft was dual-type, two wheels could be mounted to a single motor. The direction of motor rotation was possible by inverting the direction of the current flow through the motor with the help of motor drivers.

The movement of the robotic platform could be controlled by directing the rotation of drive motors using a pre-programmed microcontroller. Arduino Mega was the microcontroller board used which was interfaced with the motor via a motor shield. Arduino is an open-source microcontroller having a wide range of applications and easy-to-use. The microcontroller board Arduino Mega (Fig. 3.8) was based on Atmega2560 and came with more flash memory and RAM including 256 kB of Read Only Memory (ROM), 8 kB of Random Access Memory (RAM), 4 kB of Electrically Erasable Programmable Read-Only Memory (EEPROM). It had 54 digital I/O pins, out of which 15 pins could be used for Pulse Width Modulation (PWM) outputs, and 16 analogue input pins. It also contained a crystal oscillator of 16 MHz, 4 UARTs (hardware serial ports), an In-Circuit Serial Programming (ICSP) header, a power jack, a Universal Serial Bus (USB) connection, and a reset button. The microcontroller board could be powered either by connecting it to the computer via USB connection or by an external source like a battery or AC-to-DC adapter. The operating voltage for the Arduino Mega was 5V which made it compatible with other electronics components too. Arduino microcontroller board was programmed in Arduino software (Integrated Development Environment (IDE)) using C, C++, or JAVA programming languages. The motor shields used were based on the L298 IC, which was a high voltage high current full-bridge driver with two H-bridges (Fig. 3.9). An L298N motor driver allowed the operator to control the speed as well as the direction of two DC motors simultaneously. It could withstand a maximum operating supply voltage up to 35 V, and a total DC current of 4 A. Its continuous working current per channel was 2 A. A total of three motor drivers were used for controlling all six driving motors. The motor drivers were powered from the external power source (battery) rather than from the Arduino microcontroller board, in order to avoid damages to the board. The skid steering mechanism was employed for steering control of the prototype.

Fig. 4.7 DC worm gear motor

Fig. 4.8 Arduino Mega microcontroller board

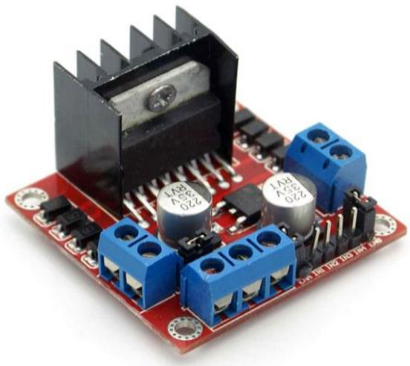

Fig. 4.9 Motor driver

4.4.2Wireless Control system

In this project, the wireless control system was based on Radio Frequency (RF) protocol. Flysky FS i6 2.4GHz Six-channel Transmitter Remote Controller with FS-iA6 Receiver was procured to serve as the transmitter and receiver unit (Fig. 4.10). This worked in the frequency range from 2.405-2.475 GHz and bandwidth of 500 kHz. The system comprised of a high-quality multidirectional antenna for covering the whole frequency band and a highly sensitive receiver for long-range communication. It contained two gimbals, three two-position switches, one three-position switch and two vario-meters. The transmitter and receiver unit had to be paired first, using the bind plug. Each transmitter had its unique ID which was used to connect it with the receiver unit. Hence interference from other transmitter units could be avoided. Four 6V 1.5A batteries

were used for powering the remote and 5V (4 – 6.5V) DC for the receiver. The receiver was connected to the Arduino Mega microcontroller board for processing the received signals from the transmitter.

Fig. 4.10 Transmitter remote controller with receiver

4.4.3 Real-time video transmission system

Monitoring and the direction control of the robot could be accomplished with the help of a real-time video transmission system. For the real-time video streaming, a V380 Wireless IP Camera having 720-pixel resolution was selected in this project (Fig. 4.11). V380 camera was a Wi-Fi enabled motion detection camera which allowed two-way live video communications. It could also support a memory card (64 GB) for recording the data. One of the significant advantages of this camera was its low internet data consumption. It provided a free movement along the horizontal and vertical axis, i.e., pan 355° and tilt 120°, which facilitated a wide-angle view. This helped to attain an almost 360° view all around the camera. The camera was configured with a mobile phone using the "V380 app", which helped to monitor the real-time data captured and control the motion of the camera. The camera had an adaptor and a USB cable for powering. Here the battery power could be utilized for powering the camera. Therefore, a DC-DC buck converter should be used for stepping down the input voltage to 5 V. LM2596 DC-DC buck converter was a step-down regulator capable of providing variable output voltages

ranging from 3.3 – 12 V and driving load current up to 3 A. It was a switch-mode power supply having higher conversion efficiency (Fig. 4.12).

The camera was mounted at the front of the robotic frame, which enabled the operator with better visibility for getting a proper wide-angle view of the surroundings. The live-video would be displayed on the display screen of the mobile phone, which was connected with the Wi-Fi camera via the V380 app. These arrangements enabled the operator to control the robot with the captured real-time video.

Fig. 4.11 Wireless IP Camera

Fig. 4.12 LM2596 buck converter

4.4.4 Operational unit

A 3.35 m spray boom was adopted for this design which helped to improve the field coverage with minimum runs of the platform. The sprayer unit was designed to be operated for spraying the liquid formulations over the crop. Boom positions had to be varied accordingly with the crop height. A geared DC motor operated cable drive slider mechanism, used in raising and lowering of the automobile windows, could be used for the raising and lowering of the sprayer unit (Fig. 4.13). This mechanism was operated using a 12 V electric motor having rated speed of 60 RPM and 2.9 Nm rated torque coupled with a cable drive guidance system. Since the boom length was higher than the track width of the platform, there would be difficulty in turning or transporting the platform from one place to another. The boom should be in its full span only during the operating condition. Therefore, another DC motor operated cable drive slider mechanism

could be employed for the opening and closing of the spray boom. The sprayer unit could be actuated using relays which provided robust connections. An eight channel relay board module with a relay driver circuit was used for controlling the operations. ULN2003 IC was the relay driver used. It is a high voltage and high current array IC capable of withstanding a peak current of 600 mA. This relay driver circuit could drive the relays ON or OFF based on the signals received from the microcontroller for actuating the operational components.

Fig. 4.13 DC motor operated cable drive slider mechanism

A positive-displacement pump along with the sprayer fittings were procured and attached to the boom to perform the spraying operation. A 12 V 4.5 A high-pressure diaphragm pump having a cut-off pressure of 8.5 bar and a flow rate of 7.5 $Lmin^{-1}$ was fitted for pumping the spray solution from the tank. The pump was low-cost, portable, and required less maintenance. Two plastic cans, each having 10 L capacity, were used for carrying the spray liquid. The inlet of the pump was connected to the spray tank and the outlet to the boom with nozzles via laterals and fittings.

4.4.5 Power supply unit

All the functional components of the rover and the drive motors were required to be powered by a battery. Each of the drive motor consumed a continuous current of 3 A and hence a total of 18 A was required for driving the six 12 V geared DC motors. Other

functional units would also consume some amount of current. The operation of the robot was envisaged for a minimum duration of one hour. Therefore, a 12 V 35 Ah battery was selected which was considered sufficient to power the entire system. In order to step down the voltage from the input supply to the required output, a buck converter (DC to DC power converter) was used. The commonly used step-down switching regulator LM2596 was selected for this project. They are monolithic integrated circuits that allocate every active function for the buck converter. This series of regulators were capable of taking up input voltages ranging from 4.5V to 40V and regulate into fixed output voltages ranging from 3.3 – 12 V. It was capable of driving a maximum load current of 3A. It was composed of a fixed-frequency oscillator with internal frequency compensation. They were popularly used in power modules because of their high current capability. A 5V regulator was adopted for stepping down the 12V input voltages to an output of 5V.

The battery was required to be charged when it got drained. AC power source could not be used directly to charge the battery. Therefore, the Switched-Mode Power Supply (SMPS) and voltage regulator were used to charge the battery. SMPS is a power supply consisting of switching regulators to convert electrical power from AC to DC. The solid-state switches in it could stabilize the unregulated voltages, by changing the load current ON and OFF, and generate a smooth regulated DC output. It transferred power from DC or AC sources to DC loads and was capable of offering higher power conversion with minimum loss. A voltage regulator used in supplement with SMPS could step-down and maintain a constant voltage level as required.

4.5 Development of the prototype of semi-autonomous robotic platform

The prototype of semi-autonomous robotic platform was developed in accordance with the conceptual design as given in section 3.5. The functional units were developed and attached on to the fabricated chassis for developing the prototype.

4.5.1 Development of drive mechanism

A six-wheel-drive skid steering mechanism was adopted for driving the robot. The drive motors were mounted at the bottom of each leg with the aid of L-brackets. A

nylon rod, having 15 mm external diameter and 8 mm internal diameter, was attached to the output shaft of each motor. It helped to extend the output shaft for mounting the wheels on it. Since the motor had a dual output shaft, two wheels were mounted on a single motor (Fig. 4.14). Therefore, a total of twelve numbers of wheels were used and an effective wheel width of 12.5 cm was achieved on each leg. It was assumed that the dual wheels on a motor would helps to improve the traction performances.

Fig. 4.14 Motor-wheel assembly

The direction of motor rotation was controlled by the microcontroller for establishing the skid-steering. The DC motors were interfaced with the microcontroller via L298N motor drivers, which could enable the speed and direction control with respect to PWM and H-bridge techniques. In PWM method, the average value of input voltages was adjusted by turning ON/OFF the power at a faster rate. The average voltage is proportional to the duty cycle, i.e., ratio of amount of time the signal is ON to the amount of time the signal is OFF in a single time period, expressed in percentage. The average voltage applied to the motor would be higher (high speed) for a higher duty cycle and vice-versa. The H-bridge technique could control the direction of motor rotation by changing the polarity of input voltages. It consisted of four switching elements with a motor at the centre forming an H-like configuration. The direction of current flow was changed by activating two particular switching elements at the same time. This causes the change in direction of motor rotation. This dual channel H-bridge driver was capable of driving two DC motors (A and B). Logic control inputs (HIGH [5V], LOW [GND]) were

used for the motor control. EnA and EnB were PWM-enabled pins for speed control of motor A and motor B respectively. If En was HIGH, the motor got enabled and control the speed and if En was LOW the motor got disabled/OFF. In1 and In2 were the direction control pins for motor A and, In3 and In4 for motor B. The direction control of the motor based on the logic inputs is given in Table 4.3. The motor driver had three power pins, viz, motor power supply (V_S), logic power supply (V_{CC}) and ground (GND). V_S pin could supply power to the motor ranging between 5 – 35 V. The V_{CC} was connected to 5 V pin of Arduino for switching logic circuitry.

Three motor drivers were used for driving six DC motors, in which each motor driver was connected to two DC motors on each side. All the drivers received the same output signals from the microcontroller which enabled uniform motion for the motors on each side, i.e., motors on each side were driven by same signals from the microcontroller. The pin-out diagram of the motor driver is shown in Fig. 4.15.

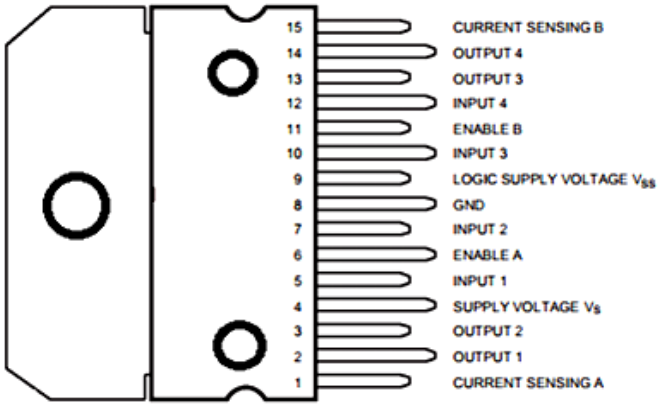

Fig. 4.15 Pin out diagram of motor driver

Table 4.3 Direction control of motor

Input 1	Input 2	Direction of motor rotation
High	Low	Clockwise (Forward)
High	High	Motor OFF
Low	High	Anticlockwise (Backward)
Low	Low	Motor OFF

4.5.2 Development of sprayer unit

A sprayer boom was developed and mounted at the rear-side of the chassis. The constructional details of the unit are shown in Fig. 4.16. An rectangular tube (38 mm × 10 mm) having 50 cm length was welded vertically to the centre of another rectangular tube with 100 cm length to form a T- connection. For making spray boom, two pieces of square tubes (25 mm × 25 mm) having 130 cm length were connected to the 100 cm rectangular tube, one on each end, by means of nut and bolt. Two supporting pieces were also provided vertically at 40 cm spacing from the central T-connection. Aluminium C-channels, having 4 cm width and 50 cm length, were connected to the chassis for attaching the developed sprayer unit. This C-channel could enable the movement of the unit.

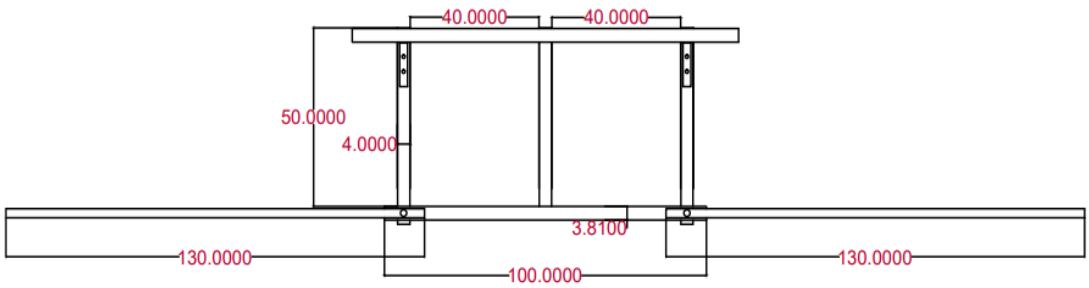

Fig. 4.16 Constructional details of the sprayer assembly

The movement of the sprayer unit was established by a geared DC motor along with its cable-drive guidance system. This cable drive system could transfer the rotating motion of the geared motor to reciprocating motion. Two geared DC motor operated cable-drive slider mechanism were employed, one for opening/closing of spray boom and other for lowering/raising the unit. The direction of rotation of the DC motor was controlled by a two-way control switch, in which one switch position could help the motor to rotate in the clockwise direction for raising the unit and another switch position could rotate the motor in opposite direction for lowering the unit. A Double Pole Double Throw (DPDT) relay was used as the two-way control switch. To protect the motor from overheating, limit switches were provided on each end at a safest extreme point. In addition, two more DPDT relays were connected to limit switches at each end. When the limit switch on one end got activated, the DPDT relay provided at that end would actuate

the two-way control switch of motor to change its switching position for reversing the motor rotation in opposite direction. For activating these DC motors and the sprayer pump according to the joystick command from the user, Single Pole Double Throw (SPDT) relays were provided.

4.5.3 Development of wireless communication

The Flysky FS i6 2.4 GHz 6-channel transmitter remote controller and FS-iA6 receiver would be pre-bounded. Initially, the transmitter and receiver were paired for establishing the communication and the following procedure was followed:

- The bind cable provided was connected to B/VCC port of the receiver.
- Receiver was powered via another port. Then LED started to blink quickly indicating that it was powered.
- The bind key on transmitter was pressed while powering on the transmitter. Then, the LED on the receiver started to light instead of blinking. The pairing was successfully completed.

Here, five channel positions were required for controlling the prototype. Channel 1 – 4 were enabled with the right and left gimbals. Any of the switches could be assigned for Channel 5. The auxiliary channel function on the transmitter was used for assigning the two-position switch (SwA) as channel 5. Function setup —> Aux. Channels —> Select channel using “OK” key —> Select the switch using “UP” and “DOWN” key —> Hold “CLOSE” key to save. Table 4.4 represents the channel positions for each operation control of the prototype.

Table 4.4 Channel positions for the robot control

Channel position	Operation
Channel 1	Up-down movement of sprayer unit
Channel 2	Open-close movement of boom
Channel 3	Forward-reverse motion of prototype
Channel 4	Right-left turn of prototype
Channel 5	Switch ON/OFF of spray pump

4.5.4 Control unit of the robot

The control unit was developed as the central processing unit of the robotic platform for governing the operations to be carried out. It comprised of the microcontroller board, motor drivers, voltage regulators, wireless receiver unit, relay driver circuit, DPDT relays, jumper wires and other terminal connectors. Fig. 4.17 and Fig. 4.18 represents the Arduino Mega wired connection diagram and relay control diagram of the control unit, respectively.

The control unit was powered by the 12V battery, interfaced with an LM2596 buck converter for stepping down the voltage to 5V. The signals from the transmitter were received by the receiver unit and transferred to the Arduino Mega microcontroller board. The 5V (V_{CC}) and GND power wires of the Arduino were connected to V_{CC} and GND of receiver unit. Each channel of the six-channel receiver unit (ch1, ch2, ch3, ch4, ch5) was connected with the Arduino digital pins 7, 8, 9, 10, 11. The DC motors were connected to the Arduino board via the motor shields L298N. In the motor driver, the motor power supply terminal (Vs) was connected to the external 12V supply. The logic circuitry terminal (V_{CC}) was connected to 5 V pin of Arduino board and GND pin was also connected to Arduino GND pin. Each motor driver drove two motors, a right motor and a left motor. Three motor drivers were used to drive a total of six motors. The input lines (In1, In2, In3, In4) and enable lines (EnA, EnB) of the motor driver were driven by the Arduino digital output pins (2, 3, 4, 5, 22, 23). Arduino output pins 22 and 23 were capable of pulse width modulation. These PWM signals helped to maintain an average value of voltage by turning ON/OFF the power at a faster rate. The H-bridge in the L298N driver aid to change the direction of the current flow which in turn helped to change the rotation direction of the motor. Two DC motors were connected to the output terminals A (out1 and out2) and B (out3 and out4) of the motor driver. All the DC motors on the right side were driven by the same input lines (In1, In2) and enable line (EnA). Similarly, input lines (In3, In4) and enable line (EnB) drives all motors on the left side. If the In1 was HIGH and In2 was LOW, the right motors will move forward and vice versa. Same as in the case of left side motors too.

The operational unit was controlled by means of relays which were interfaced with the microcontroller via a relay driver circuit ULN2003. The Arduino digital output pins (28, 29, 30, 31, and 32) were connected to the inputs of the relay driver. The relay driver output pins for Arduino pin 32 was connected to G5LE SPDT relay for switching ON/OFF the spray pump. The relay driver output for the Arduino pin 28 and 30 were connected to G5LE-1 SPDT relays and Arduino pin 29 and 31 were connected to DPDT relays for actuating the geared DC motors in slider mechanism; one for raising/lowering sprayer unit and other for open/close of spray boom. The joystick control for actuating the DC motors were initiated by these SPDT relays. The direction of rotation of the motor was changed with the help of DPDT relays. Limit switches and another supporting relays were assisted to these DPDT relays, for enabling the direction control of motor. Fig. 4.19 depicts the control unit of the prototype. It was made as compartments for arranging the components within minimum space. The receiver unit with antenna, microcontroller unit, and relay circuit board were placed at the top compartment. Motor drivers and the relays were placed in the middle and SMPS was connected at the bottom most portion. In order to reduce heat losses, DC fans were employed at the sensitive points.

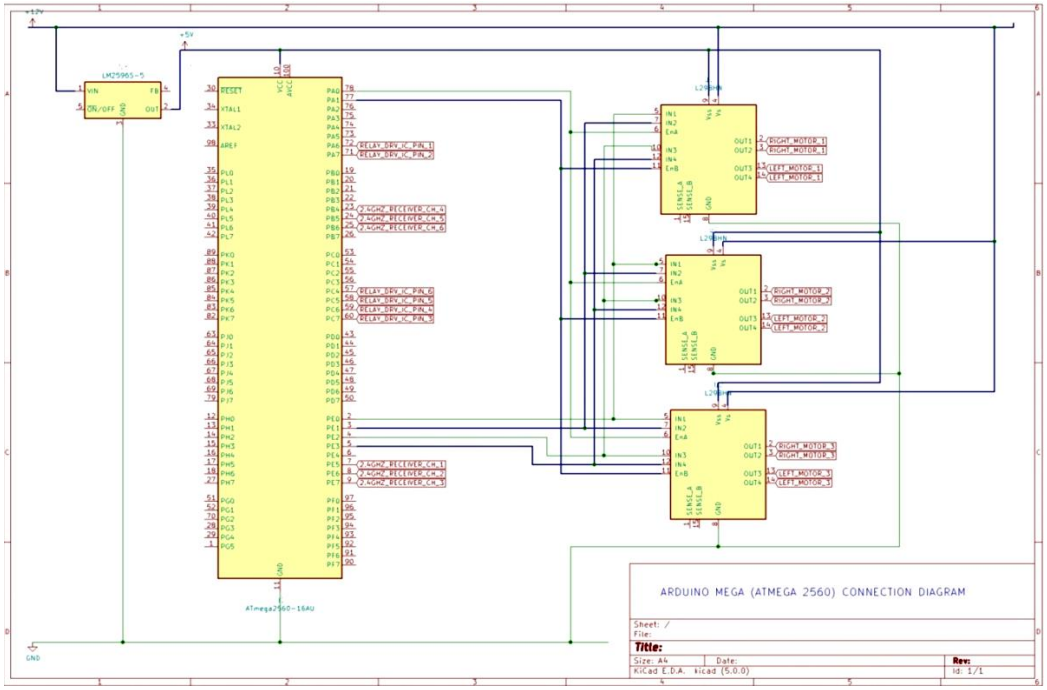

Fig. 4.17 Circuit diagram of microcontroller for motion control

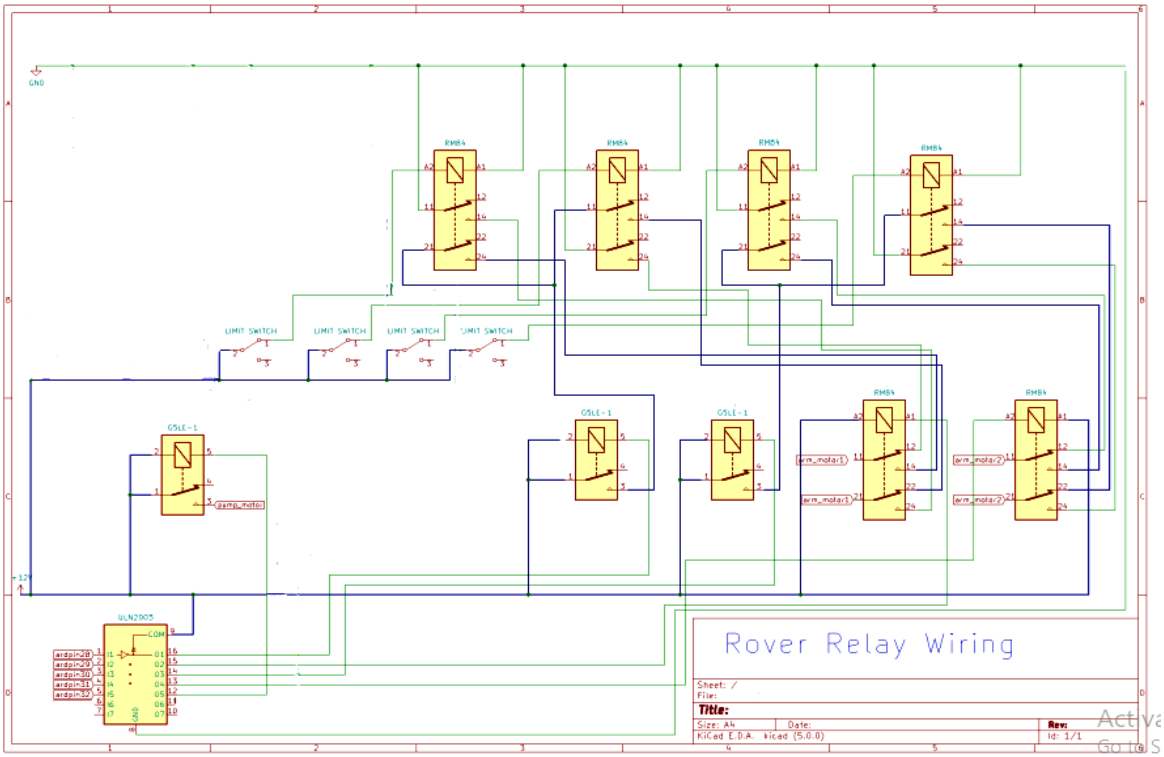

Fig. 4.18 Circuit diagram of relay control for sprayer unit

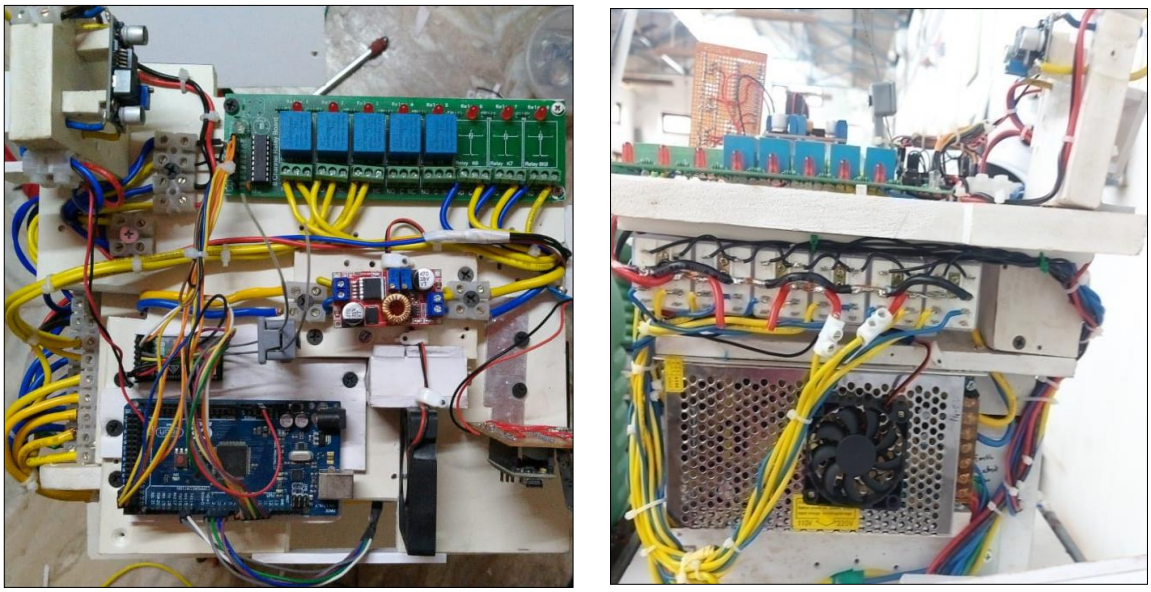

(a) **(b)**

Fig. 4.19 Control unit of the platform - (a) top view and (b) side view

4.5.5 Programming the Arduino microcontroller

The program code generated was based on the sequence of instructions defined in an algorithm to solve or perform definite operations of the prototype. The overall concept of the system approach could be presented as two distinct algorithms, one for motion control and other for sprayer control. The motion control algorithm defined the semi-autonomous control of the prototype according to the user commands. The flow charts of motion control and sprayer control algorithms of the prototype are given in Fig. 4.20 and Fig. 4.21, respectively.

The principle of working of the motion control algorithm could be detailed in the following steps:

Step 1: Start the program.

Step 2: *Initialize* the system parameters. Set the variables of the receiver channel (ch3, ch4, move-value, turn-value). A lower stop range value and an upper stop range value was defined as thresholds to the channels for both move and turn motions. Set the motor driver variables like In1, In2, In3, In4, Motor right enable and Motor left enable as PWM pins. Setup the channel pins as INPUT and PWM pins of motor driver as OUTPUT.

Step 3: *Read the pulse width* of each channel and map its value (980 to 1999) to -255 to 255 for both move-value and turn-value. The pulse width of Channel 3 was represented as move-value for forward and reverse motion. Similarly, channel 4 represented the turn-value for left and right turn. Channel values were limited within the ranges provided.

Step 4: If the move-value and turn-value were between the lower stop range value and upper stop range value as defined in step 2, the "robot control state = 0" condition occurred and stops the robot. At this condition, the In1 = In2 = In3 = In4 = 0 and motor right enable = motor left enable = LOW. Otherwise turn to step 5.

Step 5: If the turn-value was higher than upper stop range value, turn to the condition "robot control state = 1". At this condition, In1 = In4 = 0, In2 = In3 = motor speed and motor right enable = motor left enable = HIGH. Then the robot turns right otherwise move to step 6.

Step 6: If the turn-value was lesser than the lower stop range value, the "robot control state = 2" occurred where In1 = In4 = motor speed, In2 = In3 = 0 and enable pins = HIGH. Then the robot turned left otherwise moved to step 7. In both step 5 and step 6, the channel 3 was within the threshold limit (lower stop range value < move-value < upper stop range value)

Step 7: If move-value was higher than the upper stop range value, the "robot control state = 3" condition occurred and moved the robot in forward direction. Because, during this condition the In1 = In3 = motor speed, In2 = In4 = 0 and enable pins= HIGH. If the condition was not satisfied, then shift to step 8. In the step 7 and step 8, the turn-value was within its lower and upper stop range value.

Step 8: If move-value was lesser than lower stop range value, the condition "robot control state = 4" occurred in which In1 = In3 = 0, In2 = In4 = motor speed and enable pins = HIGH. Then robot moved in reverse direction. If the condition was not satisfied, then moved to step 3 to read the pulse width and repeat the processes until the microcontroller is turned OFF.

The algorithm for sprayer unit control was detailed as given in the following steps:

Step 1: Start the program

Step 2: Initialize the system parameters. Initializes the variables of receiver channel (ch1, ch2, ch5, up-down value, open-close value, swA value) and relays (Re01, Re02, Re03, Re04, Re05). Setup the channel pins as INPUT and relay pins as OUTPUT.

Step 3: Read the pulse width of each channel and map its values (980 to 1999) to 0 to 255. Channel values would be limited within these ranges.

Step 4: After reading the control signals, the relays were controlled accordingly. The relay control comes under a looping function.

a. If the up-down value was greater than 200, the Re01 would be enabled and resulted in upward movement of the sprayer unit (*Boom up*). Otherwise turned to step 4b.

b. If the up-down value was lesser than 100, both the Re01 and Re02 would be enabled and resulted in lowering of sprayer unit (*Boom down*). Otherwise both Re01 and Re02 would be disabled and turned to step 3. Repeat the process.
c. If the open-close value was higher than 200, the Re03 would be enabled and resulted on opening of the spray boom (*Boom open*). If not moved to next step 4d.
d. If the open-close value was lower than 100, both the Re03 and Re04 would be enabled and resulted in closing of the spray boom (*Boom close*). Or else Re01 and Re02 would be disabled and moved to step 3. Repeat the process.
e. If the switchA value was higher than 200, the Re05 became enabled and turn ON the spray pump. Or else Re05 remain disabled and the pump would be OFF.

The program code prepared and compiled in the Arduino IDE software was uploaded to the microcontroller board for performing the operations. The program was detailed in Appendix IV.

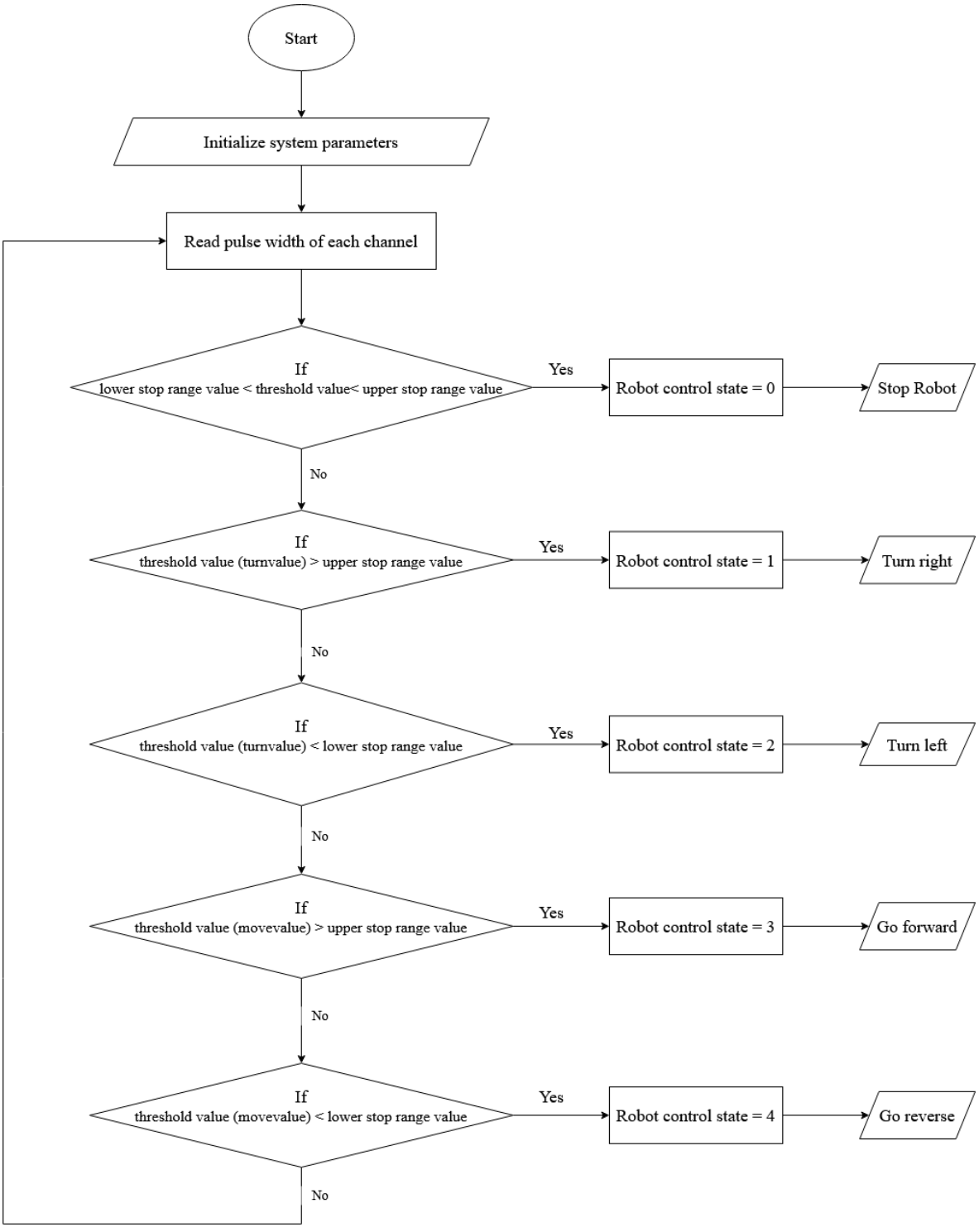

Fig. 4.20 Flow chart of motion control algorithm

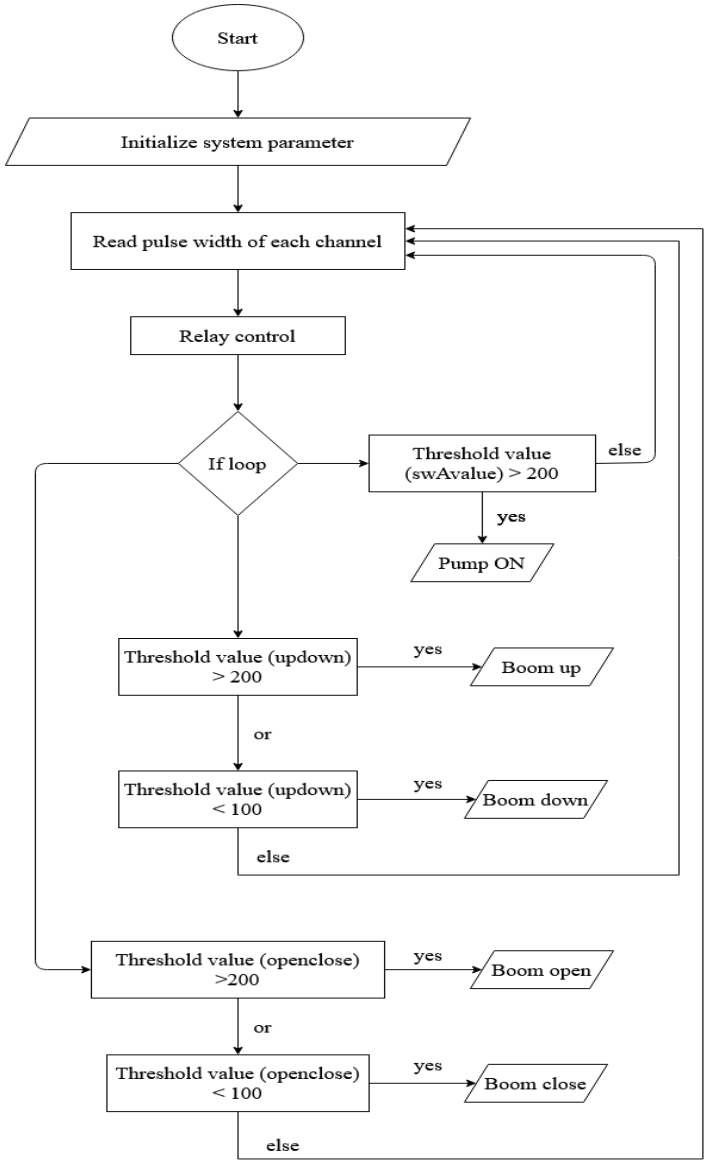

Fig. 4.21 Flow chart of sprayer unit control algorithm

After developing the functional components, they were assembled on to the chassis. The geared motors with wheels were mounted at the bottom of the leg and the sprayer unit was attached on the rear portion. The control unit, battery, wireless camera, spray tanks, spray pump and power window motors were arranged on the top of the chassis carriage in such a way to result in an uniform load distribution. The whole unit was powered by the battery unit.

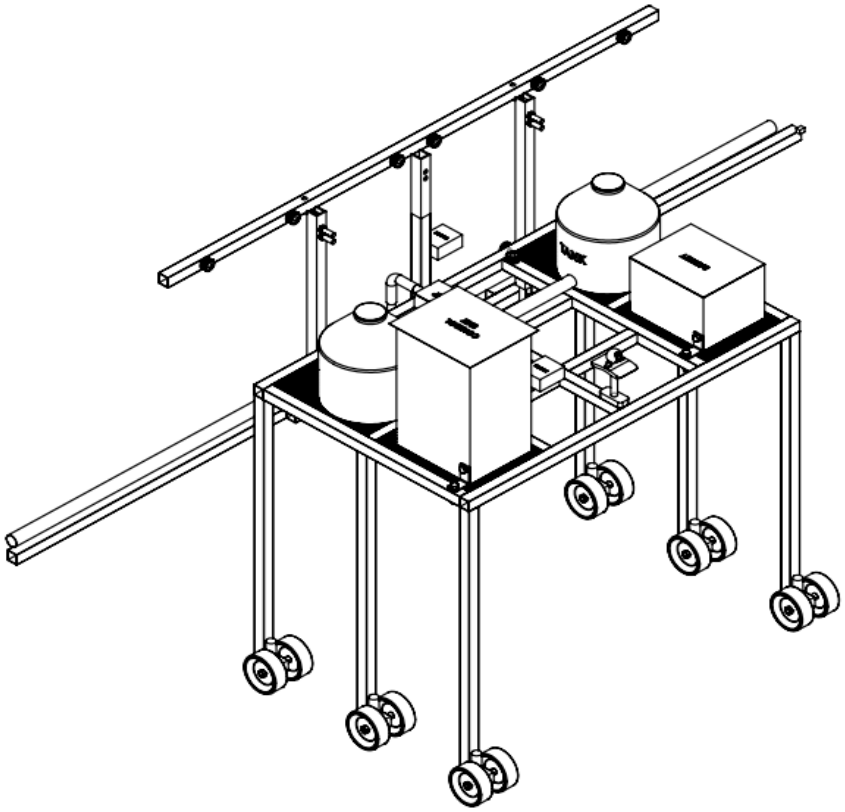

Fig. 4.22 Isometric view of the prototype

Fig. 4.23 Developed prototype of semi-autonomous robotic platform

Table 4.5 Specification of the developed prototype

Sl. No.	Components	Specifications
1.	Chassis	: Dimension(L×B): 135 × 80 cm
		: Ground clearance: 100 cm
		: Track width: 75-135 cm
		: Material: Galvanized Iron tubes, lead screws (8 mm diameter)
		: Weight: 18.45 kg
2.	Drive unit	
	a. Drive motor	: Motor type: DC worm gear motor (GW5840-31ZY) with dual output shaft
		: Operating voltage: 12V
		: Stall Torque: 140 kg_f-cm
		: No-load speed: 27 RPM
		: Continues current: 3 A
		: Output power: 10 - 20 W
	b. Wheels	
		: Wheel type: Rigid rubber wheels
		: Dimension: 12.7 cm diameter, 2.54 cm width
3.	Wireless control system	: Type: Radio frequency protocol
		: Model: Flysky FS i6 2.4GHz Six-channel Transmitter Remote Controller with FS-iA6 Receiver
		: Operating frequency: 2.405-2.475 GHz
		: Bandwidth: 500 kHz

4. Control unit

a. Microcontroller board	:	Arduino Mega (Atmega2560)
		Memory: 254 kB
b. Motor driver	:	Model: L298N
	:	Max. operating current: 4 A
	:	Max. operating voltage: 46 V
c. Relay control for sprayer unit	:	Relay circuit: ULN2003 IC
	:	Relays: SPDT, DPDT

5. Operational unit

a. Boom	:	Overall boom length: 335 cm
b. Motor	:	Type: Geared DC motors (12V)
	:	Rated speed: 60 RPM
	:	Rated torque: 2.9 Nm
c. Tank	:	Capacity: 10 L
d. Pump	:	Type: Positive displacement pump
	:	Make & model: FIELD STAR Model SL-DP16
	:	Flow rate: 7.5 l/min
	:	Operating voltage & current: 12 V, 4.5 A

6. Real-time video transmission unit

a. Wireless IP camera	:	Model: V380 Wireless IP Camera
	:	Resolution: 720 pixels
	:	Wide angle view: 360°
b. Buck converter	:	Model: LM2596 DC-DC buck converter(12V to 5V)
	:	Input voltages: 4.5V to 40V

		: Output voltages: 3.3V- 12V
7.	Power supply	
	a. Battery	: 12V 35 Ah Lead acid battery
	b. Voltage regulator	: Model: LM2596 DC-DC buck converter (12 to 5V)
		: Input voltages: 4.5V to 40V
		: Output voltages: 3.3V – 12 V
		: Continuous current: 3A
8.	Charging unit	: Switched-Mode Power Supply (SMPS)
	Overall weight	**: 52.35 kg**

4.6 Evaluation of the prototype semi-autonomous robotic platform

The prototype, consisting of DC motor drive system, control unit, wireless communication system, sprayer unit and real-time video streaming unit, was developed to move in between the crop rows and turn at the end of the rows for subsequent operation, as per the operator guidance. The developed unit was evaluated under both laboratory and field conditions.

4.6.1 Laboratory test

The physical and working characteristics of the developed prototype were assessed before evaluating on the field. It helped to analyze the effectiveness of functional units.

4.6.1.1 Machine dimensions and weight

The overall machine parameters were measured and given in Table 4.6.

Table 4.6 Machine parameters

Sl. No.	Specifications	Quantity
1	Overall width	335 cm
2	Overall length	100 cm
3	Overall height	150 cm

4	Wheel track	135 cm
5	Wheel base	80 cm
6	Ground clearance	100 cm
7	Weight of prototype	
	a. Without sprayer unit	36.70 kg
	b. With sprayer unit	52.35 kg

The weight of the developed prototype was very less as compared to other agricultural robotic platforms like Amazone Bonirob (Ruckelshausen *et al.*, 2009) and Thorvald II (Grimstad and Johan, 2017). This would not only help to reduce the soil compaction but also to improve the overall operation time of the platform, since it is battery operated.

4.6.1.2 Speed of travel

The number of revolutions per unit time was 18 RPM. The measured value of speed (0.125 ms^{-1}) was lesser than the rated speed (0.2 ms^{-1}).

Table 4.7 Speed of travel of the prototype

Distance, m	Time, s	Speed, ms^{-1}
20	162	0.123
20	160	0.125
20	159	0.125
20	160	0.125
20	158	0.126
Average		**0.125**

4.6.1.3 Power requirement

The active power exerted by the robot for self-propulsion was formulated for two conditions, without payload and with payload. The weight of the prototype and its velocity of travel were the parameters influencing the power consumption. The

mechanical and electrical efficiencies for drive system were taken as 70% each. The power consumed by the prototype for its self-propulsion was 97.57 W without payload and 125.29 W with payload.

The voltage and flowing current from the battery were also measured for determining the total power requirement of the prototype at its working condition. The total power consumed by the prototype was 246.56 W without payload and 359.31W with payload condition.

Table 4.8 Actual power consumption of the prototype for self-propulsion

Condition	Load acting, kg	Torque, Nm	Speed, RPM	Power, W	Actual power consumed, W
Without payload	36.70	22.83	20	47.81	97.57
With payload	52.35	32.57	18	61.39	125.29

Table 4.9 Total power consumed by prototype

Condition	Voltage, V	Current, A	Power consumed, W	Average
Without payload	12.3	20.4	250.92	246.56 W
	12.3	19.8	243.54	
	12.2	20.1	245.22	
With payload	12.5	28.6	357.50	359.31 W
	12.4	28.9	358.36	
	12.4	29.2	362.08	

From the Table 4.8 and 4.9, it was concluded that power consumed by the prototype was directly proportional to the weight of the robot (Fig. 4.24). With increase in the load, current flowing from the battery increased and resulted on higher power consumption by the prototype. The total power consumed was very much higher than the actual power required. These variations might be due to the electromechanical losses in

the robot drive system and the control system. With payload, the power was also consumed by the sprayer unit for its operation. Therefore, total power requirement by the prototype with payload was much higher than without payload.

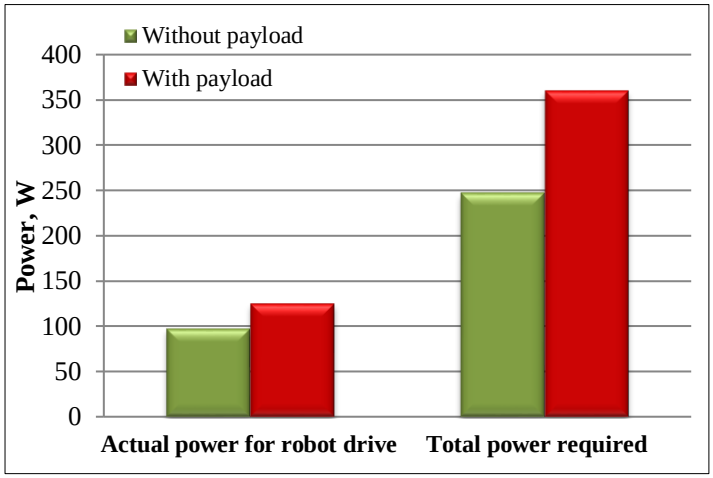

Fig. 4.24 Power consumption by prototype

4.6.1.4 Operational/locomotion features

a. Straightness in motion

The platform was made to run through the straight tracks for observing straightness in motion (Fig. 4.25). This operation was carried out with and without steering assistance. The linear deviation of the platform from the straight path without steering assistance was recorded (Appendix V). An average of 50.33±4.5 cm linear deviation to the right-side was observed for a 20 m run (Fig. 4.26). Therefore, the angular deviation from the path would be $\tan^{-1}(\frac{0.5}{20}) \approx 1.5°$.

The experiment was also conducted with steering assistance and the linear deviations from the path were noted. Fig. 4.27 represents the linear deviations observed from the straight path based on the distance travelled at 50 cm interval. When the robot got deviated from the straight path, it was altered by proper steering control and thus deviation was minimized.

Fig. 4.25 Motion of the prototype over a straight path

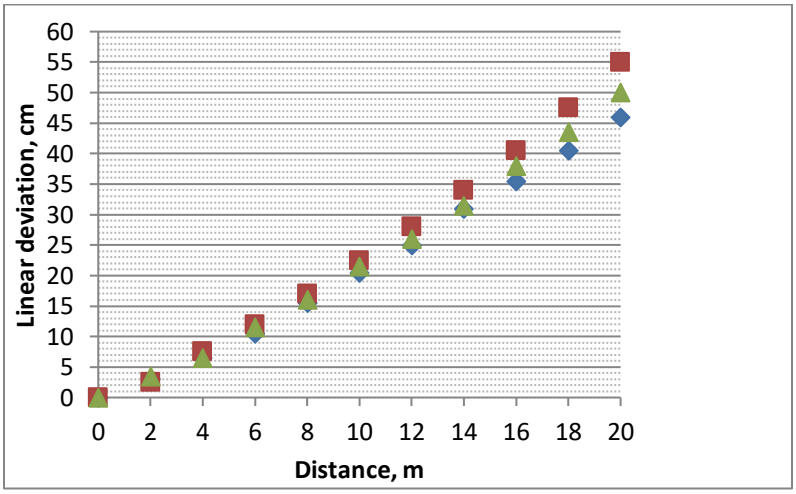

Fig. 4.26 Linear deviation for the platform without steering

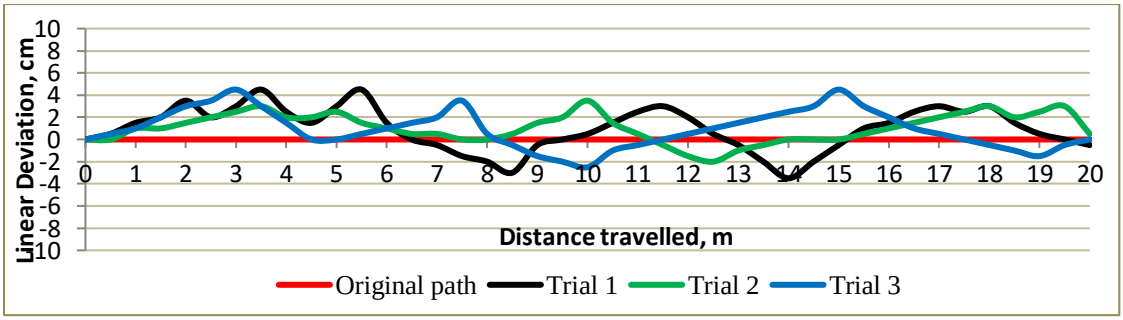

Fig. 4.27 Linear deviation for the platform with steering control

b. Range of communication

The Flysky FS i6 was featured with a maximum of 1000 m communication range. It was verified in the lab study and concluded that the user could control the prototype successfully within a range of 500 m in its line of sight. Similarly, the range was tested for the V380 camera. The wireless IP camera transmitted the real-time video effectively within 50 m and beyond that the signal strength decreases. For long range video transmission, the camera and the V380 app should be provided with internet connection and had to be connected to cloud network like IoT (Internet of Things).

c. Effectiveness of control unit

The prototype was analysed for the effectiveness of control unit. The control unit functioned satisfactorily for every command by the user, at no-load condition of wheels. Under loaded condition, the prototype performed inadequately for the commands. The prototype could perform the forward motion, reverse motion and sprayer operations, but unable to perform the complete skid turn. This inadequacy was caused by drive mechanism. The drive motors could not carry the entire load during skid-turning.

A laboratory experiment was taken up for analyzing the effectiveness of control unit for performance control and row-guidance according to the operator instructions (Fig. 4.28). Tomato plants in grow bags (available) were taken as the representative crop to form 10 m length crop row having an inter-row spacing of 60 cm and intra-row spacing of 60 cm. The average plant height was 85 cm. The travel speed of the prototype was tested as 0.125 ms^{-1}. The experiment showed that the operator could guide the prototype in between the rows without damaging the plants. The forward and reverse motion was controlled successfully but the turning motion was not satisfied with this unit. Instead of accomplishing a complete skid turn, maximum of 30-40° steering was acquired. The area covered by the prototype was calculated to be 0.0355 hah^{-1}.

Fig. 4.28 Laboratory experiment

4.6.2 Field evaluation

A basic field trial for the developed prototype was conducted on an experimental chilli plot of 0.01 ha, with head lands on both ends, for its performance evaluation (Fig. 4.29 a). While operating on the field it was observed that a non-uniform distribution of load on each ground-contact point occurred due to the undulated terrain. This resulted on suspension of wheels at non-contact points, because load would be completely carried out by the contacting points. In this condition, the drive motors were unable to propel the robot. Wheels were also subjected to sinkage due to soil compaction which resulted in wheel slip. Therefore, the tractive forces could not overcome the force due to soil resistance. The smaller wheel diameter increases the effect of soil resistance. The propulsion of the prototype was accomplished with external human assistance sometimes to complete the tests (Fig. 4.29 b). The signals from the transmitter were processed by the control unit satisfactorily. But the constraints in the drive mechanism limited its motion in the field. The performance indices of the prototype were determined and given in Table 4.10 and Appendix VI.

(a) **(b)**

Fig. 4.29 Field evaluation

4.6.2.1 Time of operation: Time required for operating the robot in 0.01 ha plot was measured to be 0.316 h.

4.6.2.2 Field capacity: The total time (productive and non-productive) taken by the robot during field operation was noted. The effective field capacity of the prototype was calculated using the equation 3.15 and it was 0.0217 hah^{-1}. The field coverage by the prototype was also calculated to be 0.0164 hah^{-1}.

4.6.2.3 Field efficiency: TFC was calculated using the equation 3.16. The speed of operation of the prototype in the field was lesser than the values obtained under laboratory conditions. The operating speed determined from the field was 0.04 ms^{-1}. The calculated value of TFC was 0.05 hah^{-1}. The field efficiency was less than 50% which indicated that the assumption of theoretical speed was not conforming to the actual field condition, especially due to the wheel slip and related inadequacies in the drive system.

4.6.2.4 Plant damage: The plant damage caused by the working of the prototype was assessed. As the machine was operated over short crops, no considerable plant damage

occurred. 1.8 % was the plant damage observed from the experimental field and was mainly due to inadequate steering control by the user.

During operation, wheel sinkage was observed at some points. It was due to the impact of higher load acting on loose soil condition. Wheel sinkage was observed to be high which prompted the redesign of wheel diameter.

Table 4.10 Performance indices of prototype

Sl. No.	Parameters	Average value
1	Time of operation, hha^{-1}	31.60
2	Theoretical field capacity, hah^{-1}	0.05
3	Effective field capacity, hah^{-1}	0.0217
4	Field efficiency, %	43.4
5	Plant damage, %	1.8
6	Sinkage, cm	3

The field capacity of the prototype was less than an Autonomous Plant Inspection (API) platform developed by Pedersen *et al.* (2006). The API platform had 1 m track width, 0.6 m ground clearance, 2 m working width and 1.8 kmph operating speed. It helped to reduce the application rate of herbicides in comparison with the conventional methods. However the initial investments were relatively higher, which was not affordable to common farmers.

4.6.3 Cost estimation

The overall cost involved in the development of the prototype was estimated and shown in Table 4.11. One third of the total cost was accounted for the drive motors.

Table 4.11 Estimated cost of prototype

Sl. No.	Components	Quantity	Approx. cost, Rs.
1.	Materials for chassis fabrication	1	2000
2.	Geared DC motor, 12V	6	12000

3.	L298N motor drivers	3	500
4.	Rubber wheels	12	2500
5.	Lead-acid battery, 12 V 35 Ah	1	4000
6.	Arduino Mega 2560	1	900
7.	Flysky FS i6 six-channel transmitter remote controller with FS iA6 receiver	1 set	3800
8.	Switched mode power supply (SMPS), 12 V 10A and voltage regulator	1 set	1000
9.	V380 Wireless IP camera	1	1500
10.	LM296 buck converter	2	200
11.	DC motor operated cable drive slider mechanism	2	1400
12.	Relays circuit module and relays	1 set	500
13.	Limit switches	4	200
14.	High pressure diaphragm pump, 12 V	1	1000
15.	Sprayer unit accessories	-	1000
16.	Components for electrical wiring	-	1000
17.	Miscellaneous	-	2500
			36000

4.7 Design for a modified semi-autonomous robotic platform

The developed prototype could not operate effectively in the field because of insufficient drive motor characteristics; the maximum torque capacity of the motor had reduced and failed eventually after several attempts to operate in the field. Similarly, the wheel diameter assumed was not appropriate. This smaller wheel diameter increases the effect of rolling resistance and sinkage. The developed functional units of the prototype except the drive unit works satisfactorily. This necessitated in designing a modified

prototype for semi-autonomous robotic platform to operate in the field with good terrainability, trafficability and mobility features.

4.7.1 Modification of drive mechanism

The testing of developed prototype envisages the requirement of a modified drive mechanism for the robotic platform. The modified platform should consist of high torque drive motors, high power motor drivers and large wheel diameter. Modification of driving mechanism includes the selection of suitable drive motor and their replacement along with its controllers based on the observed traction requirement for the robotic platform. The geared DC motors used in electric motor cycle would be strong enough to drive the platform. They are 24V brushed DC motor having 8 Nm rated torque and 300 RPM rated speed. The specifications of the motor are given in Table 4.12. The Arduino control of this high power motor would be accomplished via a high power motor driver module. The BTS7960 is a fully integrated high current half bridge driver module used for motor drive applications. It is a part of NovalithIC^{TM} family consisting of a P-channel high-side Metal Oxide Semiconductor Field Effect Transistor (MOSFET) and a N-channel low-side MOSFET with an integrated driver IC (74HC244 chip) in one package. It is featured with logic level inputs. This integrated driver IC effectively isolates the microcontroller and motor driver, and protects the Arduino from over-voltage, over-current, under-voltage, short circuit and over-temperature. It can handle maximum current up to 43A and operating frequency (PWM) up to 25 kHz combined with active freewheeling. The specifications of BTS7960 are given in Table 4.13.

Table 4.12 Specifications of the drive motor

Model number	MY1016Z
Voltage	24 V DC
Rated speed (after reduction)	300 RPM
Full load current	13.4 A
No load current	2.2 A

Output power	250 W
Rated torque	8 Nm
Stall torque	40 Nm
Efficiency	78%
Weight	1.9 kg

Table 4.13 Specifications of BTS7960 motor driver

Model number	IBT-2
Input voltage	6 – 27 V
Maximum current	43 A
Operating Frequency	25 kHz
Input level	3.3 – 5 V
Control mode	PWM
Duty cycle	0 – 100 %

The conceptual design was developed for a modified robotic platform (Fig. 4.30). The same chassis, with some alterations, could be utilized for the modified design. A four-wheel drive mechanism, using four 24 V geared DC motor, was conceptualized for the robot. Its motion control would be accomplished by the skid-steering mechanism. A suspension (shock absorber) could be provided on each leg to maintain uniform load distribution on each ground-contact points. In order to avoid sinkage and accomplish better terrainability, the wheel diameter had to be enhanced. Four pneumatic wheels having 30.48 cm (12 inch) diameter and 12.7 cm (5 inch) width were selected for this design. The motor speed (300 RPM) has to be lowered to a required speed of 30 RPM, which could also enhance the output torque. Therefore, a reducer unit with 10:1 transmission ratio was required to be employed. The DC motor and wheel were coupled

via the reducer unit. Two 12V 60 Ah battery connected in series could serve as the energy input for the system.

The torque exerted by the motor with reducer ($\tau_{exerted}$) could be calculated using equation 3.13.

$$\tau_{exerted} = \frac{250 * 60}{2\pi * 30} = 79.6\ Nm$$

The maximum forward velocity achievable by the modified robot, with a rated speed of 30 RPM and wheel diameter 30.48 cm approximately, was also calculated as below:

$$v = \frac{\pi * 0.3 * 30.48}{60} = 0.478\ ms^{-1}$$

The gross weight of the robot was approximated to 70 kg and the net tractive force acting on the moving robot was calculated as 254.24 N, using the equation given in section 3.2.3.2. Therefore the torque required for driving the prototype would be

$$\tau_{total} = 254.24 * \frac{30.48}{2} * \frac{1}{100} = 38.13\ \text{Nm}$$

Considering a factor of safety of 1.2,

$$\tau_{total} = 38.13 * 1.2 = 45.76.11\ Nm$$

$$Required\ torque\ on\ each\ motor, \tau_{each\ motor} = \frac{45.76}{4} = 11.44\ Nm$$

Torque exerted by the selected motor was higher than the required torque. Hence, the design was safe.

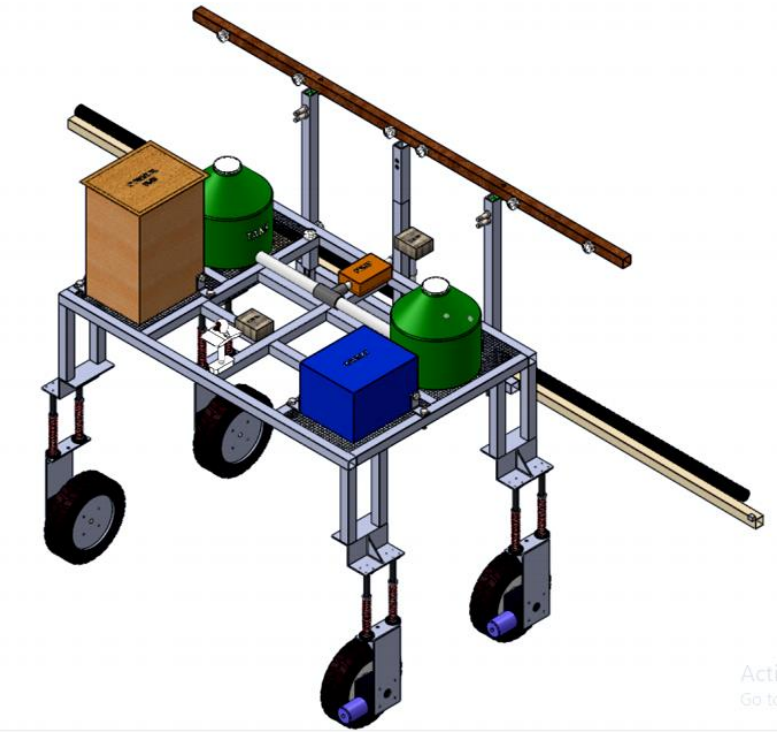

Fig. 4.30 Conceptual design of the modified robotic platform

Table 4.14 Estimated cost of modified semi-autonomous robotic platform

Sl. No.	Components	Quantity	Approx. cost, Rs.
1.	Materials for chassis fabrication with suspension	1 set	4000
2.	Geared DC motor, 24 V	4	18000
3.	Reducer unit	4	6000
4.	BTS7960 motor drivers	2	2000
5.	Pneumatic wheels, 12 inch diameter	4	5000
6.	12 V 60 Ah Lithium-ion battery	2	15000
7.	Arduino Mega 2560	1	900
8.	Flysky FS i6 six-channel transmitter remote controller with FS iA6 receiver	1 set	3800

9.	Switched mode power supply (SMPS), 12 V 10A and voltage regulator	1 set	1000
10.	V380 Wireless IP camera	1	1500
11.	LM296 buck converter	2	200
12.	DC motor operated cable driver slider mechanism	2	1400
13.	Relays circuit module and relays	1 set	500
14.	Limit switches	4	200
15.	High pressure diaphragm pump, 12 V	1	1000
16.	Sprayer unit accessories	-	1000
17.	Components for electrical wiring	-	1000
18.	Miscellaneous	-	2500
			65000

Summary and Conclusion

CHAPTER V

SUMMARY AND CONCLUSION

The world population is increasing tremendously and expected to be 9.7 billion by 2050. The agriculture production should enhance by 70 % by 2050 but it is estimated to increase by 25 % only. Agriculture is the primary source of livelihood in many countries and the Indian economy mainly depends on agricultural sector which accounts for 18% of India's Gross Domestic Product (GDP). The efficiency and productivity of agriculture has to be improved to meet the various challenges in food production, including climate change. The conventional farming methods are struggling for survival due to labour shortage which makes agriculture uneconomical and inefficient. This has led to the increased use of agricultural machines, even though they are costly. The emerging means to tackle labour shortage is by technological process, through the application of automation and robotics in agriculture. Automation in agriculture has emerged as a promising methodology for increasing the crop productivity without sacrificing the product quality, by saving time and labour, using specified tools and technology. Because of reduced soil compaction, less impact on environment, low cost, less input energy required, multi-purpose use and high precision, most of the researchers are interested in developing smaller autonomous farm vehicles instead of larger machines.

The present advancements in programming and technology have made robotics easy and less complicated. In addition to the technological easiness, the cost factor should also be considered such that it is compatible to the common farmer. Hence a robotic platform, capable of providing all the advantages of agrobots at reduced cost could boost the pace of advancement of Indian agriculture. In most of the countries, intercultural operations are carried out by human labourers and it is a tedious process. In Kerala, no notable research works were carried out in the field of agricultural automation. Therefore, this investigation was undertaken aiming at the development of a semi-autonomous robot capable of performing intercultural operations on row crops.

A semi-autonomous robotic platform which was conceptualized for performing the intercultural operations in row crops would be required to move through the space

between the rows and perform the intended operations like spraying. It should be capable of navigating within the field and performing the intended operation according to the user command. A wireless remote controller could be used to transmit the control signals from the operator and the signals received by the robot would be processed, via a microcontroller unit, for achieving the output functions.

The agronomic characteristics of the crop (Chilli) affecting the design of robotic chassis were assessed. The crop spacing and plant height were the parameters considered in this study. The plant height would be changing throughout its growth period and the maximum plant height might vary according to the crop variety cultivated. Therefore, the plant height at its various growth stages was recorded for determining the maximum height. These agronomic parameters determined the wheel track and height of the robotic chassis. The track width of the chassis depends upon the row spacing and the number of crop rows to be covered in single span. As the crop spacing differed with the variety used, a variable chassis had to be provided for changing its track width from a minimum of 75 cm to a maximum of 135 cm. The optimum plant height was recorded as 100 cm. As the prototype would be operating over the crop, a maximum ground clearance of 100 cm was allocated in order to avoid the plant damage. A rectangular carriage having a length of 135 cm and breadth of 80 cm was provided for the chassis. The carriage was supported by six legs for six-wheel independent drive mechanism. Thus the basic dimension of the chassis was 135 cm × 80 cm × 100 cm.

The wheel variables were decided based on the rolling resistance and terramechanics relationships. It was concluded that larger diameter had lesser effect on the rolling resistance and sinkage. But it could increase the net torque required on the wheel which in turn increase the total power requirement of the robot. Therefore, a medium-sized rubber wheels with 12.7 cm (5 inch) diameter and 2.54 cm (1 inch) width was selected based on its market availability and cost. One of the important aspects in consideration for the development of a mobile robot was the selection of drive motors. The capacity of the motor to drive the robot would be indicated with reference to motor torque. Gross weight of the robot (55 kg), wheel diameter (12.7 cm) and velocity of travel

(0.2 ms^{-1}) are parameters which decide traction characteristics. The net force acting on the moving robot was calculated to be 199.75 N (20.38 kg_f). Therefore the total torque acting on the robot was 129.43 kg_f-cm and the torque on each motor was 21.57 kg_f –cm. The rotational speed for the motor was obtained as 30 RPM.

A six-wheel drive skid-steering drive mechanism was provided to the robot. Six high torque 12V DC geared motors with stall torque of 140 kg_f-cm and a no-load speed of 27 rpm were used as drive motors. The movement of the robotic platform could be controlled by directing the rotation of drive motors using a pre-programmed microcontroller with the help of motor drivers. Arduino Mega was the microcontroller used which was interfaced with the motors via L298N motor driver. Since the drive motor had a dual-type output shaft, two wheels were connected to a single motor which resulted in 12.5 cm effective wheel width. Three motor drivers were used for driving six dc motors, in which each motor driver was connected to the dc motors on each side. All the drivers received the same output signals from the microcontroller which enabled uniform motion for the motors on each side, i.e., motors on each side were driven by same signals from the microcontroller. A wireless control system was based on Radio Frequency (RF) protocol using Flysky FS i6 2.4GHz Six-channel Transmitter Remote Controller with FS-iA6 Receiver unit. This wireless control system could govern the robot's operations, viz, the forward movement, reverse movement, left-side turn or right-side turn of the robotic platform, switching ON/OFF the spray pump, lowering or raising of the sprayer boom unit, and bending or straightening of the sprayer boom.

The width of operation was one of the design considerations adopted during the development of the sprayer unit. A 3.35 m spray boom was provided to the boom which also helped to improve the field coverage with minimum mobility of the platform. The sprayer unit was designed to be operated for spraying the liquid formulations over the crop. As the crop height varied in its different growth stages, the boom position had to be changed accordingly. Similarly, the boom needed to be folded when not operated. Therefore, geared DC motor operated cable drive slider mechanisms were employed for

changing the boom positions. A simple and robust method for sprayer control was by means of relays with relay driver interfacing circuits.

For a semi-autonomous robot, the motion and direction control was carried out by human interactions. A V380 Wireless IP Camera having 720-pixel resolution was used which allows two-way live video communications. The camera is configured with the smart phone using the "V380 app", which helped to monitor the real-time data captured and control the motion of the camera. All the functional components of the rover and the drive motors were powered by means of a battery. A 12 V 35 Ah battery was selected which was sufficient to power the entire system. LM2596 buck converters were used for stepping down the input voltage 12 V to 5 V.

The control unit was developed as the principal control unit of the robotic platform for governing the operations to be carried out. It comprised of the microcontroller, motor drivers, voltage regulators, wireless receiver unit, relay driver circuit, DPDT relays, jumper wires and other terminal connectors. After proper circuit connection of all hardware components, the microcontroller was programmed in Arduino IDE software using C++ language. After developing the functional components, they were assembled on to the chassis. The geared motors with wheels were mounted at the bottom of the leg and sprayer unit was attached on the rear portion. The control unit, battery, wireless camera, spray tanks, spray pump and DC motors in slider mechanism were arranged on the top of the chassis carriage in such a way to result in an uniform load distribution.

The salient findings obtained from the evaluation of the developed prototype in both laboratory and field conditions are listed below:

- The weight of the prototype was less than other agricultural robotic platforms. It helped to reduce the soil compaction and improved hours of operation.
- The speed of travel obtained was less than the desired speed (0.2 ms^{-1}).
- The actual power consumed by the prototype for its self-propulsion was 97.57 W without payload and 125.29 with payload. The total power consumed by the prototype was 246.56 W without payload and 359.31W with payload. The total

power consumed by the prototype increased with increase in the load and was much higher than the actual power estimated. These variations were likely to be due to the electromechanical losses in the robot drive and control system.

- The average linear deviation of the platform from a straight path, without steering assistance was recorded as 50.33±4.5 cm. Deviation could be rectified by proper steering control.
- The communication range obtained with the Wi-Fi camera was 50 m and less than 500 m for the wireless control unit.
- The control unit functioned satisfactorily for every command by the user, at no-load condition of wheels. Under loaded condition, the prototype performed inadequately for the commands. It could perform forward motion, reverse motion and sprayer operations, but was unable to turn properly. The drive motors were not capable of withstanding the load requirement during skid-turning, as the power required during turning was greater than that for forward/reverse motion.
- A non-uniform distribution of load on each ground-contact point occurred due to the undulated terrain. The wheels were also subjected to sinkage resulting in wheel slip. The rolling resistance and effect of sinkage increased due to smaller wheel diameter. Therefore the drive motors could not propel the robot in such conditions.

The developed functional units of the prototype except the drive unit worked satisfactorily. This necessitated in redesigning it to develop a modified prototype with good terrainability, trafficability and mobility features.

Modified design

The same chassis, with some alterations, could be utilized for the modified design. A four-wheel drive mechanism, using four 24 V geared DC motors, was conceptualized for the robot. The drive mechanism of the modified design comprised of high torque motors, high power motor drivers and larger diameter pneumatic wheels. 24 V brushed DC motors having 8 Nm rated torque and 300 RPM rated speed were selected to be used in the modified prototype. A high power motor driver module BTS7960 was

selected for their control. A suspension was required to be provided on each leg to maintain uniform load distribution on each ground-contact points. Four pneumatic wheels having 30.48 cm diameter and 12.7 cm width were selected for this design. The motor speed (300 RPM) should be lowered to a required speed of 30 RPM, which could also enhance the output torque. Therefore, a reducer unit with 10:1 transmission ratio needs to be employed. Two 12 V 60 Ah battery connected in series could serve as the power source for the system. The torque exerted by the motor with reducer would be 79.6 Nm which was higher than the required torque on each motor. Therefore, the design would be safe. The cost for modified prototype was estimated to be Rs.65000/-.

The dead load of the chassis could also be lowered by using less weight- high strength materials like Carbon Fibre Reinforced Polymer (CFRP) or Aluminium alloys. Similarly, the lead acid batteries could be replaced with Lithium Polymer batteries for reducing battery weight.

Future scope of work

- The platform can serve as a multipurpose agricultural robot with the attachment of suitable gadgets. The soil conditions like pH, temperature, moisture content etc. along with agro-climatic parameters like humidity and atmospheric temperature can be monitored if suitable sensors are mounted on the platform.
- Automatic weed control unit using image processing technique may be employed with the platform. Crop and field monitoring can be accomplished with the robotic platform.
- The battery powered platform can be modified with a solar power unit in order to make use of renewable energy as well as to improve hours of operation.

References

REFERENCES

Adamides, G., Katsanos, C., Constantinou, I., Christou, G., Xenos, M., Hadzilacos, T. and Edan, Y. 2017a. Design and development of a semi-autonomous agricultural vineyard sprayer: Human-robot interaction aspects. *J. Field Robotics*. 34(8): 1407-1426.

Adamides, G., Katsanos, C., Parmet, Y., Christou, G., Xenos, M., Hadzilacos, T. and Edan, Y. 2017b. HRI usability evaluation of interaction modes for a tele-operated agricultural robotic sprayer. *Appl. Ergonomics*. 62: 237-246.

Aishwarya, B. V., Archana, G. and Umayal, C. 2015. Agricultural robotic vehicle based pesticide with efficiency optimization. In *2015 IEEE Technological Innovation in ICT for Agriculture and Rural Development (TIAR). IEEE*. pp.59-65.

Akbar, S. A., Chattopadhyay, S., Elfiky, N. M. and Kak, A. 2016. A novel benchmark RGBD dataset for dormant apple trees and its application to automatic pruning. In *Proceedings of the IEEE conference on computer vision and pattern recognition workshops.* pp: 81- 88.

Al-Sahib, N. K. A. and Azeez, M. Z. 2015. Build and Interface Internet Mobile Robot using Raspberry Pi and Arduino. *Innovative Syst. Des. & Eng.* 6(1): 106-114.

Amer, G., Mudassir, S. M. M. and Malik, M. A. 2015. Design and operation of Wi-Fi Agribot Integrated system. In *2015 International Conference on Industrial Instrumentation and control (ICIC), IEEE.* pp: 207-212.

[Anonymous]. 2019. Department of Agriculture, Cooperation & Farmers Welfare. http://agricoop.nic.in/sites/default/files/AR_2018-19_Final_for_Print.pdf [1 March 2020].

Arefi, A., Motlagh, A. M. and Teimourlou, R. F. 2010. A segmentation algorithm for the automatic recognition of tomato at harvest. *J. Food Agric. & Environ*. 8(3-4): 815-819.

Arguenon, V., Bergues-Lagarde, A. Rosenberger, C., Bro, P. and Smari, W. 2006. Multi-agent based prototyping of agriculture robots. *In Collaborative technologies and systems (CTS), International Symposium, IEEE*. pp: 282-288.

Azeta, J., Bolu, C. A., Hinvi, D., Abioye, A. A., Boyo, H., Anakhu, P. and Onwordi, P. 2019. An Android Based Mobile Robot for Monitoring and Surveillance. 2nd international conference on sustainable materials processing and manufacturing (SMPM). *Procedia Manufacturing*. 35:1129–1134.

AuatCheein, F.A. and Carelli, R. 2013. Agricultural robotics: Unmanned robotic service units in agricultural tasks. *IEEE: Industrial Electronics Magazine*. 7(3): 48-58. http://doi.org/10.1109/MIE.2013.2252957.

Bac, C. W., Henten, E. J., Hemming, J. and Edan, Y. 2014. Harvesting robots for high-value crops: State-of-the-art review and challenges ahead. *J. Field Robotics*. 31(6): 888-911.

Bak, T. and Jakobsen, H. 2004. Agricultural Robotic Platform with Four-Wheel Steering for Weed Detection. *Biosystems Eng*. 87(2): 125–136.

Bakker, T., Wouters, H., van Asselt, K., Bontsema, J., Tang, L. and Muller, J.. 2008. A vision based row detection system for sugar beet. *Comput. & Electr. Agric*. 60(1): 87-95.

Bakker, T., Van Asselt, K., Bontsema, J., Muller, J. and Van Straten, G. 2011. Autonomous navigation using a robot platform in a sugar beet field. *Biosystems Eng*. 109(4): 357-368.

Bawden, O., Ball, D., Kulk, J., Perez, T. and Russell, R. 2014. A Lightweight, Modular Robotic Vehicle for the Sustainable Intensification of Agriculture. *Proceedings of the 16th Australasian Conference on Robotics and Automation.* Australian Robotics and Automation Association Inc., Australia. pp: 1-9.

Bechar, A. and Vigneault, C. 2016. Agricultural robots for field operations: Concepts and components. *Biosystems Eng.* 149: 94-111. http://doi.org/10.1016/J.BIOSYSTEMSENG.2016.06.014.

Bechar, A. and Vigneault, C. 2017. Agricultural robots for field operations. Part 2: Operations and systems. *Biosystems Eng.* 153: 110-128. http://doi.org/10.1016/J.BIOSYSTEMSENG.2016.11.004.

Bekker, M.G. 1956. *Theory of Land Locomotion*. University of Michigan Press. 522p.

Belforte, G., Deboli, R., Gay, P., Piccarolo, P. and Aimonino, D. R. 2006. Robot design and testing for greenhouse applications. *Biosystems Eng*. 95(3): 309-321.

Bell, T. 2000. Automatic tractor guidance using carrier-phase differential GPS. *Comput. & Electr. Agric*. 25(2): 53–66. http://doi:10.1016/s0168-1699(99)00055-1.

Benson, E. R., Reid, J. F. and Zhang, Q. 2003. Machine vision-based guidance system for an agricultural small-grain harvester. *Trans. ASAE*. 46(4): 1255-1264.

Bergtold, J. S., Raper, R. L. and Schwab, E. B. 2009. The economic benefit of improving the proximity of tillage and planting operations in cotton production with automatic steering. *Appl. Eng. Agric*. 25(2): 133-143.

Bochtis, D. D., Sorensen, C. G. and Busato, P. 2014. Advances in agricultural machinery management: A review. *Biosystems Eng*. 126: 69-81. http://doi.org/10.1016/j.biosystemseng.2014.07.012.

Bokade, A. U. and Ratnaparkhe, V. R. 2016. Video Surveillance Robot Control using Smartphone and Raspberry Pi. *IEEE: International Conference on Communication and Signal Processing*. pp: 2094-2097.

Bonadies, S. and Gadsden, S.A. 2019. An overview of autonomous crop row navigation strategies for unmanned ground vehicles. *Eng. Agric., Environ. & Food*. *12*(1): 24-31.

Budiharto, W. 2014. Design of Tracked Robot with Remote Control for Surveillance. *Proceedings of the 2014 International Conference on Advanced Mechatronic Systems*. pp: 342-346.

Bulanon, D. A., Burks, T. E. and Alchanatis, V. 2009. Fruit visibility analysis for robotic citrus harvesting. *Trans. Asabe*. 52(1): 277-283.

Ceccarelli, M., Figliolini, G., Ottaviano, E., Mata, A. S. and Criado, E. J. 2000. Designing a robotic gripper for harvesting horticulture products. *Robotica*. 18: 105-111.

Ceres, R., Pons, F. L., Jimenez, A. R., Martin, F. M. and Calderon, L. 1998. Design and implementation of an aided fruit harvesting robot (Agribot). *Ind. Robot*. 25(5): 337.

Cheein, F. A., Steiner, G., Paina, G. P. and Carelli, R. 2011. Optimized eif-slam algorithm for precision agriculture mapping based on stems detection. *Comput. & Electr. Agric.* 78(2): 195-207.

Chen, L. Q., Wang, P. P., Zhang, P., Zheng, Q., He, J. and Wang, Q. J. 2018. Performance analysis and estimation of a maize inter-row self-propelled thermal fogger chassis. *Int. J. Agric. & Biol. Eng*. 11(5): 100-107.

Cho, S. I., Chang, S. J., Kim, Y. Y. and An, K. J. 2002. AE - automation and emerging Technologies: Development of a three-degrees-of-freedom robot for harvesting lettuce using machine vision and fuzzy logic control. *Biosystems Eng*. 82(2): 143-149.

Choi, K. H., Han, S. K., Han, S. H., Park, K. H., Kim, K. S. and Kim, S. 2015. Morphology-based guidance line extraction for an autonomous weeding robot in paddy fields. *Comput. & Electr. Agric*. 113: 266-274.

Coccia, M. 2013. Driving forces of technological change: The relation between population growth and technological innovation. *Technological Forecast. and Social Change.* 82: 52–65. http://doi:10.1016/j.techfore.2013.06.001.

Cook, J. T. and Frank, D. A. 2008. Food security, poverty, and human development in the United States. *Annals of the New York Academy of Sciences*. 1136(1): 193-209.

Cordesses, L., Thuilot, B., Martinet, P. and Cariou, C. 2000. Curved Path Following of a Farm Tractor Using a CP-DGPS. *IFAC Proc.* 33(27): 489–494. http://doi:10.1016/s1474-6670(17)37977-6.

Corollaro, M. L., Aprea, E., Endrizzi, I., Betta, E., Dematt‘e, M. L., Charles, M., Bergamaschi, M., Costa, F., Biasioli, F., Grappadelli, L.C. and Gasperi, F. 2014. A combined sensory-instrumental tool for apple quality evaluation. *Postharvest Biol. & Technol.* 96: 135-144.

Cui, Y., Gejima, Y., Kobayashi, T., Hiyoshi, K. and Nagata, M. 2013. Study on Cartesian-type strawberry-harvesting robot. *Sensor Lett*. 11(6-7): 1223-1228.

Dar, I., Edan, Y. and Bechar, A. 2011. An adaptive path classification algorithm for a pepper greenhouse sprayer. *Paper presented at the American Society of Agricultural and Biological Engineers Annual International Meeting*, August 7-10. Louisville, Kentucky. p1.

Dattatraya, G. D., Mhatardev, M. V., Shrihari, L. M. and Joshi, S. G. 2014. Robotic Agriculture Machine. *Int. J. Innovative Res. Sci., Eng. & Technol.* 3(4): 454-462

Davidson, J. R., Hohimer, C. J. and Mo, C. 2016. Preliminary Design of a Robotic System for Catching and Storing Fresh Market Apples. *IFAC-PapersOnLine.* 49(16): 149–154.

De-An, Z., Jidong, L., Wei, J., Ying, Z. and Yu, C. 2011. Design and control of an apple harvesting robot. *Biosystems Eng*. 110(2): 112-122.

Decker, M., Fischer, M. and Ott, I. 2017. Service robotics and human labor: A first technology assessment of substitution and cooperation. *Robotics & Autonomous Syst*. 87: 348-354. http://doi.org/10.1016/J.ROBOT.2016.09.017.

Dhahri, S. and Omri, A. 2020. Foreign capital towards SDGs 1 & 2– Ending Poverty and hunger: The role of agricultural production. *Struct. Change & Econ. Dyn.* 53: 208-221. http://doi:10.1016/j.strueco.2020.02.004.

Diels, E., Odenthal, T., Keresztes, J., Vanmaercke, S., Verboven, P., Nicolai, B., Saeys, W., Ramon, H. and Smeets, B. 2016. Development of a visco-elastoplastic contact force model and its parameter determination for apples. *Postharvest Biol. & Technol*. 120: 157-166.

Dixit, D. S. and Dhayagonde, M. S. 2014. Design and implementation of e-surveillance robot for video monitoring and living body detection. *Int. J. Sci. & Res. Publ*. 4(4): 297-299.

Donis-Gonzalez, I. R., Guyer, D. E. and Pease, A. 2016. Postharvest non-invasive classification of tough-fibrous asparagus using computed tomography images. *Postharvest Biol. & Technol*. 121: 27-35.

Eberhardt, M. and Vollrath, D. 2018. The effect of agricultural technology on the speed of development. *World Dev*. 109: 483-496. http://doi.org/10.1016/J.WORLDDEV.2016.03.017.

Edan, Y., Shufeng, H. and Naoshi, K. 2009. Automation in Agriculture. *Springer Handbook of Automation, Springer*. pp: 1095-1128.

Food and Agriculture Organization. 2009. *How to feed the world in 2050.* Technical Report. p.1. http://www.fao.org/wsfs/forum2050/wsfs-forum/en/.

Fennimore, S.A., Slaughter, D.C., Siemens, M.C., Leon, R.G. and Saber, M.N. 2016. Technology for automation of weed control in specialty crops. *Weed Technol.* 30(4): 823–837.

Ferdoush, S. and Li, X. 2014. Wireless Sensor Network System Design using Raspberry Pi and Arduino for Environmental Monitoring Applications. The 9th International Conference on Future Networks and Communications. *Procedia Comput. Sci.* 34: 103-110.

Gat, G., Gan-Mor, S. and Degani, A. 2016. Stable and robust vehicle steering control using an overhead guide in greenhouse tasks. *Comput. & Electr. Agric.* 121: 234-244.

Gohiya, C. S., Sadistap, S. S., Akbar, S. A. and Botre, B. A. 2013. Design and Development of Digital PID Controller for DC Motor Drive System Using Embedded Platform for Mobile Robot. *3rd IEEE International Advance Computing Conference* (IACC). pp.52-55.

Gonzalez-de-Soto, M., Emmi, L., Garcia, I. and Gonzalez-de-Santos, P. 2015. Reducing fuel consumption in weed and pest control using robotic tractors. *Comput. & Electr. Agric.* 114: 96-113.

Grimstad, L., Pham, C. D., Phan, H. T. and From, P. J. 2015. On the design of a low-cost, light-weight, and highly versatile agricultural robot. In *Paper presented at the 2015 IEEE international workshop on advanced robotics and its social impacts (ARSO)*. pp: 1-6.

Grimstad, L. and Johan, P. 2017. Thorvald II - a Modular and Re-configurable Agricultural Robot. *IFAC PapersOnLine.* 50 (1): 4588–4593.

Grift, T. 2007. Robotics in Crop Production. *Encyclopedia of Agric., Food, & Biol. Eng.* pp: 1-3.

Guo, T., Guo, J., Huang, B. and Peng, H. 2019. Power consumption of tracked and wheeled small mobile robots on deformable terrains–model and experimental validation. *Mechanism and Machine Theory*. 133: 347-364.

Hague, T., Marchant, J. A. and TIllet, N. D. 2000. Ground based sensing systems for autonomous agricultural vehicles. *Comput. & Electr. Eng.* 25(1-2): 11-18.

Hassan, M. U., Ullah, M. and Iqbal, J. 2016. Towards autonomy in agriculture: Design and prototyping of a robotic vehicle with seed selector. *In Robotics and artificial intelligence (ICRAI), 2016 2nd international conference*. pp: 37-44.

Hayashi, S., Shigematsu, K., Yamamoto, S., Kobayashi, K., Kohno, Y., Kamata, J. and Kurita, M. 2010. Evaluation of a strawberry-harvesting robot in a field test. *Biosystems Eng.* 105: 160-171.

Hiremath, Van der Heijden, G. W. A. M., Van Evert, F. K., Stein, A., and Ter Braak, C. J. F. 2014. Laser range finder model for autonomous navigation of a robot in a maize field using a particle filter. *Comput. & Electr. Agric*. 100: 41-50.

Hoyo, A., Guzman, J. L., Moreno, J. C. and Berenguel, M. 2015. Teaching Control Engineering Concepts using Open Source tools on a Raspberry Pi board. *IFAC-PapersOnLine.* 48(29): 99-104.

Ishibashi, M., Iida, M., Suguri, M. and Masuda, R. 2013. Remote Monitoring of Agricultural Robot using Web Application. *4th IFAC Conference on Modelling and Control in Agriculture, Horticulture and Post Harvest Industry*. pp: 138-142.

Irie, N., Taguchi, N., Horie, T. and Ishimatsu, T. 2009. Asparagus harvesting robot coordinated with 3-D vision sensor. In *2009 IEEE International Conference on Industrial Technology.* pp. 1-6.

Jadhav, S. and Hambarde, S. 2016. Android based Automated Irrigation System using Raspberry Pi. *Int. J. Sci. & Res.* 5(6): 2345-2351.

Jinlin, X. and Liming, X. 2010. Autonomous Agricultural Robot and Its Row Guidance. *IEEE International Conference on Measuring Technology and Mechatronics Automation.* pp: 725-729.

Joe Joe, L. B., Tesfit, A. M., Temesgen, B. T., Temesgen, G. H. and James, P. S. 2019. Development of Microcontroller Based Drip-Irrigation Control System in Eritrea. *Trends in Biosci*. 12(3): 261-264.

Jokisch, B. D. 2002. Migration and agricultural change: The case of smallholder agriculture in highland Ecuador. *Human Ecol*. 30(4): 523-550.

Juman, M. A., Wong, Y. W., Rajkumar, R. K., Kow, K. W. and Yap, Z. W. 2019. An incremental unsupervised learning based trajectory controller for a 4 wheeled skid steer mobile robot. *Eng. Appl. Artif. Intell*. 85: 385-392.

Kadiyala, S., Harris, J., Headey, D., Yosef, S. and Gillespie, S. 2014. Agriculture and nutrition in India: mapping evidence to pathways. *Annals of the New York Academy of Sciences.* 1331(1): 43–56. http://doi:10.1111/nyas.12477.

Kajol, R., Kashyap, K. A. and Kumar T. G. K. 2018. Automated Agricultural Field Analysis and Monitoring System Using IOT. *Inf. Eng. & Electr. Business*. 11(2): 17-24.

Kashyap, C., Kashyap, B. Y., Guruprasad, K., Shrinivasa, D. and Shrivastava, P. K. 2019. Recent Development of Automation and IoT in Agriculture. *Int. J. Recent Technol. & Eng*. 8(2): 820-823.

KAU (Kerala Agricultural University) 2011. *Package of Practices Recommendations: Crops* (14th Ed.). Kerala Agricultural University, Thrissur, 360p.

Kebir, S. T,.Bouhedda, M., Mekaoui, S., Guesmi, M. and Douakh, A. 2016. Gesture Control of Mobile Robot Based Arduino Microcontroller. *IEEE: 8th International Conference on Modelling, Identification and Control (ICMIC)*. pp: 1081-1085.

Kepner, R.A., Beiner, R. and Barger, E.L. 1982. *Principles of farm machinery*. AVI Publ. 486 p

Khot, L. R., Tang, L., Blackmore, S. B. and Norremark, M. 2006. Navigational context recognition for an autonomous robot in a simulated tree plantation. *Trans. of the Asabe*. 49(5): 1579-1588.

Kim, Y. D., Yang, Y. M., Kang, W. S. and Kim, D. K. 2014. On the design of beacon based wireless sensor network for agricultural emergency monitoring systems. *Comput. Standards & Interfaces*. 36: 288-299.

Krinkin, K., Stotskaya, E. and Stotskiy, Y. 2016. Design and Implementation Raspberry Pi-based Omni-wheel Mobile Robot. *Proceeding of the Ainl-IsmwFruct Conference, IEEE*. pp: 39-45.

Kulkarni, C., Grama, S., Suresh, P.G., Krishna, C. and Antony, J. 2014. Surveillance Robot Using Arduino Microcontroller, Android APIs and the Internet. *Proceedings of 2014 First International Conference on Systems Informatics, Modelling and Simulation, IEEE.* pp: 83-87.

Lampridi, M. G., Kateris, D., Vasileiadis, G., Marinoudi, V., Pearson, S., Sørensen, C. G., Balafoutis, A. and Bochtis, D. 2019. A case-based economic assessment of robotics employment in precision arable farming. *Agron.* 9(4): 1-14. http://doi.org/10.3390/agronomy9040175.

Lin, H., Dong, S., Liu, Z. and Yi, C. 2015. Study and experiment on a wheat precision seeding robot. *J. Robotics.* pp: 1-9.

Lunadei, L., Diezma, B., Lleo, L., Ruiz-Garcia, L., Cantalapiedra, S. and Ruiz-Altisent, M. 2012. Monitoring of fresh-cut spinach leaves through a multi-spectral vision system. *Postharvest Biol. & Technol.* 63(1): 74-84.

Luo, L., Tang, Y., Zou, X., Ye, M., Feng, W. and Li, G. 2016. Vision based extraction of spatial information in grape clusters for harvesting robots. *Biosystems Eng*. 151: 90-104.

Madhusudhan, L. 2015. Agriculture Role on Indian Economy. *Business and Econ. J.* 6(4): 1.

Maria, E. and Ishii, K. 2019. Soil Compaction and Rolling Resistance Evaluation of a Locomotion System with an Adjustable Contact Patch for a Grape Transporting Robot. *J. Robotics, Networking & Artif. Life.* 6(3): 148–151.

Marinoudi, V., Sorensen, C. G., Pearson, S. and Bochtis, D. 2019. Robotics and labour in agriculture. A context consideration. *Biosystems Eng. 184: 111-121*. http://doi:10.1016/j.biosystemseng.2019.06.013.

McKibben, E. G. and Davidson, J. B. 1940. Transport wheels for agricultural machines IV. Effect of outside and cross-section diameters on the rolling resistance of pneumatic implement tires. *Agric. Eng.* 21(2): 57-58.

Mehta, S. S. and Burks, T. F. 2014. Vision-based control of robotic manipulator for citrus harvesting. *Comput. & Electr. Agric*. 102: 146-158.

Michler, J. D. 2020. Agriculture in the process of development: A micro-perspective. *World Dev.* 129: p.104888. http://doi:10.1016/j.worlddev.2020.104888.

Mohanty, S. K. and Mishra, S. 2019. Regulatory Reform and Market Efficiency: The Case of Indian Agricultural Commodity Futures Markets. *Res. Int. Business & Finance.* 52: p.101145. http://doi:10.1016/j.ribaf.2019.101145.

Moreno, F. A., Cielniak, G. and Duckett, T. 2013. Evaluation of laser rangefinder mapping for agricultural spraying vehicles. In *Conference towards autonomous robotic systems, Springer.* pp: 210-221.

Morimoto, E., Suguri, M. and Umeda, M. 2005. Vision-based navigation system for autonomous transportation vehicle. *Precision Agric*. 6(3): 239-254.

Munera, S., Besada, C., Blasco, J., Cubero, S., Salvador, A., Talens, P. and Aleixos, N. 2017. Astringency assessment of persimmon by hyper spectral imaging. *Postharvest Biol. & Technol.* 125: 35-41.

Nagasaka, Y., Umeda, N., Kanetai, Y., Taniwaki, K. and Sasaki, Y. 2004. Autonomous guidance for rice transplanting using global positioning and gyroscopes. *Comput. & Electr. Agric*. 43(3): 223-234.

Natu, A.S. and Kulkarni, S.C. 2016. Adoption and utilization of drones for advanced precision farming: A review. *Int. J. on recent & Innovation trends in Computing and commun.* 4(5): 563 – 565

Nof, S.Y. 2009. *Springer handbook of automation*. Springer Science & Business Media.1812p.

Noguchi, N. and Barawid Jr., O. C. 2011. Robot Farming System Using Multiple Robot Tractors in Japan Agriculture. *Proceedings of the 18th World Congress: The International Federation of Automatic Control Milano, Italy.* pp: 633-637.

Nuske, S., Achar, S., Bates, T., Narasimhan, S. and Singh, S. 2011. Yield estimation in vineyards by visual grape detection. In *Intelligent robots and systems (IROS). IEEE/RSJ international conference.* pp: 2352-2358.

Oberti, R., Marchi, M., Tirelli, P., Calcante, A., Iriti, M., Hŏcevar, M., Baur, J., Pfaff, J., Schütz, C. and Ulbrich, H . 2013. Selective spraying of grapevines diseases by a modular agricultural robot. *J. Agric. Eng.* 44: 149-153.

Oberti, R., Marchi, M., Tirelli, P., Calcante, A., Iriti, M., Tona, E., Hocevar, M., Baur, J., Pfaff, J., Schutz, C. and Ulbrich, H. 2016. Selective Spraying of Grapevines for Disease Control Using a Modular Agricultural Robot. *Biosystems Eng*. 146: 203-215.

Oerke, E. C. and Dehne, H. W. 2004. Safeguarding production d losses in major crops and the role of crop protection. *Crop Prot*. 23(4): 275-285.

Ogawa, Y., Kondo, N., Monta, M. and Shibusawa, S. 2006. Spraying Robot for Grape Production. *Field & Serv. Robotics*. 24: 539–548.

Oltean, S. E. 2019. Mobile Robot Platform with Arduino Uno and Raspberry Pi for Autonomous Navigation. The 12th International Conference Inter-disciplinarity in Engineering. *Procedia Manufacturing*. 32:572-577.

O'Neill, D.W., Fanning, A.L., Lamb, W.F. and Steinberger, J.K. 2018. A good life for all within planetary boundaries. *Sustain*. 1 (2): 88–95. https://doi.org/10.1038/ s41893-018-0021-4.

Ortiz, J. M. and Olivares, M. 2006. A vision based navigation system for an agricultural field robot. *Paper presented at the Robotics Symposium, 2006. LARS '06, IEEE 3rd Latin American.* pp: 106-114.

Pace, B., Cefola, M., Renna, F. and Attolico, G. 2011. Relationship between visual appearance and browning as evaluated by image analysis and chemical traits in fresh-cut nectarines. *Postharvest Biol. & Technol.* 61(2-3): 178-183.

Patnaik, A. and Narayanamoorthi, R. 2014. Weed Removal in Cultivated Field by Autonomous Robot using LABVIEW. *IEEE Sponsored 2nd International Conference on Innovations in Information Embedded and Communication Systems*. pp: 1-5.

Pedersen, S. M., Fountas, S., Have, H. and Blackmore, B. S. 2006. Agricultural robots system analysis and economic feasibility. *Precision Agric*. 7(4): 295-308. http://doi.org/10.1007/s11119-006-9014-9.

Perez, A. J., Lopez, F., Benlloch, J. V. and Christensen, S. 2000. Colour and shape analysis techniques for weed detection in cereal fields. *Comput. & Electr. Agric*. 25(3): 197-212.

Pexa, M., Mader, D., Čedík, J., Peterka, B., Mueller, M., Valášek, P. and Hloch, S. 2020. Experimental verification of small diameter rollers utilization in construction of roller test stand in evaluation of energy loss due to rolling resistance. *Measurement*. 152: 107287 - 107301.

Prasad, R. and Ma, Y. 2019. Hierarchical Control Coordination Strategy of Six Wheeled Independent Drive (6WID) Skid Steering Vehicle. *IFAC PapersOnLine*. 52(5): 60–65.

Ramesh, A. P. and Pasupathy, N. 2019. Design and Implementation of Remote Sensing Robotic Platform for Precision Agriculture. *Int. J. Innovative Technol. & Exploring Eng.* 8(11): 2396- 2399.

Ramya, V. and Palaniappan, B. 2012. Web Based Embedded Robot For Safety And Security Applications Using Zigbee. *Int. J. Wireless & Mobile Networks*. 4(6): 155-174.

Rashid, H., Mahmood, A., Shekha, S., Reza, S. M. T. and Rasheduzzaman, Md. 2016. Design and Development of a DTMF Controlled Room Cleaner Robot with Two Path-Following Method. *19th International Conference on Computer and Information Technology*. pp: 484-489.

Reguera, P., García, D., Domínguez, M., Prada, M. A. and Alonso, S. 2015. A Low-Cost Open Source Hardware in Control Education. Case Study: Arduino-Feedback Ms-150. *IFAC-PapersOnLine*. pp: 117–122.

Rovira-Mas, F., Chatterjee, I., and Saiz-Rubio, V. 2015. The role of GNSS in the navigation strategies of cost-effective agricultural robots. *Comput. & Electr. Agric*. 112: 172-183.

Ruckelshausen, A., Biber, P., Dorna, M., Gremmes, H., Klose, R., Linz, A., Rahe, F., Resch, R., Thiel, M., Trautz, D. and Weiss, U. 2009. BoniRob–an autonomous field robot platform for individual plant phenotyping. *Precision Agric*. 9(841): p1.

Sammons, P., Furukawa, T. and Bulgin, A. 2005. Autonomous Pesticide Spraying Robot for use in a Greenhouse. In *Australian Conference on Robotics and Automation*. 1(9): 1-9.

Shivaprasad, B. S., Ravishankara, M. N. and Shoba, B. N. 2014. Design and Implementation of Seeding and Fertilizing Agriculture Robot. *Int. J. Appl. or Innovation in Eng. & Manag*. 3(6): 251-255.

Sistler, F. 1987. Robotics and intelligent machines in agriculture. *IEEE: Journal on Robotics and Automation.* 3(1): 3-6.

Slaughter, D., Giles, D. and Downey, D. 2008. Autonomous robotic weed control systems: A review. *Comput. & Electr. Agric*. 61(1): 63-78.

Sowjanya, K. D., Sindhu, R., Parijatham, M., Srikanth, K. and Bhargav, P. 2017. Multipurpose Autonomous Agricultural Robot. *IEEE: International Conference on Electronics, Communication and Aerospace Technology.* pp: 696-699.

Sreekantha, D. 2016. Automation in agriculture: a study. *Int. J. Eng. Sci. Invention Res. & Dev*. 2: 134-139.

Srivastava, A. 2010. Robo Kisan – a helping hand to the farmer. *Proceedings of the International Multi Conference of Engineers and Computer Scientists 201, Hong Kong*. pp: 5-8.

Srivastava, A., Vijay, S., Negi, A., Shrivastava, P. and Singh, A. 2014. DTMF Based Intelligent Farming Robotic Vehicle. *IEEE International Conference on Embedded Systems.* pp: 206-210.

Steyn, W. and Warnich, J. 2015. The impact of tyre diameter and surface conditions on the rolling resistance of mountain bikes. file:///C:/Users/HP/AppData/Local/Temp/innovate_10_2015_the-impact-of-tyre-diameter-and-surface-conditions-on-the-rolling-resistance-of-mountain-bikes.zp73367.pdf. [18 June 2020].

Subramanian, V., Burks, T. F. and Arroyo, A. A. 2006. Development of machine vision and laser radar based autonomous vehicle guidance systems for citrus grove navigation. *Comput. & Electr. Agric*. 53(2): 130-143.

Sud, U., Ahmad, T., Gupta, V., Chandra, H., Sahoo, P., Aditya, K., Singh, M. and Biwas, A. 2015. *Research on improving methods for estimating crop area, Yield and production under mixed, repeated and continuous cropping.* New Delhi, India: ICAR-Indian Agricultural Statistics Research Institute, 119pp.

Sujaritha, M., Annadurai, S., Satheeshkumar, J., Sharan, S. K. and Mahesh, L. 2017. Weed detecting robot in sugarcane fields using fuzzy real time classifier. *Comput. & Electr. Agric*. 134: 160-171.

Sulakhe, A. and Karanjkar, M. N. 2015. Design and Operation of Agriculture Based Pesticide Spraying Robot. *Int. J. Electr. & Commun. Technol*. 6(4): 49-51.

Tamaki, K., Nagasaka, Y., Nishiwaki, K., Saito, M., Kikuchi, Y. and Motobayashi, K. 2013. A Robot System for Paddy Field Farming in Japan. *IFAC Proc*. 46(18): 143–147. http://doi:10.3182/20130828-2-sf-3019.00013.

Tamburinoa, L., Bravo, G., Clough, Y. and Nicholas, K.A. 2020. From population to production: 50 years of scientific literature on how to feed the world. *Global Food Security.* 24: 1-8. https://doi.org/10.1016/j.gfs.2019.100346.

Tamre, M., Hudjakov, R., Shvarts, D., Polder, A., Hiiemaa, M. and Juurma, M. 2018. Implementation of Integrated Wireless Network and MATLAB System to Control Autonomous Mobile Robot. *Int. J. Innovative Technol. & Interdisciplinary Sci.* 1(1): 18-25.

Tarannum, N., Rhaman, M.K., Khan, S.A. and Shakil, S.R. 2015. A brief overview and systematic approch for using agricultural robot in developing countries. *J. Mod. Sci. & Technol.* 3(1): 88-101. https://zantworldpress.com/wp-content/uploads/2019/12/Paper-8.pdf.

Tedla, T.B., Bovas, J.J.L., Berhane, Y., Davydkin, M.N. and James, P.S. 2019. Automated granary monitoring and controlling system suitable for the sub-saharan region. *Int. J. Sci. & Technol. Res.* 8(12):1943-1951.

Tu, X., Gai, J. and Tan, L. 2019. Robust navigation control of a 4WD/4WS agricultural robotic vehicle. *Comput. & Electr*. *Agric.* 164: p104892.

UK-RAS White papers. 2018. Agricultural Robotics: The Future of Robotic Agriculture, available: https://arxiv.org/ftp/arxiv/papers/1806/1806.06762.pdf. [27 February 2020].

Umarkar, S. and Karwankar, A. 2016. Automated Seed Sowing Agribot using Arduino. *IEEE: International Conference on Communication and Signal Processing*. pp: 1379-1383.

Utstumo, T., Urdal, F., Brevik, A., Dorum, J., Netland, J., Overskeid, O., Berge, T. W. and Gravdahl, J. T. 2018. Robotic in-row weed control in vegetables. *Comput. & Electr. Agric*. 154: 36-45.

Van Henten, E. J., Bac, C., Hemming, J. and Edan, Y. 2013. Robotics in protected cultivation. *IFAC Proc*. 46(18): 170-177.

Vanitha, M., Selvalakhmi, M. and Selvarasu, R. 2016. Monitoring and Controlling of Mobile Robot Via Internet Through Raspberry PI Board. *IEEE: Second International Conference on Science Technology Engineering and Management (ICONSTEM).* pp: 462-466.

Vasconez, J. P., Kantor, G. A. and AuatCheein, F. A. 2019. Human–robot interaction in agriculture: A survey and current challenges. *Biosystems Eng.* 179: 35–48. http://doi:10.1016/j.biosystemseng.2018.12.005.

Wallace, B. and Rao, N. 1993. Engineering Elements for Transportation on the Lunar Surface. *Appl. Mech. Rev*. 46(6): 301-312.

Wang, N. Zhang, N. and Wang, M. 2006. Wireless sensors in agriculture and food industry—Recent development and future perspective. *Comput. & Electr. Agric*. 50: 1–14.

Wismer, R. D. and Luth, H. J. 1974. Off-road traction prediction for wheeled vehicles. *Trans. of ASAE*. 17(1): 8-14.

Wong, J. Y. 1993. *Theory of Ground Vehicles*. John Wiley & Sons Inc. New York. 560p.

World Population prospects. 2019. United Nations, Department of Economics and Social Affairs. https://population.un.org/wpp/Publications/Files/WPP2019_10KeyFindings.pdf. [1 February 2020].

Xue, J., Fan, B., Zhang, X. and Fend, Y. 2017. An Agricultural Robot for Multipurpose Operations in a Greenhouse. *International Conference on Mechanical and Mechatronics Engineering (ICMME), IEEE*. pp: 122-131.

Xue, J., Dong, S. and Yan, J. 2018. Sliding mode Variable Structure Based Path Following control of Agricultural Robots with Differential Drive. *IFACPapersOnLine*. 51(17): 455–459.

Yaghoubi, S., Akbarzadeh, N. A., Bazargani, S. S., Bazargani, S. S., Bamizan, M. and Asl, M. I. 2013. Autonomous Robots for Agricultural Tasks and Farm Assignment and Future Trends in Agro Robots. *Int. J. Mech. & Mechatronics Eng. IJMME-IJENS*. 13(3): 1-6.

Yuan, T., Xu, C. G., Ren, Y. X., Feng, Q. C., Tan, Y. Z. and Li, W. 2009. Detecting the information of cucumber in greenhouse for picking based on NIR image. *Spectrosc & Spectral Anal*. 29(8): 2054-2058.

Yusoff, K. A. M., Saminb, E. R. and Ibrahimc, K. S. B. 2012. Wireless Mobile Robotic Arm. International Symposium on Robotics and Intelligent Sensors. *Procedia Eng.* 41: 1072 – 1078.

Zhang, Q. 2013. Opportunity of robotics in specialty crop production. *IFAC Proc.* 46(4): 38-39.

Zhao, D. A., Lv, J. D., Ji, W., Zhang, Y. and Chen, Y. 2011. Design and control of an apple harvesting robot. *Biosystems Eng*. 110(2): 112-122.

Zhu, A. B., Wang, B. K., Tian, C., Zhang, H. and Chen, W. 2012. Dynamics modeling method and performance simulation for maneuvering system of tracked vehicle. *J. Machine Des. Natl.* 29(9): 57-60.

Appendices

APPENDIX I

Plant height of three varieties of chilli at various growth stages

Growth stages	Anugraha					Ujwala					White kanthari				
	I	II	III	IV	V	I	II	III	IV	V	I	II	III	IV	V
15 days after transplanting	9	15	10	12	16	12.5	15	11	16.5	9	15.5	15	18	14.5	13
Flowering stage	38	46	40	44	49.5	46	52	42	55	45	62	62	65	58	56
15 days after flowering	50	56.5	52	52	58	59	63	57.5	66.5	56	78.5	76	82	73	72
Full growth period	66	70	60.5	63	69.5	71	75	70	77	69	108	105	110	103	96.5

APPENDIX II

Calculation of torque on each drive motor

m = 55 kg

μ = 0.2 - 0.4 for tilled soil condition = 0.2

α = 10°

$F_r = \mu * m * g * cos\alpha = 0.2 * 55 * 9.8 * cos10° = 106.16\ N$

$F_g = m * g * sin\alpha = 55 * 9.8 * sin10° = 93.59\ N$

$F_a = m * a \approx 0$

$F_d = \frac{1}{2} * \rho * A_f * C_d * V^2 \approx 0$

$\therefore F_t = F_r + F_g + F_a + F_d = 106.16 + 93.59 = 199.75\ N$

Assume, Diameter of the wheel = 5 inches = 12.7 cm

$$\tau_{total} = F_t * r$$

$$\tau_{total} = 199.75 * \frac{12.7}{2} = 1268.41\ Ncm = 129.42\ kg_f cm$$

Torque on each motor, $\tau = \frac{\tau_{total}}{no.of\ motors} = \frac{129.42}{6} = 21.57\ kg_f cm$

Considering a FoS 1.2, $\tau = 21.57 * 1.2 = 25.88\ kg_f cm$

APPENDIX III

a. Specification of DC motor

Model	**DC worm gear motor GW5840-31ZY**
Operating voltage	12 V
No-load speed	27 RPM
No-load current	$\leq$ 350 mA
Stall torque	140 kg_f-cm
Rated torque	80 kg_f-cm
Rated speed	20 RPM
Rated current	$\leq$ 1.6 A
Output power	10-20 W
Diameter of output shaft (dual type)	8 mm

b. Specifications of microcontroller unit

Microcontroller	**ATmega2560**
Operating Voltage	5V
Digital I/O Pins	54 (of which 15 provide PWM output)
Analog Input Pins	16
DC Current per I/O Pin	20 mA
DC Current for 3.3V Pin	50 mA
Flash Memory	256 KB
RAM	8 KB
EEPROM	4 KB
Clock Speed	16 MHz

c. Specifications of motor driver

Model	**L298N 2A**
Driver Chip	Double H Bridge L298N
Motor Supply Voltage	0-46V
Motor Supply Current	2A
Logical Voltage	5V
Driver Voltage	5-35V
Driver Current	2A
Logical Current	0-36mA
Maximum Power (W)	25W

d. Specifications of wireless communication system

i. Transmitter specifications

Model	**Flysky FS-i6X**
Channels	6 – 10 (default 6)
RF range	2.408 – 2.475 GHz
Bandwidth	500 kHz
RF channel	135
RF power	<20 dBm
Modulation type	GFSK
Antenna	Dual antenna (26 mm)
Power	Four 6.5 V DC (1.5 A)
Low voltage warning	<4.2 V

ii. Receiver specifications

Model	**Flysky FS-iA6**
Channels	6
RF range	2.408 – 2.475 GHz
Bandwidth	500 kHz
RF channel	135
RF receiver sensitivity	- 105 dBm
Modulation type	GFSK
Antenna	Dual antenna (26 mm)
Power	4-6.5V
i-Bus port	No

APPENDIX IV

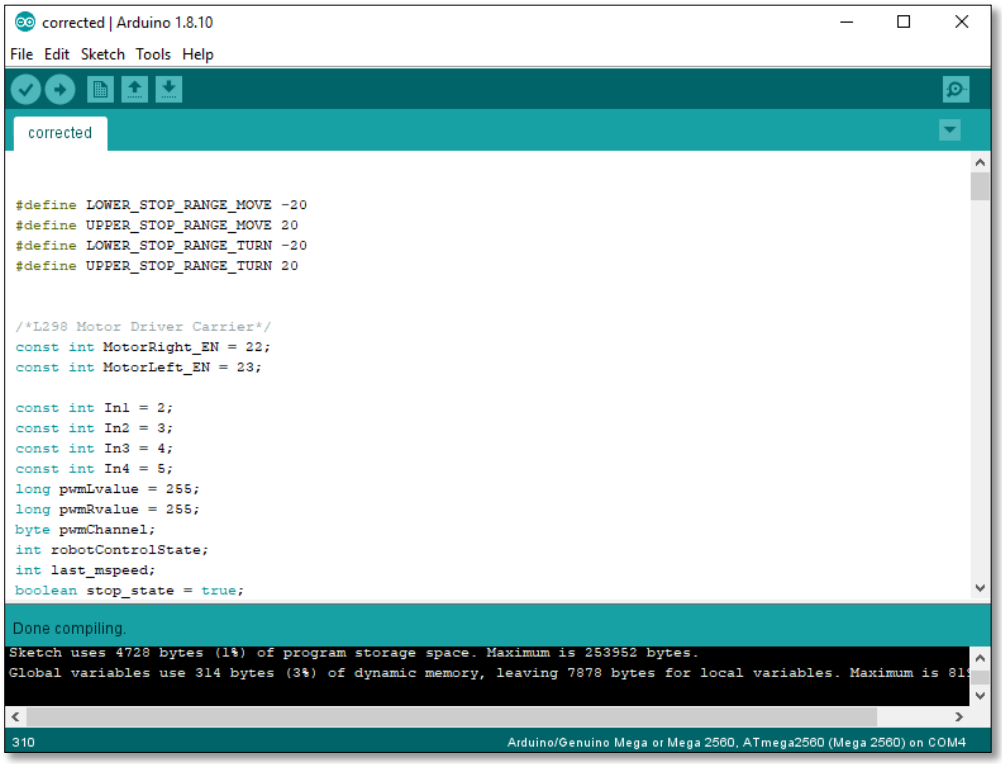
corrected | Arduino 1.8.10
File Edit Sketch Tools Help
corrected
#define LOWER_STOP_RANGE_MOVE -20
#define UPPER_STOP_RANGE_MOVE 20
#define LOWER_STOP_RANGE_TURN -20
#define UPPER_STOP_RANGE_TURN 20
/*L298 Motor Driver Carrier*/
const int MotorRight_EN = 22;
const int MotorLeft_EN = 23;
const int In1 = 2;
const int In2 = 3;
const int In3 = 4;
const int In4 = 5;
long pwmLvalue = 255;
long pwmRvalue = 255;
byte pwmChannel;
int robotControlState;
int last_mspeed;
boolean stop_state = true;
Done compiling.
Sketch uses 4728 bytes (1%) of program storage space. Maximum is 253952 bytes.
Global variables use 314 bytes (3%) of dynamic memory, leaving 7878 bytes for local variables. Maximum is 81
310
Arduino/Genuino Mega or Mega 2560, ATmega2560 (Mega 2560) on COM4

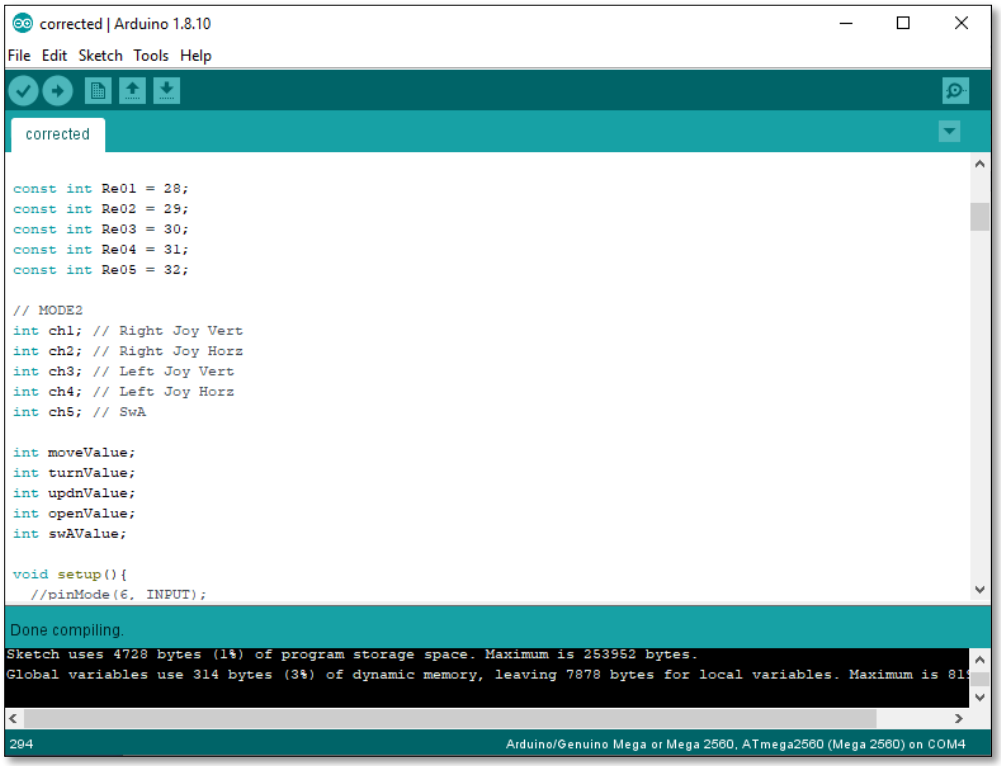
corrected | Arduino 1.8.10
File Edit Sketch Tools Help
corrected
const int Re01 = 28;
const int Re02 = 29;
const int Re03 = 30;
const int Re04 = 31;
const int Re05 = 32;
// MODE2
int ch1; // Right Joy Vert
int ch2; // Right Joy Horz
int ch3; // Left Joy Vert
int ch4; // Left Joy Horz
int ch5; // SwA
int moveValue;
int turnValue;
int updnValue;
int openValue;
int swAValue;
void setup(){
//pinMode(6, INPUT);
Done compiling.
Sketch uses 4728 bytes (1%) of program storage space. Maximum is 253952 bytes.
Global variables use 314 bytes (3%) of dynamic memory, leaving 7878 bytes for local variables. Maximum is 81
294
Arduino/Genuino Mega or Mega 2560, ATmega2560 (Mega 2560) on COM4

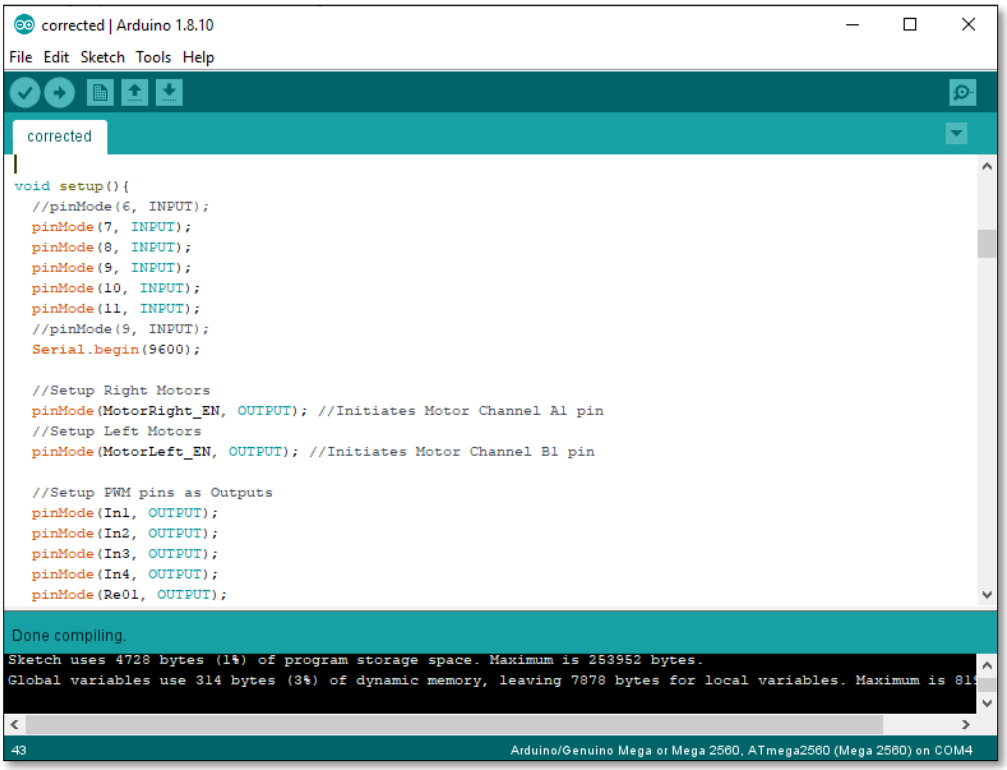
corrected | Arduino 1.8.10
File Edit Sketch Tools Help
corrected
void setup(){
//pinMode(6, INPUT);
pinMode(7, INPUT);
pinMode(8, INPUT);
pinMode(9, INPUT);
pinMode(10, INPUT);
pinMode(11, INPUT);
//pinMode(9, INPUT);
Serial.begin(9600);
//Setup Right Motors
pinMode(MotorRight_EN, OUTPUT); //Initiates Motor Channel A1 pin
//Setup Left Motors
pinMode(MotorLeft_EN, OUTPUT); //Initiates Motor Channel B1 pin
//Setup PWM pins as Outputs
pinMode(In1, OUTPUT);
pinMode(In2, OUTPUT);
pinMode(In3, OUTPUT);
pinMode(In4, OUTPUT);
pinMode(Re01, OUTPUT);
Done compiling.
Sketch uses 4728 bytes (1%) of program storage space. Maximum is 253952 bytes.
Global variables use 314 bytes (3%) of dynamic memory, leaving 7878 bytes for local variables. Maximum is 81
43
Arduino/Genuino Mega or Mega 2560, ATmega2560 (Mega 2560) on COM4

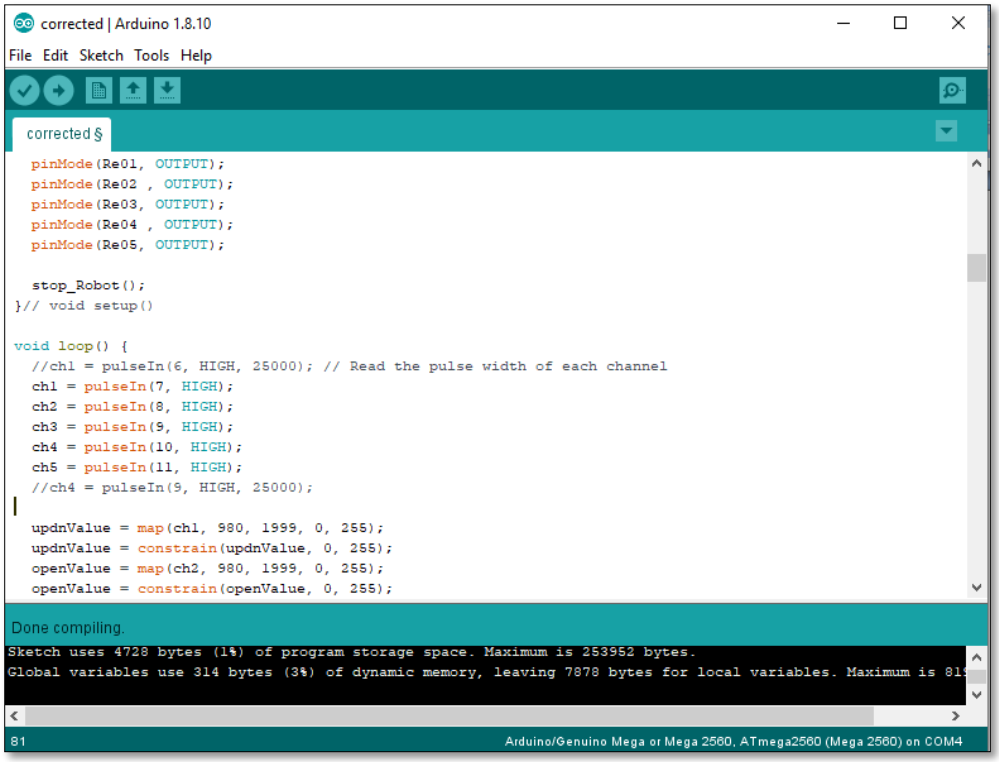
corrected | Arduino 1.8.10
File Edit Sketch Tools Help
corrected §
pinMode(Re01, OUTPUT);
pinMode(Re02 , OUTPUT);
pinMode(Re03, OUTPUT);
pinMode(Re04 , OUTPUT);
pinMode(Re05, OUTPUT);
stop_Robot();
}// void setup()
void loop() {
//ch1 = pulseIn(6, HIGH, 25000); // Read the pulse width of each channel
ch1 = pulseIn(7, HIGH);
ch2 = pulseIn(8, HIGH);
ch3 = pulseIn(9, HIGH);
ch4 = pulseIn(10, HIGH);
ch5 = pulseIn(11, HIGH);
//ch4 = pulseIn(9, HIGH, 25000);
updnValue = map(ch1, 980, 1999, 0, 255);
updnValue = constrain(updnValue, 0, 255);
openValue = map(ch2, 980, 1999, 0, 255);
openValue = constrain(openValue, 0, 255);
Done compiling.
Sketch uses 4728 bytes (1%) of program storage space. Maximum is 253952 bytes.
Global variables use 314 bytes (3%) of dynamic memory, leaving 7878 bytes for local variables. Maximum is 81
81
Arduino/Genuino Mega or Mega 2560, ATmega2560 (Mega 2560) on COM4

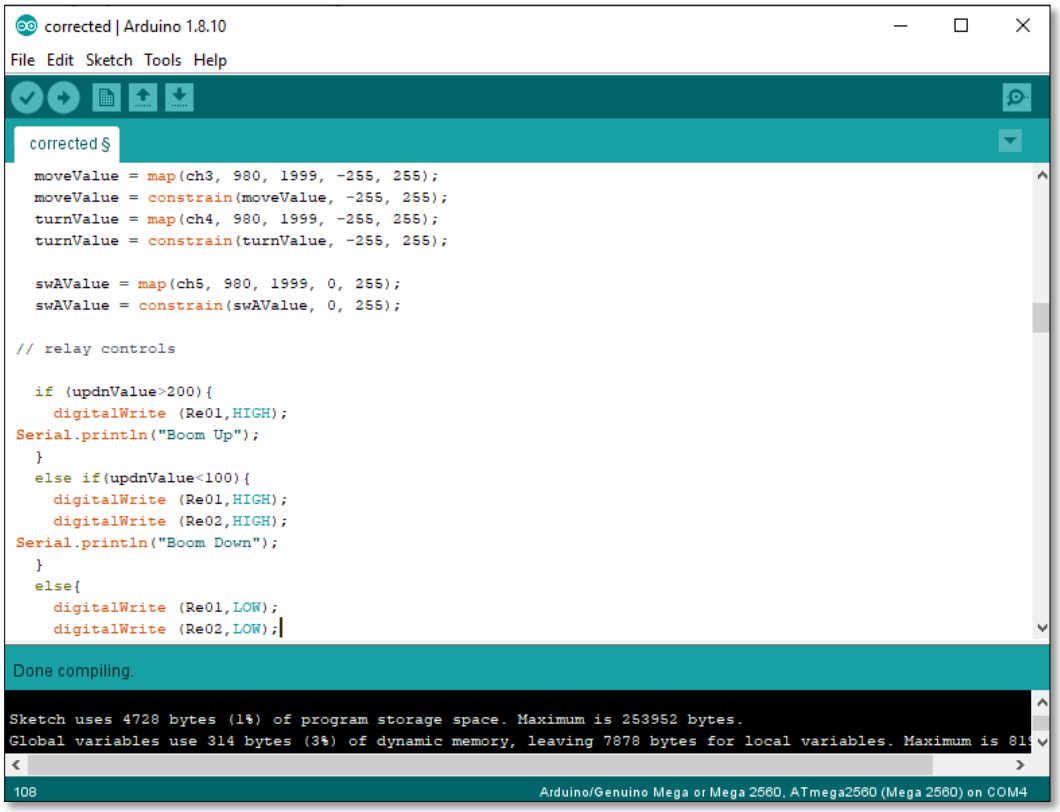
corrected | Arduino 1.8.10
File Edit Sketch Tools Help
corrected §
moveValue = map(ch3, 980, 1999, -255, 255);
moveValue = constrain(moveValue, -255, 255);
turnValue = map(ch4, 980, 1999, -255, 255);
turnValue = constrain(turnValue, -255, 255);
swAValue = map(ch5, 980, 1999, 0, 255);
swAValue = constrain(swAValue, 0, 255);
// relay controls
if (updnValue>200){
digitalWrite (Re01,HIGH);
Serial.println("Boom Up");
}
else if(updnValue<100){
digitalWrite (Re01,HIGH);
digitalWrite (Re02,HIGH);
Serial.println("Boom Down");
}
else{
digitalWrite (Re01,LOW);
digitalWrite (Re02,LOW);
Done compiling.
Sketch uses 4728 bytes (1%) of program storage space. Maximum is 253952 bytes.
Global variables use 314 bytes (3%) of dynamic memory, leaving 7878 bytes for local variables. Maximum is 81
108
Arduino/Genuino Mega or Mega 2560, ATmega2560 (Mega 2560) on COM4

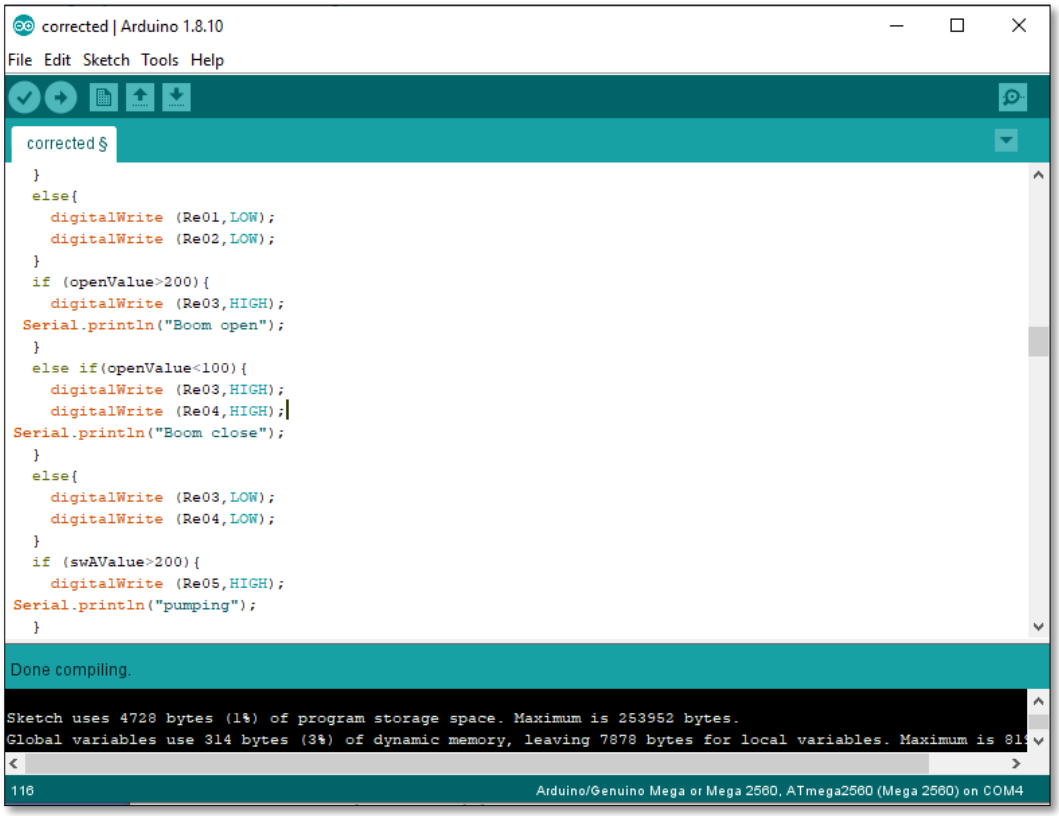
corrected | Arduino 1.8.10
File Edit Sketch Tools Help
corrected §
}
else{
digitalWrite (Re01,LOW);
digitalWrite (Re02,LOW);
}
if (openValue>200){
digitalWrite (Re03,HIGH);
Serial.println("Boom open");
}
else if(openValue<100){
digitalWrite (Re03,HIGH);
digitalWrite (Re04,HIGH);
Serial.println("Boom close");
}
else{
digitalWrite (Re03,LOW);
digitalWrite (Re04,LOW);
}
if (swAValue>200){
digitalWrite (Re05,HIGH);
Serial.println("pumping");
}
Done compiling.
Sketch uses 4728 bytes (1%) of program storage space. Maximum is 253952 bytes.
Global variables use 314 bytes (3%) of dynamic memory, leaving 7878 bytes for local variables. Maximum is 81
116
Arduino/Genuino Mega or Mega 2560, ATmega2560 (Mega 2560) on COM4

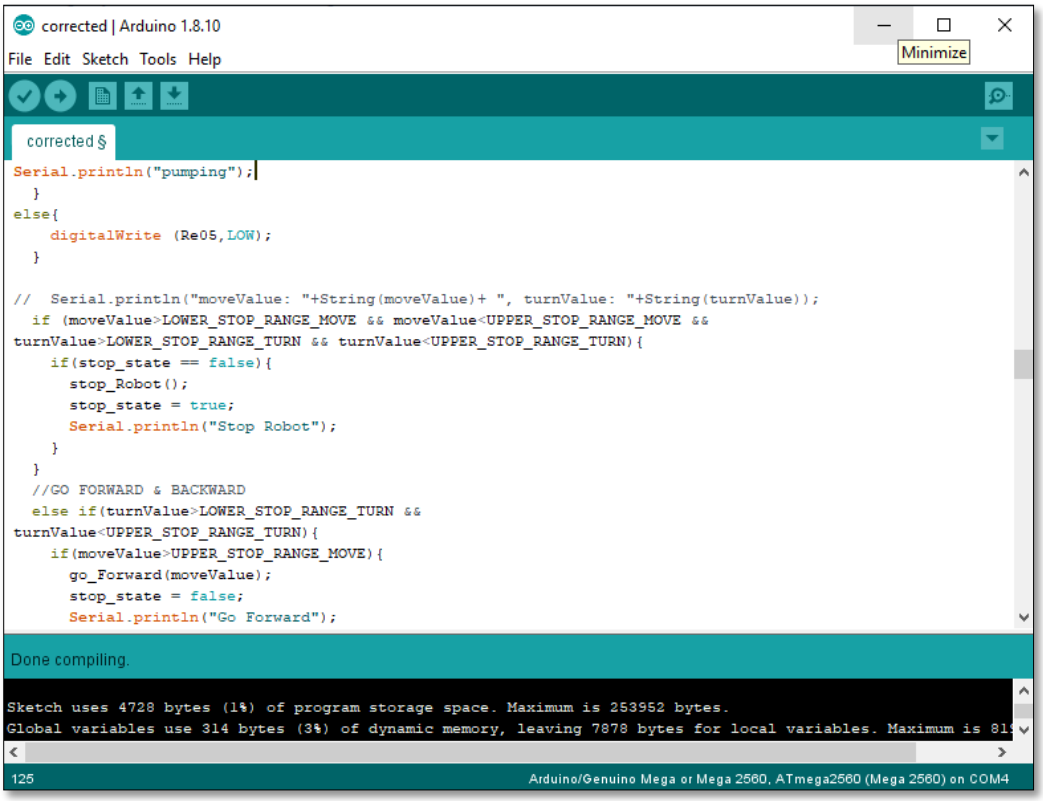
corrected | Arduino 1.8.10
File Edit Sketch Tools Help
Minimize
corrected §
Serial.println("pumping");
}
else{
digitalWrite (Re05,LOW);
}
// Serial.println("moveValue: "+String(moveValue)+ ", turnValue: "+String(turnValue));
if (moveValue>LOWER_STOP_RANGE_MOVE && moveValue<UPPER_STOP_RANGE_MOVE &&
turnValue>LOWER_STOP_RANGE_TURN && turnValue<UPPER_STOP_RANGE_TURN){
if(stop_state == false){
stop_Robot();
stop_state = true;
Serial.println("Stop Robot");
}
}
//GO FORWARD & BACKWARD
else if(turnValue>LOWER_STOP_RANGE_TURN &&
turnValue<UPPER_STOP_RANGE_TURN){
if(moveValue>UPPER_STOP_RANGE_MOVE){
go_Forward(moveValue);
stop_state = false;
Serial.println("Go Forward");
Done compiling.
Sketch uses 4728 bytes (1%) of program storage space. Maximum is 253952 bytes.
Global variables use 314 bytes (3%) of dynamic memory, leaving 7878 bytes for local variables. Maximum is 81
125
Arduino/Genuino Mega or Mega 2560, ATmega2560 (Mega 2560) on COM4

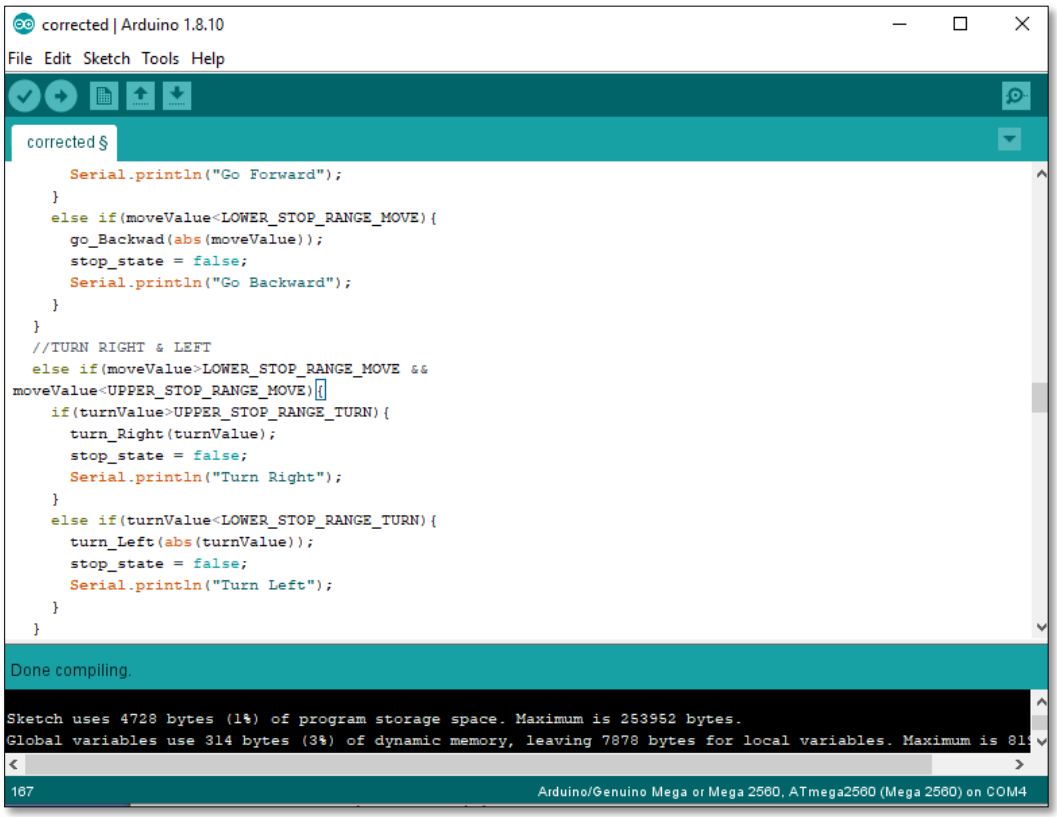
corrected | Arduino 1.8.10
File Edit Sketch Tools Help
corrected §
Serial.println("Go Forward");
}
else if(moveValue<LOWER_STOP_RANGE_MOVE){
go_Backwad(abs(moveValue));
stop_state = false;
Serial.println("Go Backward");
}
}
//TURN RIGHT & LEFT
else if(moveValue>LOWER_STOP_RANGE_MOVE &&
moveValue<UPPER_STOP_RANGE_MOVE){
if(turnValue>UPPER_STOP_RANGE_TURN){
turn_Right(turnValue);
stop_state = false;
Serial.println("Turn Right");
}
else if(turnValue<LOWER_STOP_RANGE_TURN){
turn_Left(abs(turnValue));
stop_state = false;
Serial.println("Turn Left");
}
}
Done compiling.
Sketch uses 4728 bytes (1%) of program storage space. Maximum is 253952 bytes.
Global variables use 314 bytes (3%) of dynamic memory, leaving 7878 bytes for local variables. Maximum is 81
167
Arduino/Genuino Mega or Mega 2560, ATmega2560 (Mega 2560) on COM4

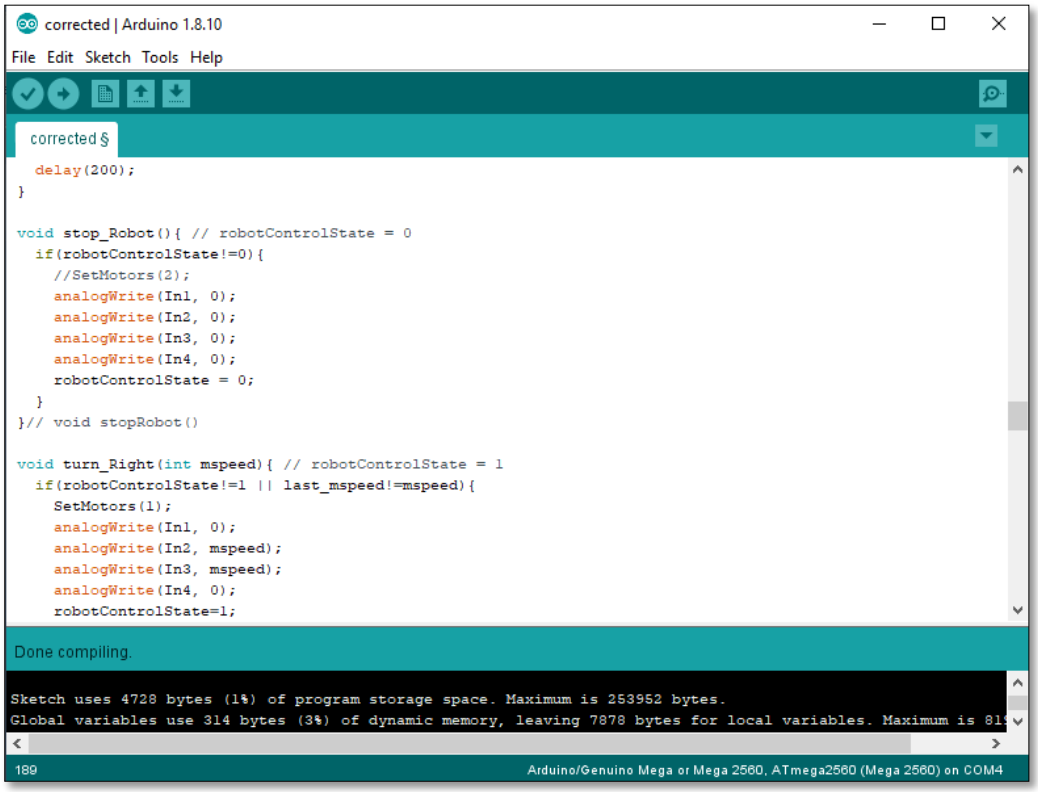
corrected | Arduino 1.8.10
File Edit Sketch Tools Help
corrected §
delay(200);
}
void stop_Robot(){ // robotControlState = 0
if(robotControlState!=0){
//SetMotors(2);
analogWrite(In1, 0);
analogWrite(In2, 0);
analogWrite(In3, 0);
analogWrite(In4, 0);
robotControlState = 0;
}
}// void stopRobot()
void turn_Right(int mspeed){ // robotControlState = 1
if(robotControlState!=1 || last_mspeed!=mspeed){
SetMotors(1);
analogWrite(In1, 0);
analogWrite(In2, mspeed);
analogWrite(In3, mspeed);
analogWrite(In4, 0);
robotControlState=1;
Done compiling.
Sketch uses 4728 bytes (1%) of program storage space. Maximum is 253952 bytes.
Global variables use 314 bytes (3%) of dynamic memory, leaving 7878 bytes for local variables. Maximum is 81
189
Arduino/Genuino Mega or Mega 2560, ATmega2560 (Mega 2560) on COM4

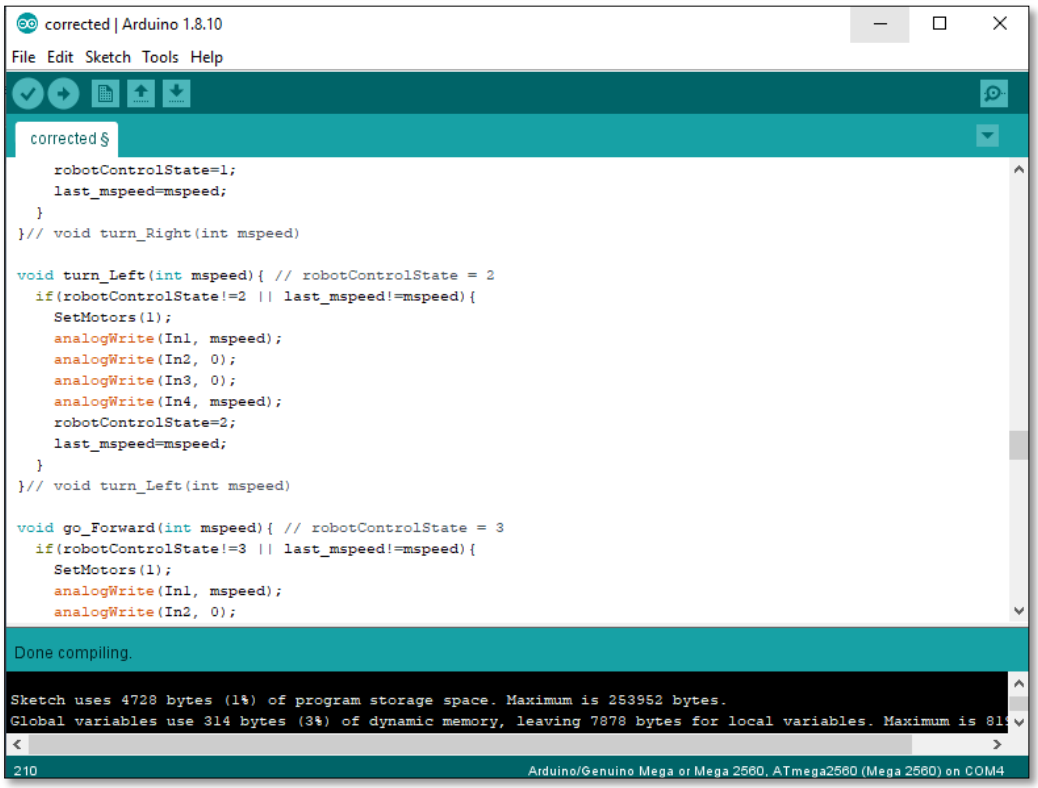
corrected | Arduino 1.8.10
File Edit Sketch Tools Help
corrected §
robotControlState=1;
last_mspeed=mspeed;
}
}// void turn_Right(int mspeed)
void turn_Left(int mspeed){ // robotControlState = 2
if(robotControlState!=2 || last_mspeed!=mspeed){
SetMotors(1);
analogWrite(In1, mspeed);
analogWrite(In2, 0);
analogWrite(In3, 0);
analogWrite(In4, mspeed);
robotControlState=2;
last_mspeed=mspeed;
}
}// void turn_Left(int mspeed)
void go_Forward(int mspeed){ // robotControlState = 3
if(robotControlState!=3 || last_mspeed!=mspeed){
SetMotors(1);
analogWrite(In1, mspeed);
analogWrite(In2, 0);
Done compiling.
Sketch uses 4728 bytes (1%) of program storage space. Maximum is 253952 bytes.
Global variables use 314 bytes (3%) of dynamic memory, leaving 7878 bytes for local variables. Maximum is 81
210
Arduino/Genuino Mega or Mega 2560, ATmega2560 (Mega 2560) on COM4


corrected | Arduino 1.8.10
File Edit Sketch Tools Help
corrected §
SetMotors(1);
analogWrite(In1, mspeed);
analogWrite(In2, 0);
analogWrite(In3, mspeed);
analogWrite(In4, 0);
robotControlState=3;
last_mspeed=mspeed;
}
}// void goForward(int mspeed)
void go_Backwad(int mspeed){ // robotControlState = 4
if(robotControlState!=4 || last_mspeed!=mspeed){
SetMotors(1);
analogWrite(In1, 0);
analogWrite(In2, mspeed);
analogWrite(In3, 0);
analogWrite(In4, mspeed);
robotControlState=4;
last_mspeed=mspeed;
}
}// void goBackwad(int mspeed)
Done compiling.
Sketch uses 4728 bytes (1%) of program storage space. Maximum is 253952 bytes.
Global variables use 314 bytes (3%) of dynamic memory, leaving 7878 bytes for local variables. Maximum is 81
208
Arduino/Genuino Mega or Mega 2560, ATmega2560 (Mega 2560) on COM4

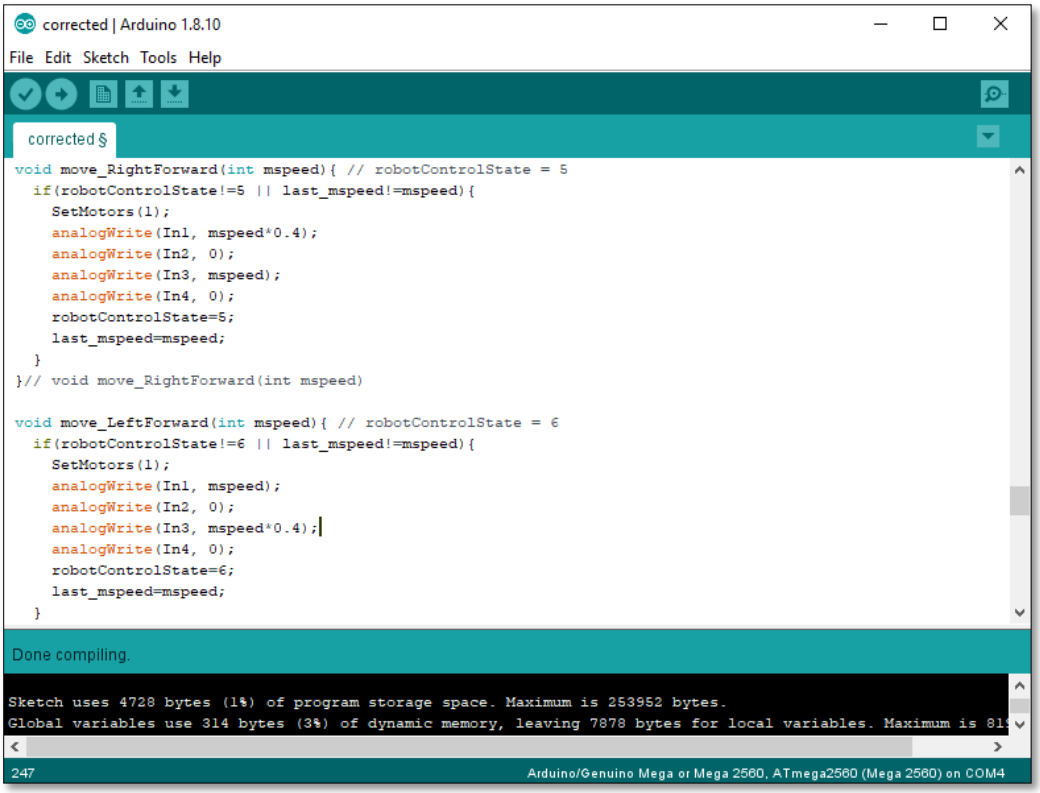
corrected | Arduino 1.8.10
File Edit Sketch Tools Help
corrected §
void move_RightForward(int mspeed){ // robotControlState = 5
if(robotControlState!=5 || last_mspeed!=mspeed){
SetMotors(1);
analogWrite(In1, mspeed*0.4);
analogWrite(In2, 0);
analogWrite(In3, mspeed);
analogWrite(In4, 0);
robotControlState=5;
last_mspeed=mspeed;
}
}// void move_RightForward(int mspeed)
void move_LeftForward(int mspeed){ // robotControlState = 6
if(robotControlState!=6 || last_mspeed!=mspeed){
SetMotors(1);
analogWrite(In1, mspeed);
analogWrite(In2, 0);
analogWrite(In3, mspeed*0.4);
analogWrite(In4, 0);
robotControlState=6;
last_mspeed=mspeed;
}
Done compiling.
Sketch uses 4728 bytes (1%) of program storage space. Maximum is 253952 bytes.
Global variables use 314 bytes (3%) of dynamic memory, leaving 7878 bytes for local variables. Maximum is 81
247
Arduino/Genuino Mega or Mega 2560, ATmega2560 (Mega 2560) on COM4

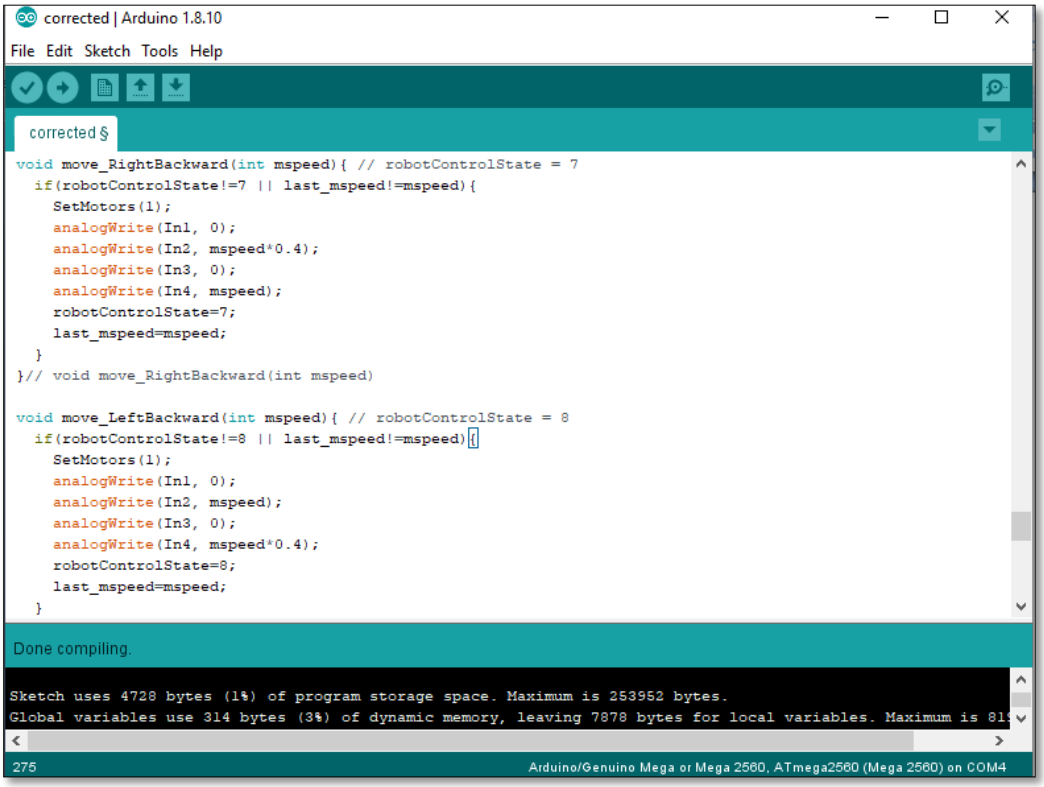
corrected | Arduino 1.8.10
File Edit Sketch Tools Help
corrected §
void move_RightBackward(int mspeed){ // robotControlState = 7
if(robotControlState!=7 || last_mspeed!=mspeed){
SetMotors(1);
analogWrite(In1, 0);
analogWrite(In2, mspeed*0.4);
analogWrite(In3, 0);
analogWrite(In4, mspeed);
robotControlState=7;
last_mspeed=mspeed;
}
}// void move_RightBackward(int mspeed)
void move_LeftBackward(int mspeed){ // robotControlState = 8
if(robotControlState!=8 || last_mspeed!=mspeed){
SetMotors(1);
analogWrite(In1, 0);
analogWrite(In2, mspeed);
analogWrite(In3, 0);
analogWrite(In4, mspeed*0.4);
robotControlState=8;
last_mspeed=mspeed;
}
Done compiling.
Sketch uses 4728 bytes (1%) of program storage space. Maximum is 253952 bytes.
Global variables use 314 bytes (3%) of dynamic memory, leaving 7878 bytes for local variables. Maximum is 81
275
Arduino/Genuino Mega or Mega 2560, ATmega2560 (Mega 2560) on COM4

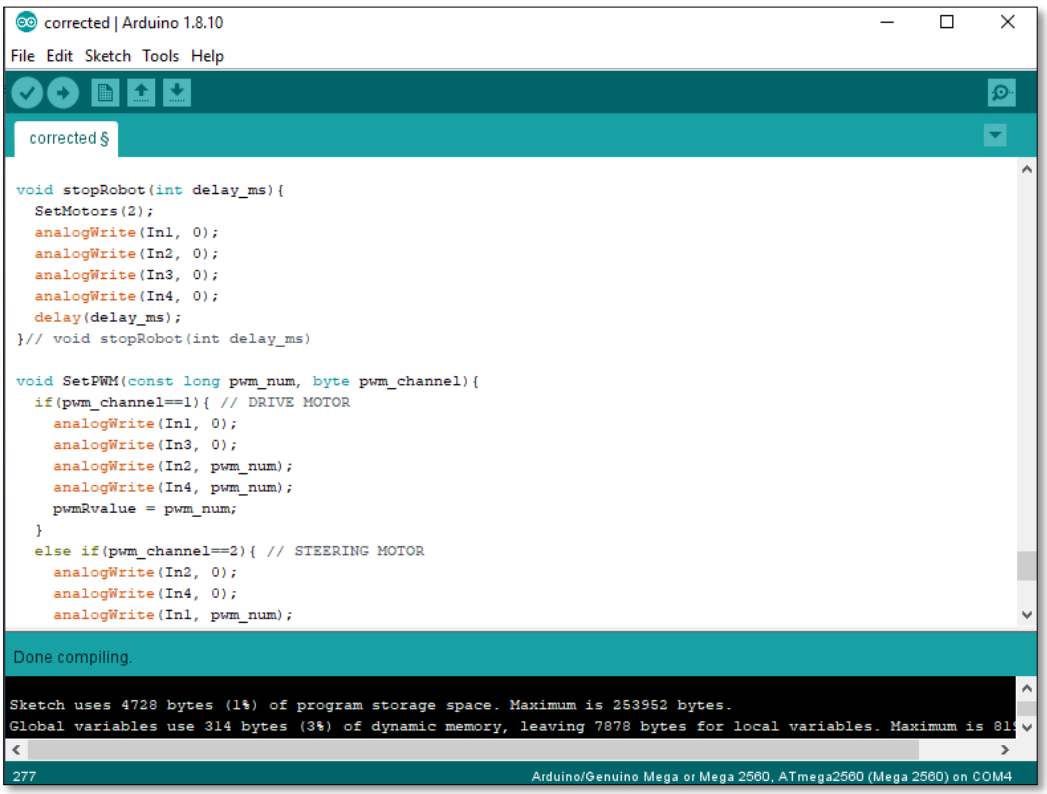
corrected | Arduino 1.8.10
File Edit Sketch Tools Help
corrected §
void stopRobot(int delay_ms){
SetMotors(2);
analogWrite(In1, 0);
analogWrite(In2, 0);
analogWrite(In3, 0);
analogWrite(In4, 0);
delay(delay_ms);
}// void stopRobot(int delay_ms)
void SetPWM(const long pwm_num, byte pwm_channel){
if(pwm_channel==1){ // DRIVE MOTOR
analogWrite(In1, 0);
analogWrite(In3, 0);
analogWrite(In2, pwm_num);
analogWrite(In4, pwm_num);
pwmRvalue = pwm_num;
}
else if(pwm_channel==2){ // STEERING MOTOR
analogWrite(In2, 0);
analogWrite(In4, 0);
analogWrite(In1, pwm_num);
Done compiling.
Sketch uses 4728 bytes (1%) of program storage space. Maximum is 253952 bytes.
Global variables use 314 bytes (3%) of dynamic memory, leaving 7878 bytes for local variables. Maximum is 81
277
Arduino/Genuino Mega or Mega 2560, ATmega2560 (Mega 2560) on COM4


corrected | Arduino 1.8.10
File Edit Sketch Tools Help
corrected §
}
else if(pwm_channel==2){ // STEERING MOTOR
analogWrite(In2, 0);
analogWrite(In4, 0);
analogWrite(In1, pwm_num);
analogWrite(In3, pwm_num);
pwmLvalue = pwm_num;
}
}// void SetPWM (const long pwm_num, byte pwm_channel)
void SetMotors(int controlCase){
switch(controlCase){
case 1:
digitalWrite(MotorRight_EN, HIGH);
digitalWrite(MotorLeft_EN, HIGH);
break;
case 2:
digitalWrite(MotorRight_EN, LOW);
digitalWrite(MotorLeft_EN, LOW);
break;
}
}// void SetMotors(int controlCase)
Done compiling.
Sketch uses 4728 bytes (1%) of program storage space. Maximum is 253952 bytes.
Global variables use 314 bytes (3%) of dynamic memory, leaving 7878 bytes for local variables. Maximum is 81
315
Arduino/Genuino Mega or Mega 2560, ATmega2560 (Mega 2560) on COM4

APPENDIX V

a. Linear deviation from the path without steering

Distance travelled, m	Linear deviation, cm			Average	Standard deviation
	Trial 1	Trial 2	Trial 3		
0	0	0	0	0	0
2	3	2.5	3.5	3	0.5
4	6.5	7.5	6.5	6.83	0.57
6	10.5	12	11.5	11.33	0.76
8	15.5	17	16	16.16	0.76
10	20.5	22.5	21.5	21.5	1
12	25	28	26	26.33	1.52
14	31	34	31.5	32.16	1.60
16	35.5	40.5	38	38	2.5
18	40.5	47.5	43.5	43.83	3.51
20	46	55	50	50.33	4.50

b. Linear deviation from the path with steering

Distance travelled, m	Linear deviation, cm		
	Trial 1	Trial 2	Trial 3
0.0	0	0	0
0.5	0.5	0	0.5
1.0	1.5	1	1
1.5	2	1	2
2.0	3.5	1.5	3

Distance travelled, m	Linear deviation, cm		
	Trial 1	Trial 2	Trial 3
10.5	1.5	1.5	-1
11.0	2.5	0.5	-0.5
11.5	3	-0.5	0
12.0	2	-1.5	0.5
12.5	0.5	-2	1

2.5	2	2	3.5
3.0	3	2.5	4.5
3.5	4.5	3	3
4.0	2.5	2	1.5
4.5	1.5	2	0
5.0	3	2.5	0
5.5	4.5	1.5	0.5
6.0	1.5	1	1
6.5	0	0.5	1.5
7.0	-0.5	0.5	2
7.5	-1.5	0	3.5
8.0	-2	0	0.5
8.5	-3	0.5	-0.5
9.0	-0.5	1.5	-1.5
9.5	0	2	-2
10.0	0.5	3.5	-2.5

13.0	-0.5	-1	1.5
13.5	-2	-0.5	2
14.0	-3.5	0	2.5
14.5	-2	0	3
15.0	-0.5	0	4.5
15.5	1	0.5	3
16.0	1.5	1	2
16.5	2.5	1.5	1
17.0	3	2	0.5
17.5	2.5	2.5	0
18.0	3	3	-0.5
18.5	1.5	2	-1
19.0	0.5	2.5	-1.5
19.5	0	3	-0.5
20.0	-0.5	0.5	0

APPENDIX VI

Total time taken = productive time + non-productive time

= 18.96 + 8.65

= 27 min = 0.46 h

$$\therefore Field\ capacity = \frac{Area\ coverd}{Total\ time} = \frac{0.01}{0.46} = 0.0217\ hah^{-1}$$

Speed of operation at field condition was measured as 0.042 m/s

$$Theoretical\ field\ capacity = \frac{w * s}{10} = \frac{3.35 * (0.042 * \frac{18}{5})}{10} = 0.05\ hah^{-1}$$

$$\therefore Field\ efficiency = \frac{EFC}{TFC} * 100 = \frac{0.0217}{0.05} * 100 = 43.4\%$$

Plant damage

Number of plants before operation = 540

Number of plants damaged after operation = 10

$$\therefore Plant\ damage = \frac{540}{10} * 100 = 1.8\%$$

Recorded values of Sinkage

Sl. No.	1	2	3	4	5
Sinkage, cm	5	3	2	3	2

Performance indices of prototype

Sl. No.	Parameters	Average value
1	Time of operation, h-ha^{-1}	31.60
2	Theoretical field capacity, ha-h^{-1}	0.05
3	Effective field capacity, ha-h^{-1}	0.0217
4	Field efficiency, %	43.4
5	Plant damage, %	1.8
6	Sinkage, cm	3

Abstract

DEVELOPMENT OF A SEMI-AUTONOMOUS ROBOTIC PLATFORM FOR INTERCULTURAL OPERATIONS IN ROW CROPS

by

ATHIRA P.

(2018-18-011)

ABSTRACT OF THESIS

Submitted in partial fulfilment of the
requirement for the degree of
MASTER OF TECHNOLOGY
IN
AGRICULTURAL ENGINEERING

(Farm Power and Machinery)

Faculty of Agricultural Engineering & Technology

Kerala Agricultural University

DEPARTMENT OF FARM MACHINERY AND POWER ENGINEERING

KELAPPAJI COLLEGE OF AGRICULTURAL ENGINEERING

AND TECHNOLOGY, TAVANUR, MALAPPURAM– 679573

KERALA, INDIA.

2020

ABSTRACT

A semi-autonomous robotic platform was conceptualized for performing the intercultural operations in row crops. It was expected to be capable of navigating within the field and performing the intended intercultural operation according to the user command.

The dimensions of the chassis (track width and ground clearance) were determined on the basis of agronomic characteristics of the crop. Wheel mounted geared motors were used for self-propulsion. The wheel variables were decided based on the rolling resistance and terramechanics relationships. A six-wheel independent drive skid-steering drive mechanism was provided to the robotic platform. Arduino Mega was the microcontroller used which was interfaced with the drive motors via L298N motor driver for speed and direction control. The microcontroller was programmed in Arduino IDE software using C++ language. The wireless communication system was based on Radio Frequency (RF) protocol using Flysky FS i6 2.4GHz Six-channel Transmitter Remote Controller with FS-iA6 Receiver unit. The monitoring guidance of the prototype was accomplished on the basis of real-time video streaming using Wi-Fi enabled wireless IP camera. The operational unit was controlled by relay driver circuits. Geared DC motor operated cable drive slider mechanisms actuated the position control of the sprayer unit.

The developed prototype was evaluated in both lab and field conditions. The speed of travel obtained was less than the rated speed. The total power consumed by the prototype increased with increase in the load. The deviation of the prototype from a straight path could be corrected by the use of steering controls by the operator. The control unit functioned satisfactorily for every command by the user. During the basic field trial, a non-uniform distribution of load on each ground-contact point occurred due to the undulated terrain. Therefore, wheels were subjected to sinkage which resulted in lack of proper traction and wheel slip. The tractive forces were then insufficient to overcome the soil resistance. The test resulted in the requirement for a modified drive mechanism for the prototype. The modified design of the drive mechanism comprised of high torque motors (24 V, 8Nm, 300 RPM DC motor) with reducer unit, high power

motor drivers (BTS7960) and larger diameter pneumatic wheels (30.48 cm diameter). A suspension could also be provided to maintain uniform load distribution on each ground-contact points. As the torque exerted by these motors would be greater than the required torque, the design was safe. The cost for modified prototype was estimated to be Rs.65000/-.